

EVOLUTIONARY MORPHOLOGY OF THE  
PRIMARY MALE REPRODUCTIVE SYSTEM AND  
SPERMATOOZOA OF GOBLIN SPIDERS  
(OONOPIDAE; ARANEAE)

ELISABETH LIPKE

*General and Systematic Zoology, Zoological  
Institute and Museum, Ernst-Moritz-Arndt  
University of Greifswald, Germany*

PETER MICHALIK

*General and Systematic Zoology, Zoological  
Institute and Museum, Ernst-Moritz-Arndt  
University of Greifswald, Germany; Division of  
Invertebrate Zoology, American Museum of  
Natural History,  
New York*

BULLETIN OF THE AMERICAN MUSEUM OF NATURAL HISTORY

Number 396, 72 pp., 48 figures, 2 tables

Issued September 24, 2015

## CONTENTS

|   |    |
|---|----|
| Abstract . . . . .  | 3  |
| Introduction . . . . .  | 3  |
| List of Abbreviations . . . . .                                 | 4  |
| Materials and Methods. . . . .                                  | 4  |
| Taxon Sampling . . . . .  | 4  |
| Histology . . . . .   | 4  |
| Transmission Electron Microscopy . . . . .                      | 4  |
| Surface Reconstruction . . . . .                                | 4  |
| Phylogenetic Reconstruction . . . . .                           | 5  |
| Results . . . . .   | 6  |
| Primary Male Reproductive System . . . . .                      | 6  |
| Sperm Transfer Forms, Spermatozoa, and Spermiogenesis . . . . . | 6  |
| Discussion . . . . .  | 51 |
| Evolutionary and Functional Implications. . . . .               | 51 |
| Phylogenetic Implications . . . . .                             | 63 |
| Conclusions . . . . .   | 65 |
| Acknowledgments . . . . .                                       | 65 |
| References . . . . .  | 66 |
| Appendix 1: Study Species . . . . .                             | 70 |
| Appendix 2: Character Matrix. . . . .                           | 72 |

## ABSTRACT

Goblin spiders (Oonopidae Simon, 1890) are distributed worldwide and among the most species-rich spider taxa. However, goblin spiders are understudied in many aspects and their phylogenetic relationships are not well resolved. As previously shown for numerous other spider groups the male and female reproductive system bears many characters of phylogenetic relevance. Moreover, the diversity of sperm structures within spiders is astonishingly diverse and often taxon specific. In the present study, we analyzed the primary male reproductive system and spermatozoa of goblin spiders for the first time. We investigated 18 species of 13 genera representing the subfamilies Orchestinae and Oonopinae by means of light and transmission electron microscopy. We scored 44 characters from the gross morphology of the reproductive system as well as spermatozoa including four new characters for the male spider reproductive system. All investigated species transfer sperm as synspermia, a method corroborating with the recently proposed “Synspermiata” clade unifying all ecribellate Haplogynae. Furthermore, goblin spiders show by far the highest diversity of sperm structures in spiders. In total, we recovered 30 unambiguous synapomorphies for different oonopid taxa. In a comparison with all other spider taxa studied to date, we identified the longest sperm (*Neoxyphinus termitophilus*) and longest sperm conjugates (*Orchestina*). Moreover and most remarkable is the presence of aflagellate sperm in *Opopaea apicalis*, which is the first report of the loss of a sperm flagellum in tetrapulmonate arachnids. These findings are of high interest not only because of their phylogenetic implications, but also with regard to their contribution to our understanding of postcopulatory sexual selection in spiders.

## INTRODUCTION

Goblin spiders (Oonopidae) are tiny animals of less than 3 mm in length, and are either soft or hard bodied (Platnick et al., 2012b). Usually oonopids bear six eyes, with the anterior median eyes absent (Forster and Platnick, 1985). Even though goblin spiders are among the most species-rich spider families and are distributed worldwide, occurring in a variety of habitats (Fannes et al., 2008), knowledge about behavior, ecology, and phylogeny is very scarce. However, our understanding of the taxonomy and systematics of this spider family has remarkably increased within the past five years, as reflected in numerous contributions (e.g., Edward and Harvey, 2009; Platnick and Dupérré, 2009a, 2009b, 2010a; Baehr et al., 2012; Baehr and Harvey, 2013; Grismado and Ramírez, 2013; Platnick et al., 2013, 2014). The family currently contains 1545 extant species in 102 genera (World Spider Catalog, 2015), but also has an extensive fossil record compared to other spider groups (e.g., Penney, 2000; Saube et al., 2012; summarized in Dunlop et al., 2015).

The monophyly of goblin spiders was debated until recently, when synapomorphies from the primary male reproductive system and tarsal organ provided substantial evidence for the monophyly of this diverse

group (Burger and Michalik, 2010; Platnick et al., 2012b).

A recent study using molecular markers provided further support for the monophyly of goblin spiders and analyzed the intrafamilial relationships for the first time (de Busschere et al., 2014). In general, goblin spiders can be divided into three subfamilies: (1) Orchestinae Chamberlin and Ivie, (2) Sulsulinae Platnick, and (3) Oonopinae Simon, with (1) and (2) branching off basally according to one suggestion of Platnick et al. (2012b). The spermophor lost its cuticular lining, as especially characteristic in Oonopinae (Platnick et al., 2012a), and Grismado et al. (2014) identified an exposed male sperm pore as synapomorphy of higher gamasomorphines. Nevertheless, the internal phylogeny of goblin spiders is still poorly resolved and needs to be addressed in future studies.

The primary male reproductive system and spermatozoa in general are highly diverse (Platnick et al., 2009) and have been shown to be phylogenetically informative for a variety of animal taxa (e.g., Jamieson et al., 1999; Giribet et al., 2002; Marotta et al., 2008). For spiders, most studies addressed the phylogenetic implications of the morphology of sperm traits (e.g., Alberti and Weinmann, 1985; Alberti, 1990; Michalik et al., 2004a;

Michalik and Alberti, 2005; Michalik and Hormiga, 2010), and only recently Michalik and Ramírez (2014) conceptualized characters of the primary male reproductive system and spermatozoa for the first time, recovering several new synapomorphies for a variety of spider taxa.

In the present study we investigated the primary male genital system and spermatozoa of goblin spiders. We will not only address hypotheses of the evolution of this organ system, but will also conceptualize characters and evaluate the phylogenetic value of those for oonopid phylogeny. Moreover, we will discuss the evolution of sperm traits with regard to the highly diverse organization of the female genital system.

#### LIST OF ABBREVIATIONS

|      |                                      |
|------|--------------------------------------|
| AF   | acrosomal filament                   |
| AV   | acrosomal vacuole                    |
| Ax   | axoneme                              |
| Chr  | condensed chromatin                  |
| Cy   | cytoplasm                            |
| Cys  | cyst of developing spermatids        |
| dC   | distal centriole                     |
| DD   | deferent duct                        |
| En   | endosymbiont                         |
| FT   | flagellar tunnel                     |
| GD   | Golgi derivatives                    |
| Gly  | glycogen                             |
| IF   | implantation fossa                   |
| LuD  | lumen of deferent duct               |
| LuE  | lumen ejaculatory duct               |
| LuT  | lumen of testis                      |
| Mi   | mitochondrion                        |
| MM   | manchette of microtubules            |
| N    | nucleus                              |
| NC   | nuclear canal                        |
| pC   | proximal centriole                   |
| prcN | precentriolar part of nucleus        |
| peN  | postcentriolar elongation of nucleus |
| Sec  | secretions                           |
| Spt  | spermatid                            |
| SSh  | secretion sheath                     |
| STF  | sperm transfer form                  |
| Syn  | synspermium                          |
| SynA | aggregation of synspermia            |
| VA   | vesicular area                       |

#### MATERIALS AND METHODS

**TAXON SAMPLING:** The present study comprises 18 species of 13 genera. Species identifications and collection sites (localities) are listed in the appendix in alphabetical order.

Vouchers are deposited in (1) the Zoological Museum of the University of Greifswald (ZIMG), Germany, (2) the Museo Argentino de Ciencias Naturales of Buenos Aires (MACN)–CONICET, Argentina, or (3) the American Museum of Natural History (AMNH), New York.

**HISTOLOGY:** Primary male reproductive systems were dissected in either the field or in the lab in 0.1 M phosphate buffer to which 1.8% sucrose was added (PB). Isolated reproductive systems were then fixed in 2.5% glutardialdehyde in PB and further processed in the lab at the University of Greifswald. Documentation of the gross morphology was performed by using a Zeiss Discovery V20 stereomicroscope with a Zeiss MCr camera. The tissue was postfixed in buffered 2% OsO<sub>4</sub>. After a wash in PB, it was dehydrated in graded ethanols and embedded in Spurr's resin (Spurr, 1969). Serial semithin sections (700 nm) were obtained using a Diatome Ultra 45° diamond knife on a Leica ultramicrotome UCT and finally stained according to procedures outlined by Richardson et al. (1960).

**TRANSMISSION ELECTRON MICROSCOPY:** Ultrathin sections (70 nm), as well as serial ultrathin sections (60 nm), were cut with a Diatome diamond knife on a Leica ultramicrotome UCT and either applied to copper mesh grids, or slot grids, covered with a thin layer of desiccated pioloform® solution (1% pioloform® in 100% chloroform). Postprocessing included staining with uranyl acetate and lead citrate according to Reynolds (1963). Finally, sections were examined using a JEOL JEM 1011 electron microscope at 80 kV and images were obtained with an Olympus Mega View III digital camera using the iTEM software.

**SURFACE RECONSTRUCTION:** For the surface reconstruction of depicted sperm transfer forms we used series of ultrathin sections, derived from the distal deferent ducts, near the genital opening. Serial sections comprising

entire synsperma of (1) *Cinetomorpha* sp. (Iguazú) (image stack = 234 sections), (2) *Escaphiella ramirezi* Platnick and Dupérré, 2009b (image stack = 1175 sections), (3) *Neotrops pombero* Grismado and Ramírez, 2013 (image stack = 162 sections), (4) *Neoxyphinus termitophilus* (Bristowe, 1938) (image stack = 250 sections), (5) *Oonops* sp. (Ibiza) (image stack = 67 sections) and (6) *Paradysderina yanayacu* Platnick and Dupérré, 2011 (image stack = 102 sections) were aligned elastically using the Fiji plug-in TrakEM2 (according to Saalfeld et al., 2012). Additionally, serial semithin sections were used to reconstruct a part of a convoluted deferent duct of *Orchestina* sp. 1 (Chile) (image stack = 77 sections) and aligned as described above. For the successive segmentation of sperm conjugates Amira 5.4.5 and Amira 5.6.0 (FEI, Visualization Science Group) were used. In each section, contours of the main cell components were delineated manually. The obtained labels were then interpolated to keep the refinement of structures and a surface was generated. Further processing was performed using the surface editor for refining the surface as a whole, as well as the smooth surface function.

**PHYLOGENETIC RECONSTRUCTION:** The present data matrix includes 19 terminals scored for 44 characters, 40 of which are conceptualized in the recent study of Michalik and Ramírez (2014). Modifications and additional characters are listed below. In addition to data obtained in the present study, sperm characters of *Oonops domesticus* Dalmas, 1916 were extracted from Alberti and Weinmann (1985) and Michalik and Ramírez (2014). The evolution of the characters was reconstructed under parsimony using the software package Mesquite 2.75 (build 566) (Maddison and Maddison, 2011) and WinClada (Nixon, 2002).

Redefinition of characters from Michalik and Ramírez (2014) (abbreviated below as MiRa), keeping original numbering:

**20. Microfilaments inside implantation fossa during spermiogenesis** (MiRa: microtubules in the implantation fossa during spermiogenesis): 0. Absent. 1. Present.

**21. Shape of postcentriolar elongation of nucleus:** 0. Round or oval. 1. Flattened. 2.

With a distinct projection. 3 (*new state*). Flag shaped; this state corresponds to postcentriolar elongations that resemble a very short, tiny band as present in e.g., *Escaphiella ramirezi* (fig. 7E).

**22. Postcentriolar elongation of nucleus** (MiRa: length of peN): 0.  $< \frac{1}{2}$  of prcN. 1. Similar to prcN. 2.  $> 2$  of prcN. 3.  $> 5$  of prcN. 4 (*new state*).  $< 1/5$  of prcN. 5. (*new state*) Absent. Character state 4 is present in, e.g., *Escaphiella ramirezi* (figs. 6, 7) and *Stenoconops peckorum* Platnick and Dupérré, 2010 (fig. 39); a postcentriolar elongation is not developed (state 5) in, e.g., *Orchestina* sp. 1 (Chile) (fig. 27).

**24. Appearance of condensed chromatin of prcN** (MiRa: appearance of surface of prcN): 0. Smooth (mainly homogeneously condensed chromatin). 1. Helical band of condensed chromatin. 2. Irregularly condensed. 3 (*new state*). Threadlike. The new character state 3 is present in *Opopaea apicalis* (fig. 25).

**36. State of coiling:** 0. Incomplete. 1. Complete. 2 (*new state*). Not coiled. The new character state 2 refers to completely uncoiled, thus stretched sperm of *Orchestina* sp. 1 (Chile) (fig. 26) and *Orchestina* sp. 2 (Argentina), where neither sperm cell component is bent or coiled.

**39. Formation of sheath:** 0. Deferent ducts. 1. Testis. 2 (*new state*). Ejaculatory duct. This character refers to the production site of the sheath that surrounds the sperm transfer forms. The new character state 2 refers to *Neoxyphinus termitophilus* (fig. 19), where a sheath is not detectable before the sperm transfer forms are located in the ejaculatory duct.

#### *New characters*

**41. Shape of prcN:** 0. Tubelike, as in, e.g., *Oonops* sp. (fig. 22). 1. Helically contorted, as in, e.g., *Cinetomorpha* sp. (Iguazú) (fig. 3). 2. Irregularly shaped as in, e.g., *Neotrops pombero* (fig. 13). 3. Distinct longitudinal ridges (e.g., *Chileotaxus sans* Platnick, 1990; Michalik and Ramírez, 2014: fig. 6G).

**42. Length of AV:** 0.  $< 0.5$  of prcN (e.g., *Neoxyphinus termitophilus*, fig. 18). 1.  $0.5$  of prcN (e.g., *Hickmanolobus mollipes* (Hickman, 1932), Lipke et al., 2014: fig. 9F). 2.  $> 0.5$  of prcN (e.g., *Oonops* sp. (Ibiza); fig. 22).

**43. Golgi derivatives (after coiling process):** 0. Absent. 1. Present (fig. 2A, C). Golgi derivatives are provided with a double membrane and contain, e.g., secretions or mitochondria (compare, e.g., figs. 2C and 6D in Lipke and Michalik, 2012).

**44. Length of axoneme in relation to prcN:** 0. Ax >prcN. 1. Ax <prcN. The length of the axoneme in relation to the nucleus is either precisely measured based on surface reconstructions, or estimated based on cross sections of the axoneme and nucleus visible in 2D TEM images.

## RESULTS

**PRIMARY MALE REPRODUCTIVE SYSTEM:** Descriptions given here refer to all investigated specimens, if not especially mentioned. The primary male genital system is composed of an unpaired testis (figs. 1A–C, 2) and two deferent ducts that emanate to form the unpaired ejaculatory duct (figs. 1D–F, 2). The testis is mainly spherical, e.g., in *Orchestina* sp. 1 (Chile) (figs. 1A, 2C), or slightly oval shaped, e.g., in *Neoxyphinus termitophilus* and *Paradysderina fusciscuta* Platnick and Dupérré, 2011 (figs. 1, 2). However, in contrast to all remaining investigated oonopids, the testis of *Oonops* sp. (Ibiza) is indented (figs. 1C, 2D). Nevertheless, due to the high compactness it has a “completely fused” appearance. Two deferent ducts are exceptionally long and convoluted in both *Orchestina* species (figs. 1D, 2C). The deferent ducts fuse near the genital opening, forming a slender ejaculatory duct (fig. 2).

**SPERM TRANSFER FORMS, SPERMATOOZOA, AND SPERMIOGENESIS:** Descriptions of sperm transfer forms, characteristics of spermatozoa, and spermiogenesis, listed below, are ordered alphabetically. Dimensions of individual sperm-cell components, if not especially mentioned, refer to proportions in relation to the nucleus (precentriolar part of nucleus + post-centriolar elongation of nucleus).

### *Cinetomorpha* sp. (Iguazú)

**SPERM TRANSFER FORM** (figs. 3, 4): Large, cone-shaped synspermia (~25 µm) consisting of four fused spermatozoa (fig. 3);

irregular membranes located in the periphery (fig. 4A–C). Cytoplasm in sperm conjugate heterogeneous; some dense granules and lamellae occur (fig. 4A–C, G). Nuclei incompletely coiled and helically contorted, chromatin irregularly condensed (fig. 4D, E). Axonemes hardly visible (fig. 4F) due a low electron density compared to the nonhomogeneous cytoplasm. A thin (~80 nm) secretion sheath, developed in the deferent ducts, surrounds each sperm conjugate (fig. 4G).

**SPERMATOOZOA** (fig. 4): **Acrosomal complex:** AV cylindrical and small (~4.9 µm); narrow subacrosomal space for the most part, slightly widening posteriorly (fig. 4E, 4E inset). AF thin, originates from narrow subacrosomal space in anterior AV and extends into a nuclear canal, but clearly ends before axonemal base. **Nucleus:** prcN elongated (~66.8 µm) (fig. 4A–C), helically contorted, and with a conspicuous, irregular chromatin-condensation pattern. The small implantation fossa contains only centrioles (fig. 4G); peN absent. NC empty for the most part in mid and late spermatids and no longer visible in mature sperm. **Axoneme:** 9+3 microtubular pattern.

**NOTES ON SPERMIOGENESIS** (fig. 5): Within the testis all stages of spermiogenesis are present. Germ cells of the same developmental stage in conjunction within cyst. The acrosomal vacuole of early spermatids irregularly electron dense, resulting in spotted appearance (fig. 5A). It is separated from the anterior pole of the nucleus by a small electron-dense plate. The two centrioles migrate toward posterior pole, where they arrange in a tandem position (fig. 5B). Chromatin starts to condense only in a small portion near the nuclear canal that contains the acrosomal filament (fig. 5C, D) while the so-called manchette of microtubules (i.e., a ring or ruffle of microtubules) surrounds the entire nuclear material (fig. 5C, D). Further development includes elongation of the nucleus. The chromatin condenses irregularly and appears “folded” (fig. 5E) with a typical “looped” appearance in cross section (fig. 5E, H). Although the axoneme has the typical 9+3 microtubular pattern (fig. 5F), the central tubuli are very short, thus the main part of the axoneme shows 9+0 microtubular pattern (fig. 5G). While spermatids start to fuse at the end of

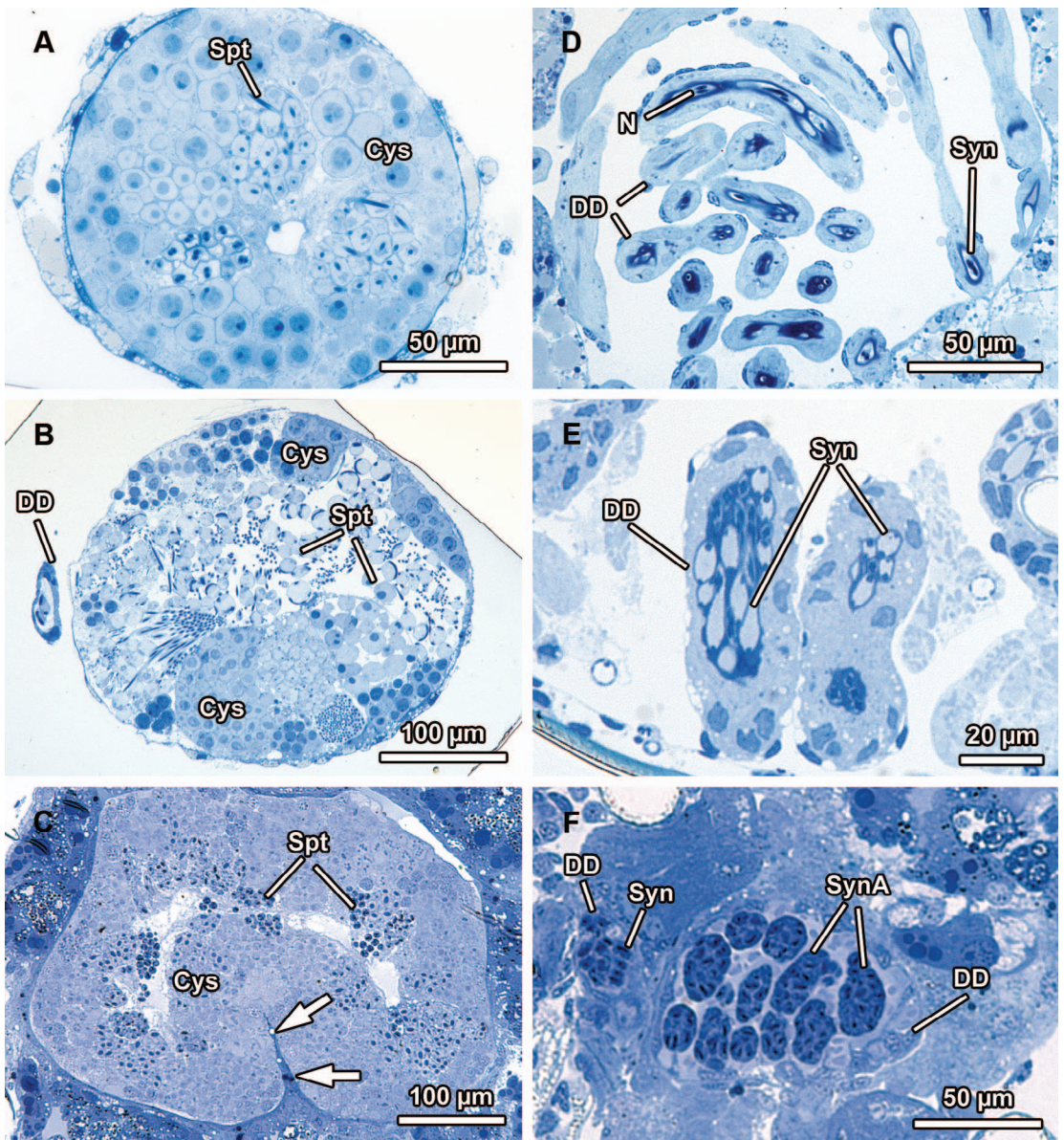


Fig. 1. Light-microscopy images of the testis and deferent ducts of selected oonopids. **A, B:** *Orchestina* sp. 1, **C, D:** *Escaphiella ramirezi* and **E, F:** *Oonops* sp.. Note the indentation of the testis of *Oonops* sp. (arrows) and the organization of synspermia that form distinct aggregates within the deferent ducts.

spermiogenesis, the manchette of microtubules disintegrates (fig. 5H).

*Escaphiella ramirezi* Platnick and Dupérré, 2009

**SPERM TRANSFER FORM** (figs. 6, 7): Very large, elongated synspermia (~70 μm) that

comprise four spermatozoa (fig. 7A, B). Overall shape of this sperm conjugate bone-like (fig. 6). A slender vesicular area surrounds all sperm-cell components (fig. 7B, D, E). The acrosomal vacuoles, which represent the anterior pole of sperm, are located in the middle of the sperm conjugate (fig. 6, arrow). Two sperm arranged opposed to each other

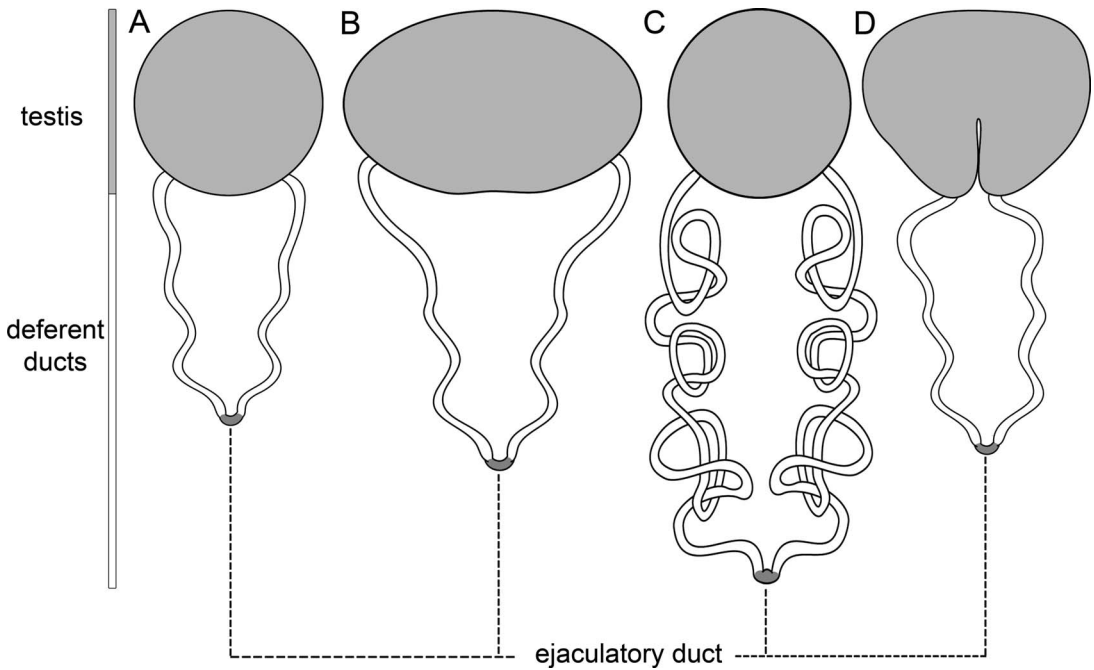


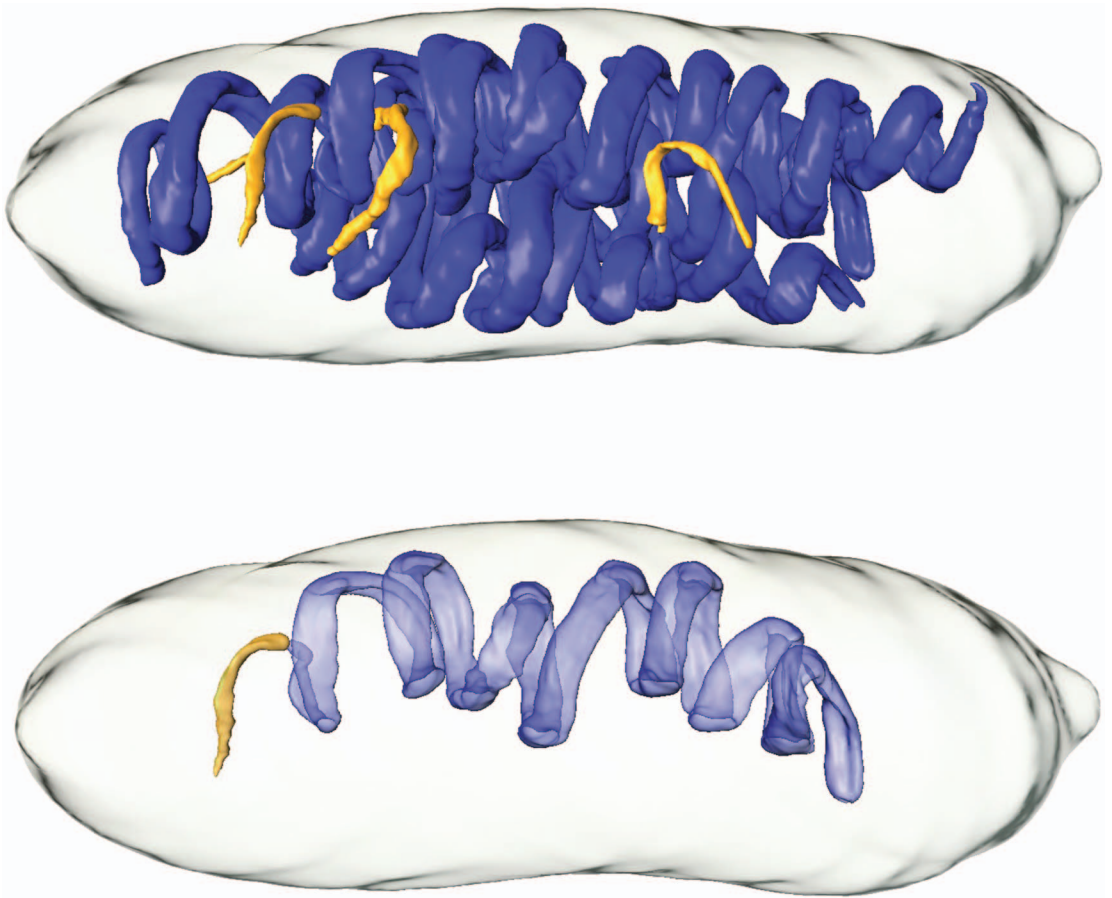
Fig. 2. Schematic drawings of the general organization of the primary male reproductive system in Oonopidae. **A:** The unpaired, completely fused testis is spherical in most investigated oonopids (*Cinetomorpha* sp. (Iguazú), *Escaphiella ramirezi*, *Gamasomorpha* cf. *vianai*, *Neotrops poguazu*, *Neotrops pombero*, *Neotrops waorani*, *Niarchos scutatus*, *Orchestina* sp. 1 (Chile)). **B:** In contrast, the testis of, e.g., *Neoxyphinius termitophilus*, *Paradysderina fusiscuta*, and *Paradysderina yanayacu* are oval. **C:** The deferent ducts of all investigated species are rather short, except those of *Orchestina* sp. 1 (Chile) and *Orchestina* sp. 2 (Argentina), which are extremely elongated and convoluted. **D:** In contrast to all remaining oonopids, the unpaired testis of *Oonops* sp. (Ibiza) is indented.

(two sperm coil clockwise, the remaining two counter clockwise). Cytoplasm of the sperm conjugate electron lucent. Numerous, circular Golgi derivatives are present, mainly located in the periphery of the sperm conjugate (fig. 7A–C) and sometimes associated with the membrane of the syncytium (fig. 7C). Synspermia surrounded by a thin (~50 nm) secretion sheath (fig. 8B, C) that is produced in the deferent ducts.

**SPERMATOZOA** (fig. 7): **Acrosomal complex:** AV very short (~1.9  $\mu\text{m}$ ), cylindrical, narrow subacrosomal space (fig. 8D). AF originates from the subacrosomal space of the acrosomal vacuole and extends into the nuclear canal; ends in the region of the axonemal base (fig. 7E); extremely elongated (~125.2  $\mu\text{m}$ ) and for most part remarkably large, resembling the most prominent cell component (fig. 7B). **Nucleus:** prcN extremely elongated (~126  $\mu\text{m}$ ) (fig. 6). Most pro-

minent part of the prcN is the nuclear canal that contains the massive acrosomal filament (see above, figs. 6, 7B–E). Condensed chromatin is restricted to a small portion around the latter (fig. 7B–E). Implantation fossa extremely small, containing only the centrioles (fig. 7E). peN very short (~1.3  $\mu\text{m}$ ) and thin, flag shaped (figs. 6, 7E). **Axoneme:** short (~58.4  $\mu\text{m}$ ), 9+3 microtubular pattern (fig. 7B, D); centrioles arranged rectangularly, proximal centriole very short.

**NOTES ON SPERMIOGENESIS** (fig. 8): Cysts of developing sperm (mainly early and mid-spermatids) present within the testis. Early spermatids characterized by a small vesicle-like AV that is attached to the cell membrane (fig. 8A). Originating from the subacrosomal space, AF comprises only a few filaments in the AV as indicated by cross sections (fig. 8A). In contrast, it expands to a massive rod composed of numerous filaments (fig. 8B–D)



■ precentriolar part of nucleus    ■ acrosomal vacuole    ■ membrane of syncytium

Fig. 3. Surface reconstruction of sperm transfer form of *Cinetomorpha* sp. (Iguazú), illustrating the shape and arrangement of all four fused sperm, as well as the arrangement of an individual sperm. Note the helically contorted nucleus. The axoneme is not shown in this surface reconstruction.

within NC. Nucleus is surrounded by a manchette of microtubules and chromatin appears fibrillar in early and midspematids (fig. 8B, C). While nucleus elongates, condensed chromatin constricted to a small portion (fig. 8D). Axoneme originates from the distal centriole (fig. 8E). Occasionally, small electron-dense spots are present in the periphery, likely inside NC, associated with AF. At the end of spermiogenesis, several spermatids start to fuse, resulting in voluminous sperm conjugates that remain connected to each other via cellular bridges (fig. 8F). A loose, electron-dense network of fused vesicles, representing an early stage vesicular

area, surrounds all main sperm cell components (fig. 8F inset).

*Gamasomorpha* cf. *vianai* Birabén, 1954

SPERM TRANSFER FORM (fig. 9): Very large (>30  $\mu\text{m}$ ), cone-shaped synsperma that presumably comprise four sperm, which are loosely arranged (fig. 9A, B). In the periphery of the sperm conjugate irregular tubelike membranes, originating from membrane invaginations, are visible (fig. 9C). The cytoplasm is heterogeneous, numerous electron-dense droplets and lamellae are visible (fig. 9B, C). The nuclei are elongated, cross sections reveal helical contortion, indicated by curls of the

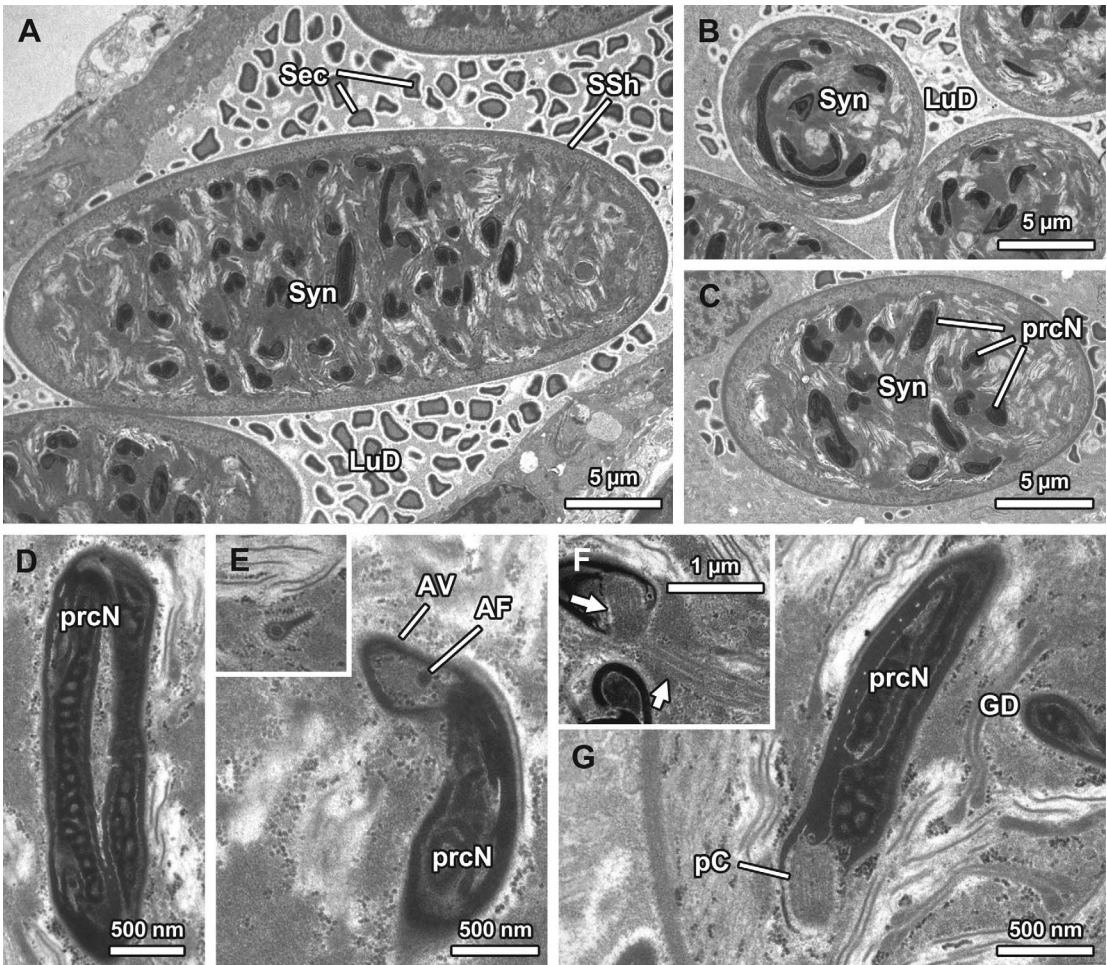


Fig. 4. Characteristics of synspermia of *Cinetomorpha* sp. (Iguazú). **A**: One entire sperm conjugate is rather large (approx. 25 μm). **B**, **C**: The nuclei of the four fused sperm are helically contorted, indicated by curls of the latter which are visible in cross sections. **D**: The chromatin condenses irregularly, resulting in a very specific chromatin-condensation pattern. **E**: The AV is conical with a widened subacrosomal space near the anterior pole of the nucleus; it appears spoonlike in cross sections (inset). **F**: The IF is very small, comprising only the two centrioles. **G**: The Ax, although hardly visible originates from the distal centriole. Note, a peN is not developed.

nuclei (fig. 9B). Numerous mitochondria are present. A thin, homogeneous secretion sheath (~80 nm) surrounds the sperm conjugates (fig. 9A, C). The chromatin of mature spermatozoa is irregularly condensed (fig. 9D).

**SPERMATOZOA** (figs. 9): **Acrosomal complex**: AV cylindrical; narrow subacrosomal space, (fig. 9C). AF originates from the subacrosomal space, extends into NC. **Nucleus**: prcN elongated (fig. 9A, B), with conspicuous chromatin-condensation pattern

(fig. 9A, D). Implantation fossa very small and contains only centrioles. peN not identifiable. NC located in the periphery, empty for the most part. **Axoneme**: short, indicated by only few cross sections that are visible in the sperm conjugate (fig. 9B); 9+3 axonemal pattern (fig. 9B).

**NOTES ON SPERMIOGENESIS** (fig. 10): The small developing acrosomal vacuole with a narrow subacrosomal space (fig. 10A inset) separated from the nucleus by a distinct electron-dense plate (fig. 10A). At the

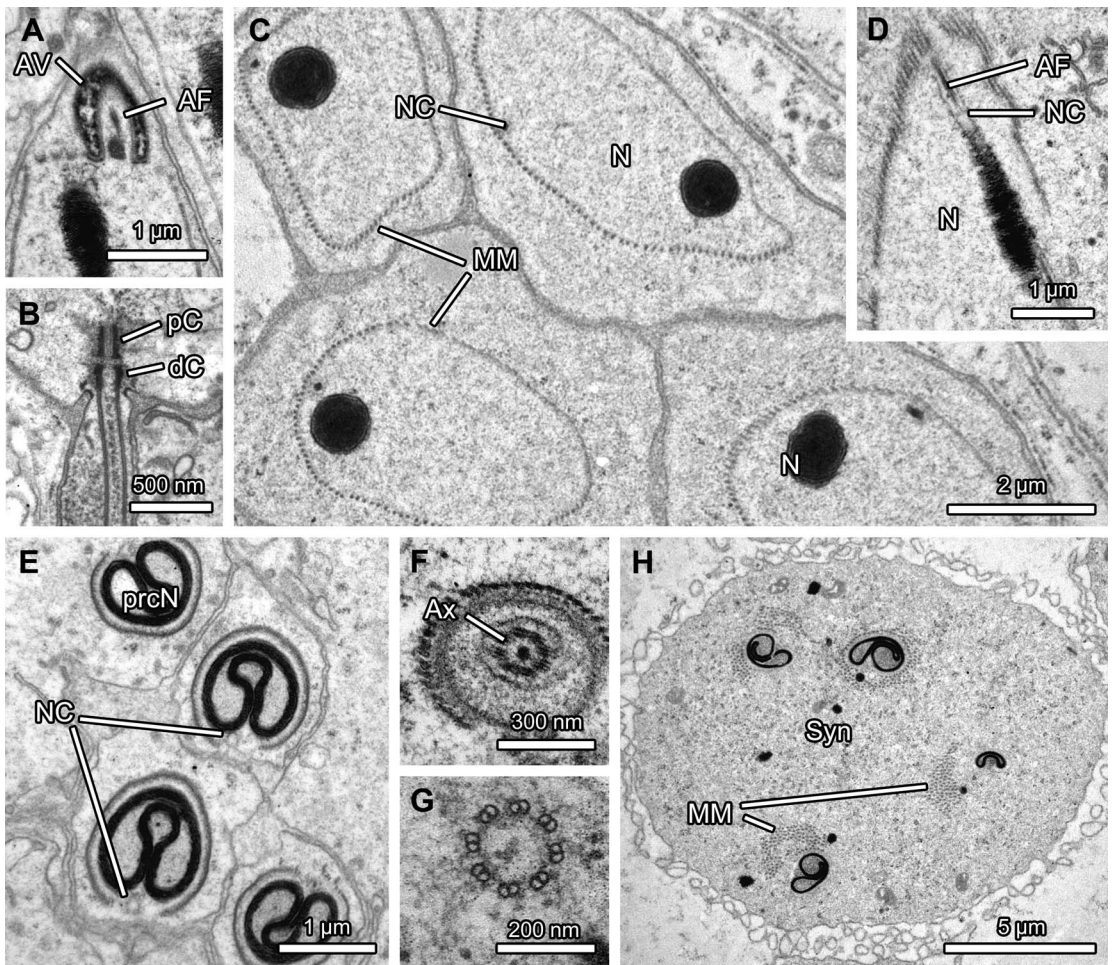


Fig. 5. Characteristics of spermiogenesis of *Cinetomorpha* sp. (Iguazú). **A:** Early spermatids are characterized by small AV that appears spotted. **B:** The two centrioles arrange in a tandem position and migrate toward the posterior pole of the nucleus initiating the formation of the implantation fossa. **C:** The chromatin condensation is restricted to a small portion of the nucleus that is often associated with the nuclear canal. **D:** The NC is located in the periphery of the developing nucleus and contains the AF. **E:** During further spermatid development, the nucleus enormously elongates and the peculiar chromatin-condensation pattern is formed. Note, the nuclear canal is empty for the most part in these spermatids. **F:** The Ax that originates from the distal centriole extends into the flagellar tunnel. **G:** Although the axoneme possesses the typical 9+3 microtubular pattern, the central tubules are very short and missing for the most part. **H:** While four spermatids fuse entirely, the manchette of microtubules disintegrates. Numerous constrictions of the membrane of the syncytium border the early sperm conjugate.

posterior pole of the nucleus both centrioles migrate toward the latter, initiating the formation of a small implantation fossa (fig. 10B). The nucleus elongates markedly while the chromatin condenses irregularly, resembling an electron-dense thread in mid-spermatids (fig. 10C). Mature spermatozoa

remain the irregularly condensed chromatin-condensation pattern (fig. 10D, E). At the end of spermiogenesis four spermatids fuse (fig. 10E) to form a very large sperm conjugate. The manchette of microtubules disintegrates during further sperm conjugate differentiation.

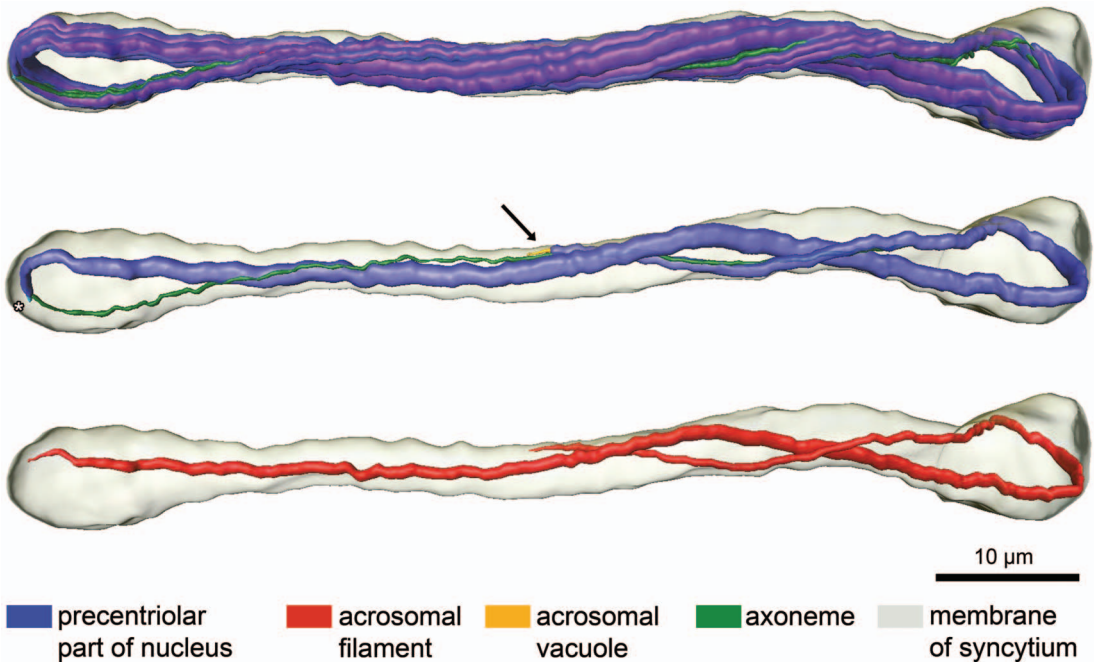


Fig. 6. Surface reconstruction of sperm transfer form of *Escaphiella ramirezi* illustrating the shape and arrangement of all four fused sperm cells, as well as the arrangement of an individual sperm and the acrosomal filament of an individual sperm. All AVs are located in the centre of the sperm conjugate (arrow), as indicated for one AV. Two sperm coil clockwise, while the remaining two coil counterclockwise. Note the extremely thick AF and the very thin, flag shaped peN (asterisk).

*Neotrops poguazu* Grismado and Ramirez, 2013

**SPERM TRANSFER FORM** (fig. 11): Oval-shaped synspermia (~10 µm), comprising four sperm (fig. 11A). In the periphery of the sperm conjugate, numerous membranes are visible (fig. 11B, arrow). Synspermia surrounded by a thin (~80 nm) secretion sheath (fig. 11B, C); cytoplasm electron dense within sperm conjugates of the ejaculatory duct (fig. 11D), some mitochondria present.

**SPERMATOOZA** (fig. 11): **Acrosomal complex:** AV conical with wide subacrosomal space (figs. 11A, C), proximally sunken into the anterior pole of prcN (fig. 11C). AF originates from subacrosomal space, extends into NC, but clearly ends before axonemal base. **Nucleus:** prcN deeply indented at its anterior pole (bowl shaped), irregularly shaped with irregularly condensed chromatin

(fig. 11A, B). peN short, flattened, (fig. 11D). NC peripheral (fig. 11A–C). **Axoneme:** proximal centriole longer than distal centriole, 9+3 microtubular pattern.

*Note on Spermiogenesis* (fig. 12): All stages of spermiogenesis present in the testis. Spermatids of the same developmental stage arranged in cysts. Early spermatids characterized by a large, oval nucleus surrounded by a manchette of microtubules and small AV (fig. 12A inset) that is separated from the nucleus by a distinct electron-dense border (fig. 12A). The AF originates from the subacrosomal space (12C). The chromatin begins condensing in the center of the nucleus and appears fibrillar (fig. 12A, B). The small implantation fossa is irregularly shaped in early spermatids (fig. 12B, B inset). There is always a small amount of electron-dense, granular material associated with the proximal centriole (fig. 12D). A collar of electron-dense,

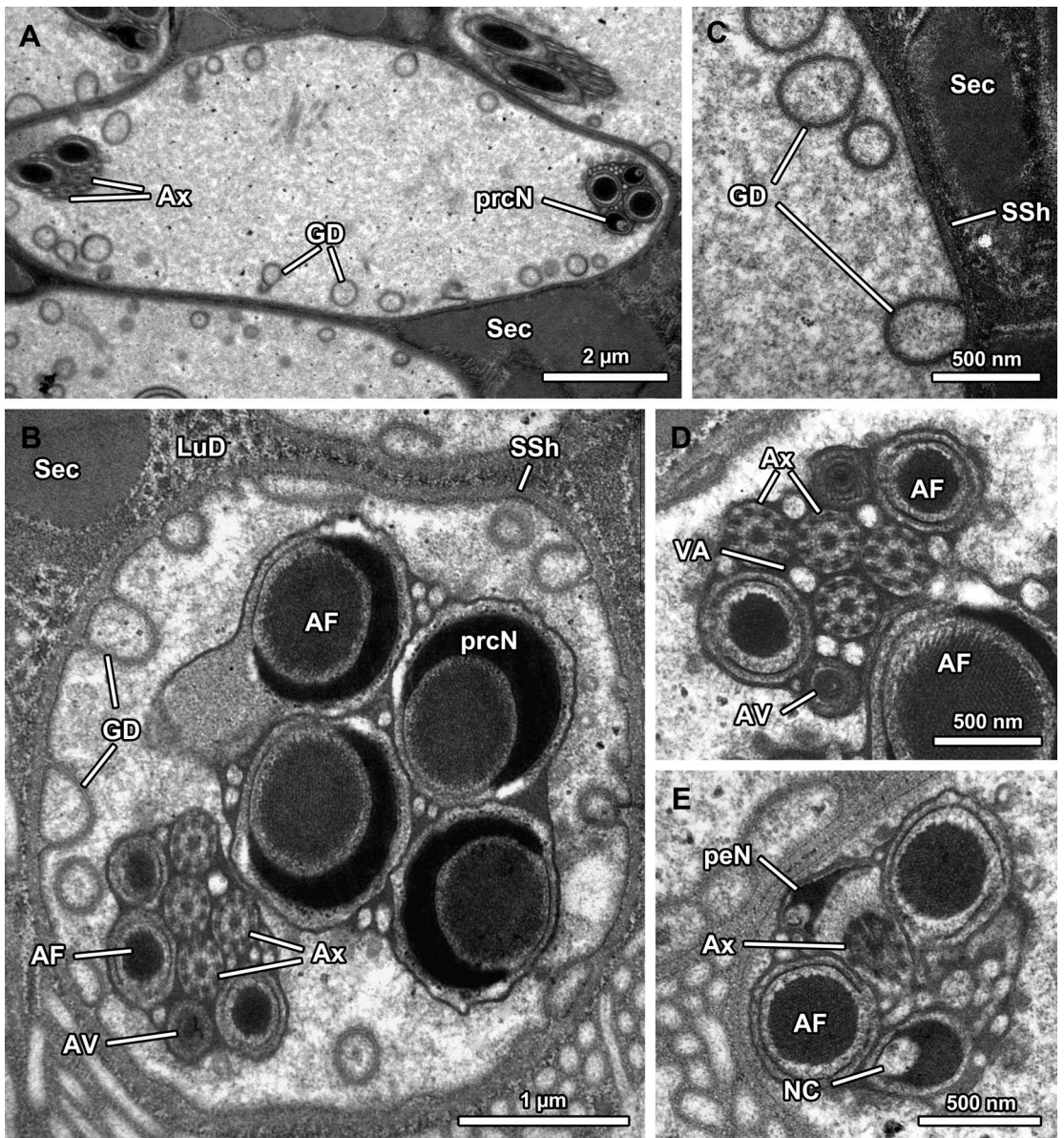


Fig. 7. Characteristics of synspermy of *Escaphiella ramirezi*. **A:** Due to the peculiar shape of the bonelike sperm conjugate cross sections are either oval shaped or spherical. **B:** A small VA surrounds the sperm cell components secondarily. **C:** Numerous Golgi derivatives, sometimes attached to the membrane of the syncytium are visible within the sperm conjugate; a thin secretion sheath surrounds the entire synspermium. **D:** The AVs have a narrow subacrosomal space from which the AF originates. **E:** The AF enlarges and extends into the NC but clearly ends before the axonemal base, the postcentriolar elongation is very short and flag shaped.

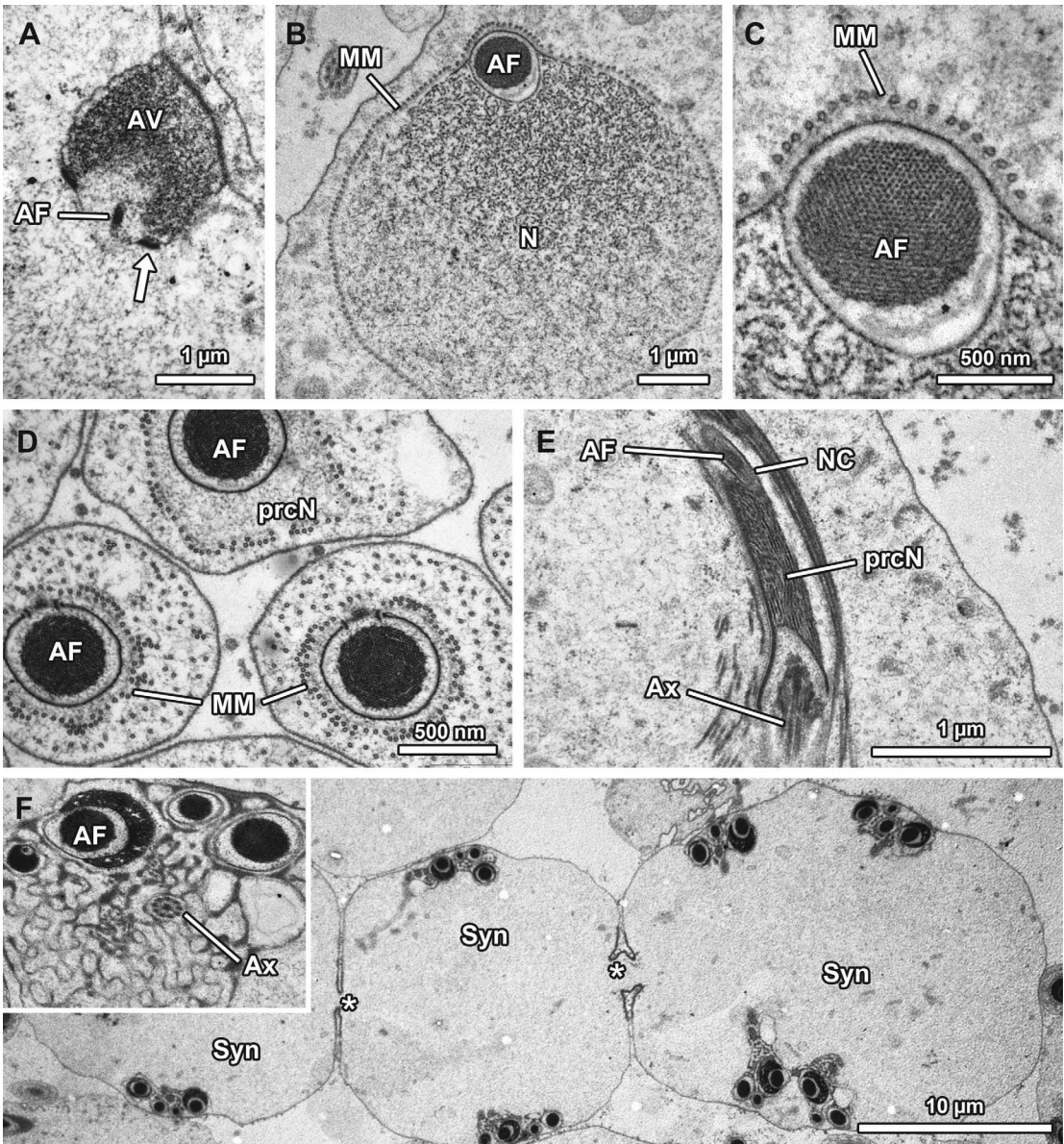


Fig. 8. Characteristics of spermiogenesis of *Escaphiella ramirezi*. **A:** The small AV of early spermatids is attached to the cell membrane and separated from the nucleus by distinct electron-dense plates (arrow). **B:** The AF is thin near its origin within the subacrosomal space but enormously expands while extending into the nucleus. **C:** Numerous filaments that build the AF are visible in cross sections. **D:** A manchette of microtubules surrounds the nucleus. The small implantation fossa contains only the centrioles. **E:** At the end of spermiogenesis the main cell components coil within the cell membrane and two spermatids fuse. **F:** These large, early sperm conjugates are still connected to each other via cellular bridges (asterisks); a loose, electron-dense network arranges around the sperm cell components, forming a small vesicular area (inset).

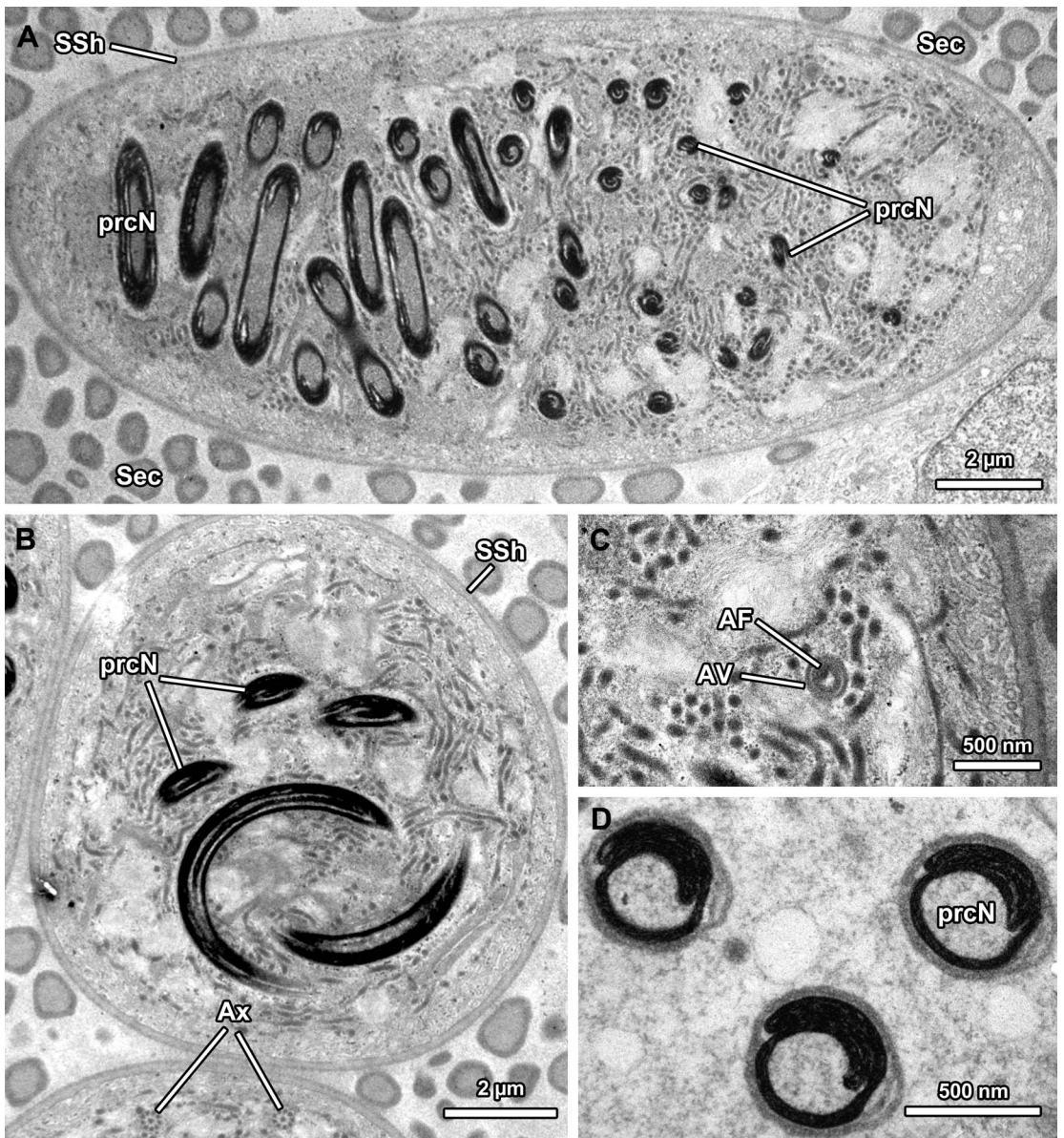


Fig. 9. Characteristics of synspermia of *Gamsomorpha cf. vianai*. **A:** Within the deferent ducts and the ejaculatory duct numerous very large sperm conjugates (>25 μm) are visible. **B:** The nuclei are helically contorted as indicated by curls of the latter that are visible in cross sections. **C:** A thin secretion sheath surrounds sperm conjugates. The periphery of the syncytium is built by numerous constrictions of its membrane. **D:** The most obvious sperm characteristic is the peculiar chromatin-condensation pattern.

platelike secretions surrounds the base of the Ax (fig. 12E). At the end of spermiogenesis late spermatids that remained connected via cellular bridges start to fuse, finally resulting in synspermia.

*Neotrops pombero* Grismado and Ramírez, 2013

SPERM TRANSFER FORM (figs. 13, 14):  
Oval-shaped synspermia (~10 μm), compris-

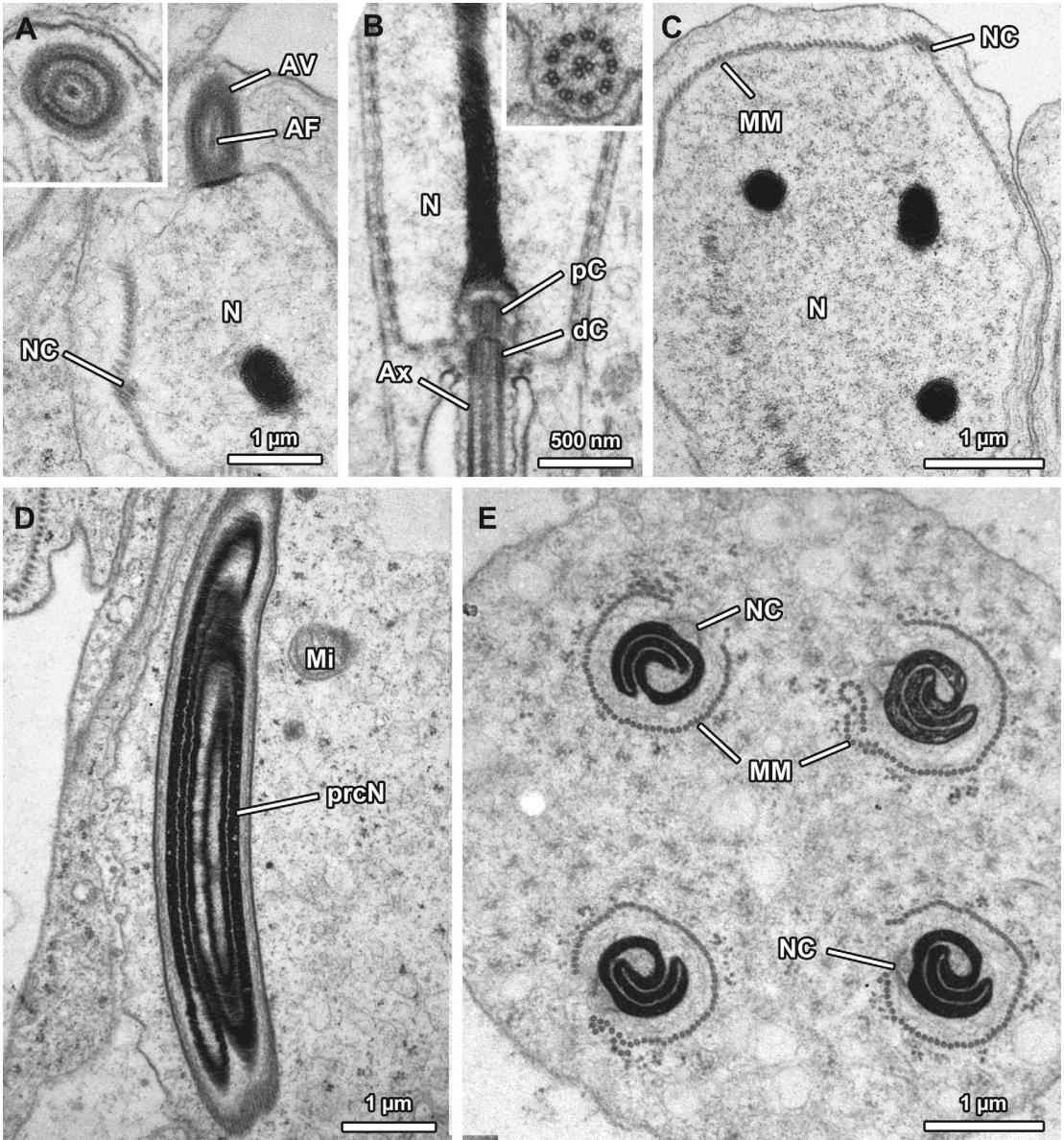


Fig. 10. Characteristics of spermiogenesis of *Gamasomorpha* cf. *vianai*. **A:** The small AV is separated from the nucleus by a distinct electron-dense border; the narrow subacrosomal space contains the AF (inset). **B:** The chromatin starts condensation selectively in small spots within the nucleus. The very small IF contains only the two centrioles, the Ax, which has a typical 9+3 microtubular pattern (inset), originates from the distal centriole and extends into a flagellar tunnel. **C:** A small NC that contains the AF is located in the periphery of the nucleus. The nucleus of all stages of spermiogenesis is surrounded by a single-layered manchette of microtubules. **D:** Late spermatids show the peculiar chromatin-condensation pattern, which resembles a furlled sleeve in longitudinal sections. **E:** At the end of spermiogenesis, four spermatids entirely fuse to form large sperm conjugates. The NC is empty for the most part; the manchette of microtubules disintegrates during further sperm conjugate development.

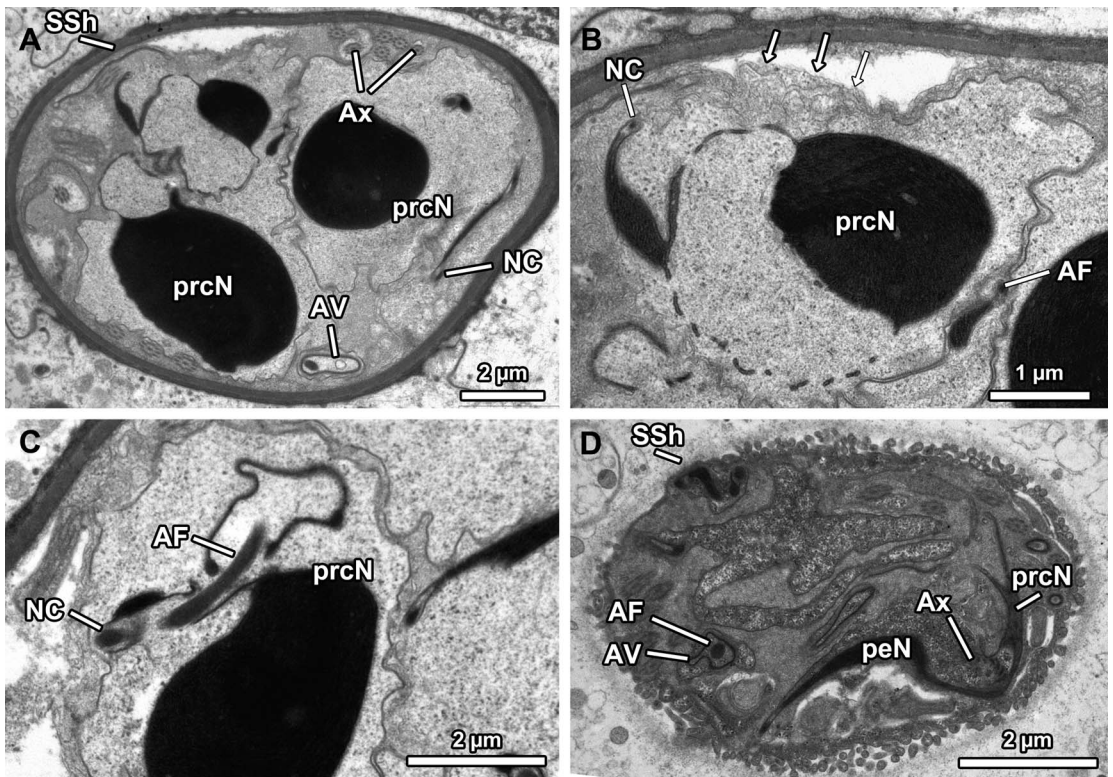


Fig. 11. Characteristics of synspermy and spermatozoa of *Neotrops pognazu*. **A:** Sperm conjugates are surrounded by a thin secretion sheath. **B:** The chromatin is irregularly condensed. **C:** The AF extends toward the nucleus and projects into the periphery of the nucleus, surrounded by the NC. **D:** Within the ejaculatory duct sperm conjugates further differentiate. This includes further condensation of cytoplasm while peripheral constrictions recess.

ing four spermatozoa that are densely packed (figs. 13, 14A, B). Small, irregular membrane stacks, as well as mitochondria, are present in the periphery (fig. 14C, D). Whereas the cytoplasm is electron lucent within sperm conjugates of the deferent duct (fig. 14C), it further condenses, finally appearing electron dense in sperm conjugates located in the ejaculatory duct (fig. 14E–F). Sperm are incompletely coiled (fig. 13). A thick (~250 nm), homogeneous secretion sheath surrounds the sperm transfer forms (fig. 14E).

**Spermatozoa** (figs. 13, 14): **Acrosomal complex:** AV conical, long (~9.8 μm); widened subacrosomal space (fig. 14A), sunken into the prcN (fig. 13). AF originates from the subacrosomal space, extends into the NC, ends clearly before axonemal base. **Nucleus:** prcN deeply indented at its anterior pole,

compact (~11.7 μm) but irregularly shaped (figs. 13, 14C), chromatin is irregularly condensed (fig. 14C, F). peN small (~5.4 μm), flattened (fig. 13). NC peripheral (fig. 14C, D). **Axoneme:** proximal centriole longer than distal centriole. 9+3 microtubular pattern (fig. 14D).

**NOTES ON SPERMIOGENESIS** (fig. 15): All stages of spermiogenesis are present in the testis. Spermatids of the same developmental stage are arranged in cysts. Early spermatids are characterized by a large AV that is accompanied by a collar of electron-dense secretions and secretion droplets (fig. 15A, A inset, B). Proximal portion of AV is deeply sunken into the anterior pole of the nucleus (figs. 15B, C). The AF originates from the subacrosomal space (fig. 15B). The nucleus is surrounded by a manchette of microtubules.

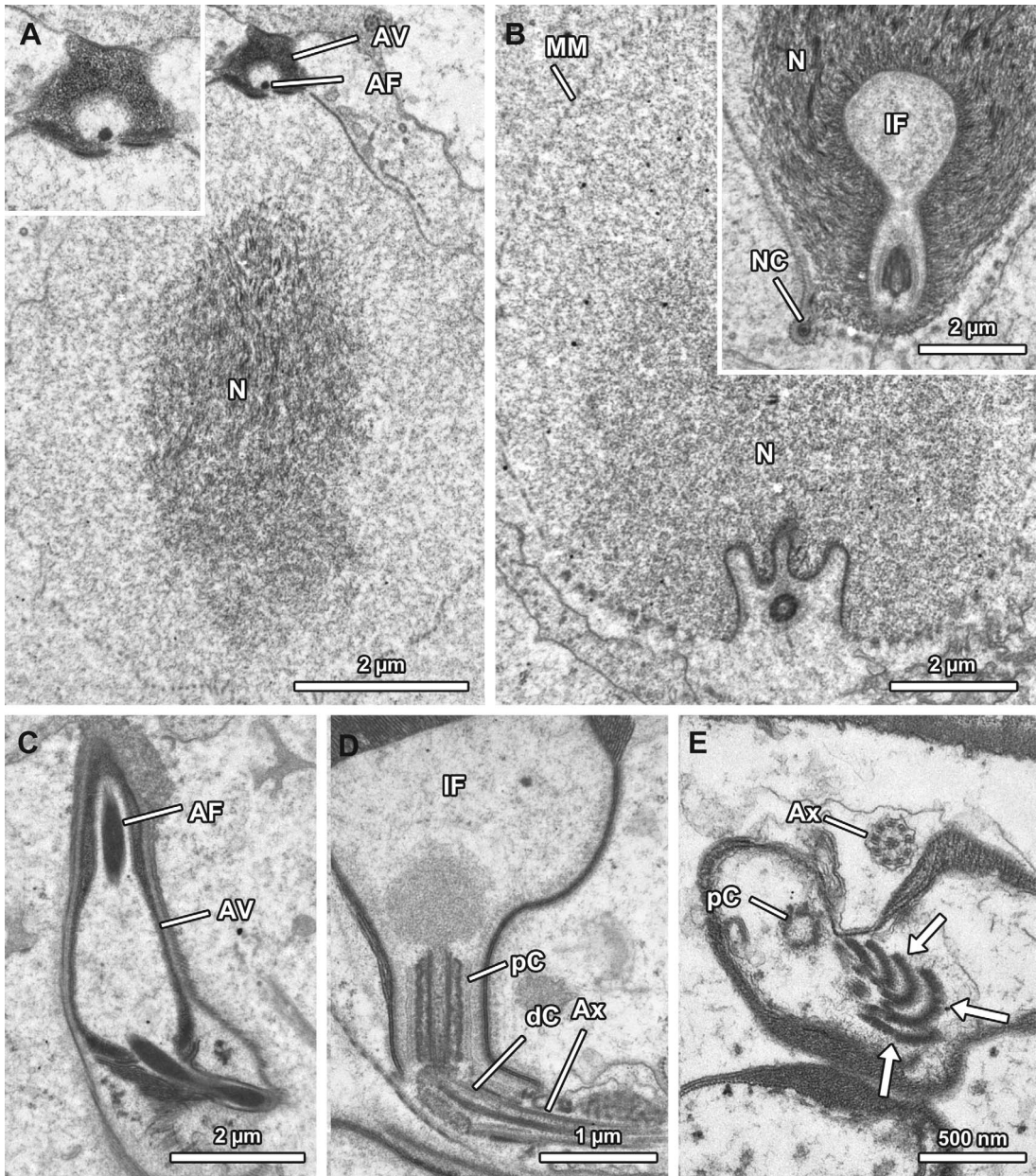


Fig. 12. Characteristics of spermiogenesis of *Neotrops poguazu*. **A:** The small AV is bordered from the nucleus by a distinct electron-dense plate (magnified in inset). **B:** The chromatin starts condensation irregularly and appears fibrillar in mid-spermatids (inset). At the posterior pole of the nucleus, an irregularly shaped IF is formed through migration of the two centrioles toward the posterior pole of the nucleus. **C:** During further development, the AV enlarges and sinks deeply into the anterior portion of the nucleus, while the subacrosomal space widens. **D:** A small amount of secretion is attached to the proximal centriole within the wide IF. Note the elongated proximal centriole, which is arranged rectangularly to the distal centriole. **E:** Distinct electron-dense lamellae are arranged around the base of the Ax (arrows).

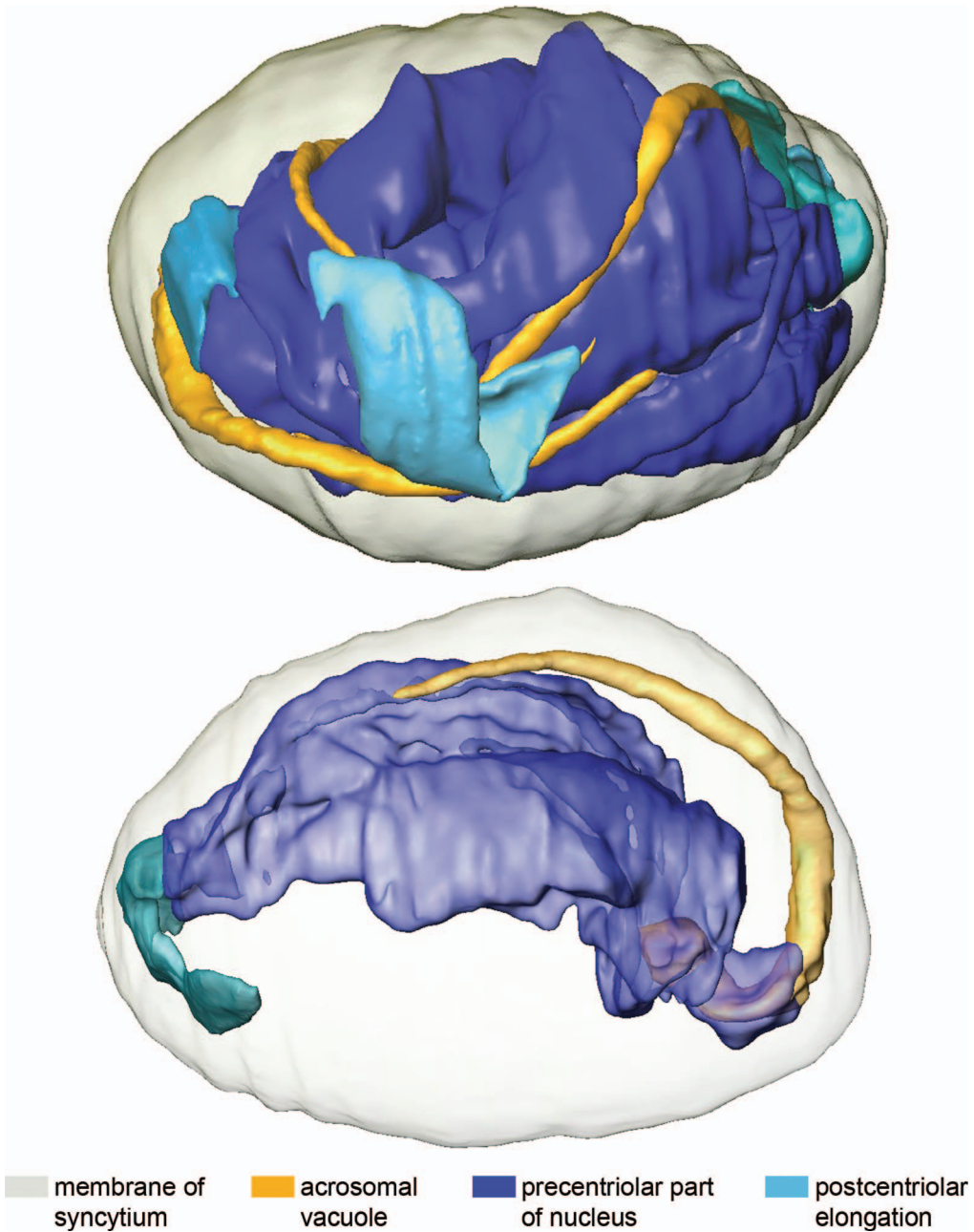


Fig. 13. Surface reconstruction of sperm transfer form of *Neotrops pombero* illustrating the shape and arrangement of all four fused sperm, as well as the arrangement of an individual sperm. Note the very long AV, which is nearly as long as the prcN. Axonemes are not shown in this reconstruction.

The chromatin appears fibrillar in mid spermatids, although it condenses irregularly (fig. 15B). Late spermatids retain this irregular condensation pattern (fig. 15C–E). The

small implantation fossa is composed of two parts, a spherical portion that contains a small amount of secretions (fig. 15D) and a narrow, tubelike portion where the cen-

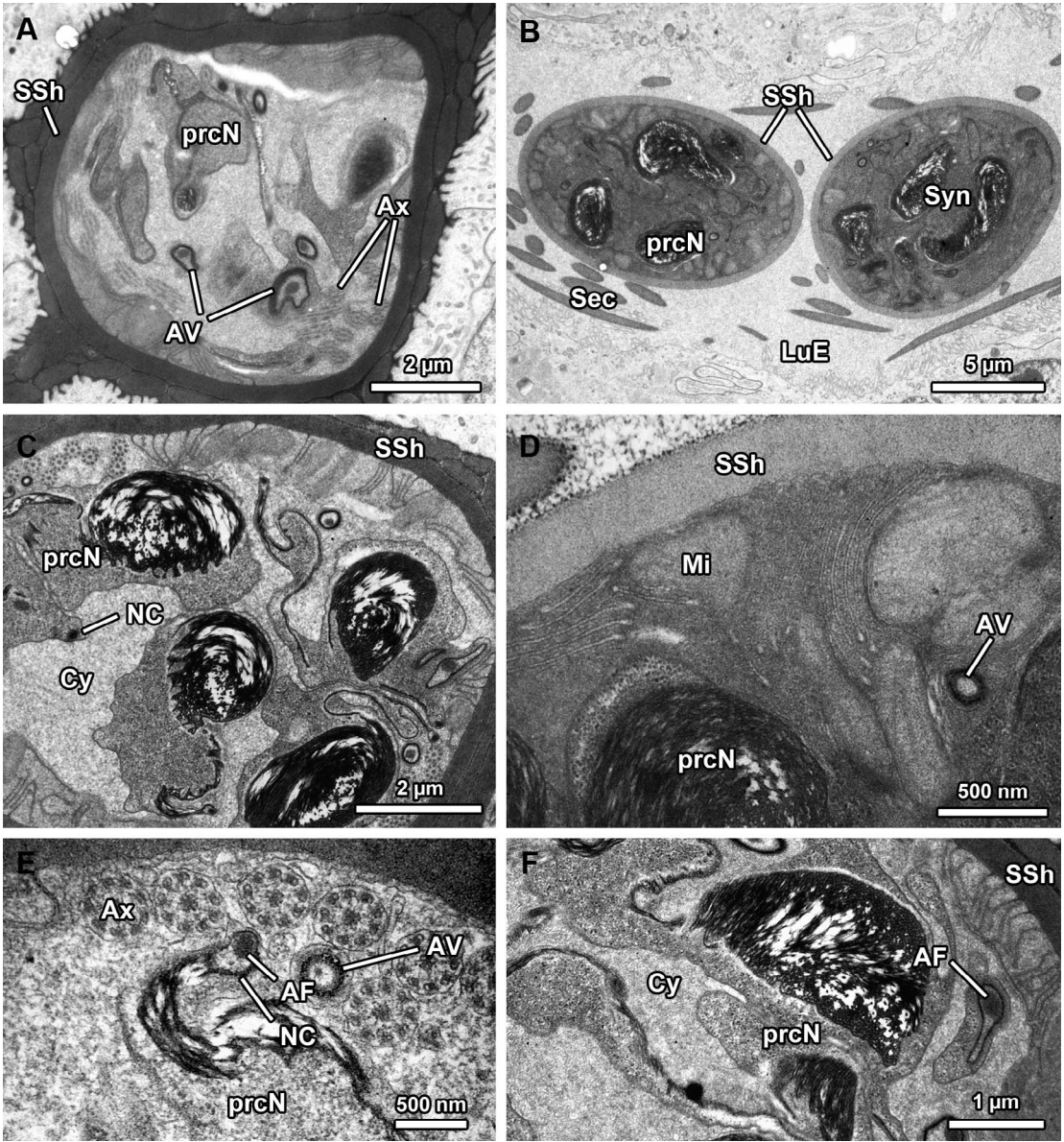


Fig. 14. Characteristics of synspermia and spermatozoa of *Neotrops pombero*. **A:** Within the proximal portion of the deferent duct, synspermia are irregularly formed and embedded in a dense matrix composed of longish, electron-dense secretions, a secretion sheath surrounds the sperm conjugates. **B:** In contrast, synspermia in the lumen of the ejaculatory duct are oval, the cytoplasm is further condensed and appears electron dense. **C:** The four fused sperm show a characteristic, irregular chromatin-condensation pattern. The condensed chromatin appears fibrillar and possesses numerous electron-lucent streaks. **D:** Numerous membrane stacks, as well as a few mitochondria are visible in the periphery of the sperm conjugate. **E:** The NC in the periphery of the nucleus is located on a distinct projection. **F:** The posterior portion of the AV is deeply sunken into the anterior pole of the nucleus and thus partly surrounded by the latter.

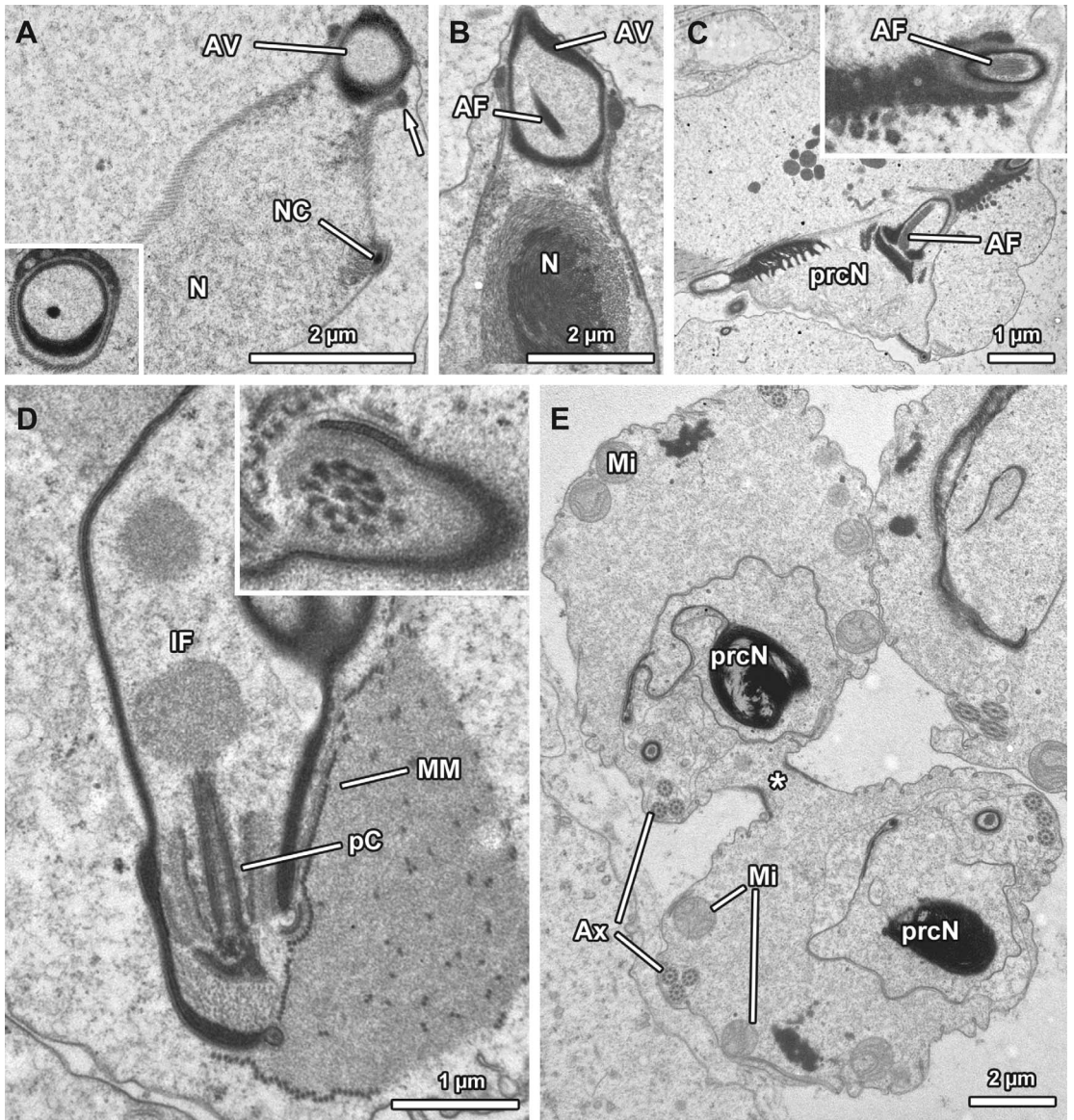


Fig. 15. Characteristics of spermiogenesis of *Neotrops pombero*. **A:** The posterior portion of AV is already sunken into the anterior pole of the nucleus in early spermatids; the AF is thin, the subacrosomal space is widened (inset). Note distinct electron-dense spots (arrow) that occur at the anterior pole of the nucleus. **B:** The chromatin appears fibrillar and starts condensation in the center of the nucleus. **C:** The elongating AV is accompanied by electron-dense secretions (magnified in inset). **D:** The proximal centriole is enlarged and nearly twice as long as the distal centriole; the base of the axoneme is surrounded by few electron-dense secretions (inset). **E:** At the end of spermiogenesis, the main sperm cell components coil within the cell membrane, while the spermatids are still connected with each other via cellular bridges (asterisk). Finally four spermatids fuse and form oval synspermia. Note mitochondria within the cytoplasm.

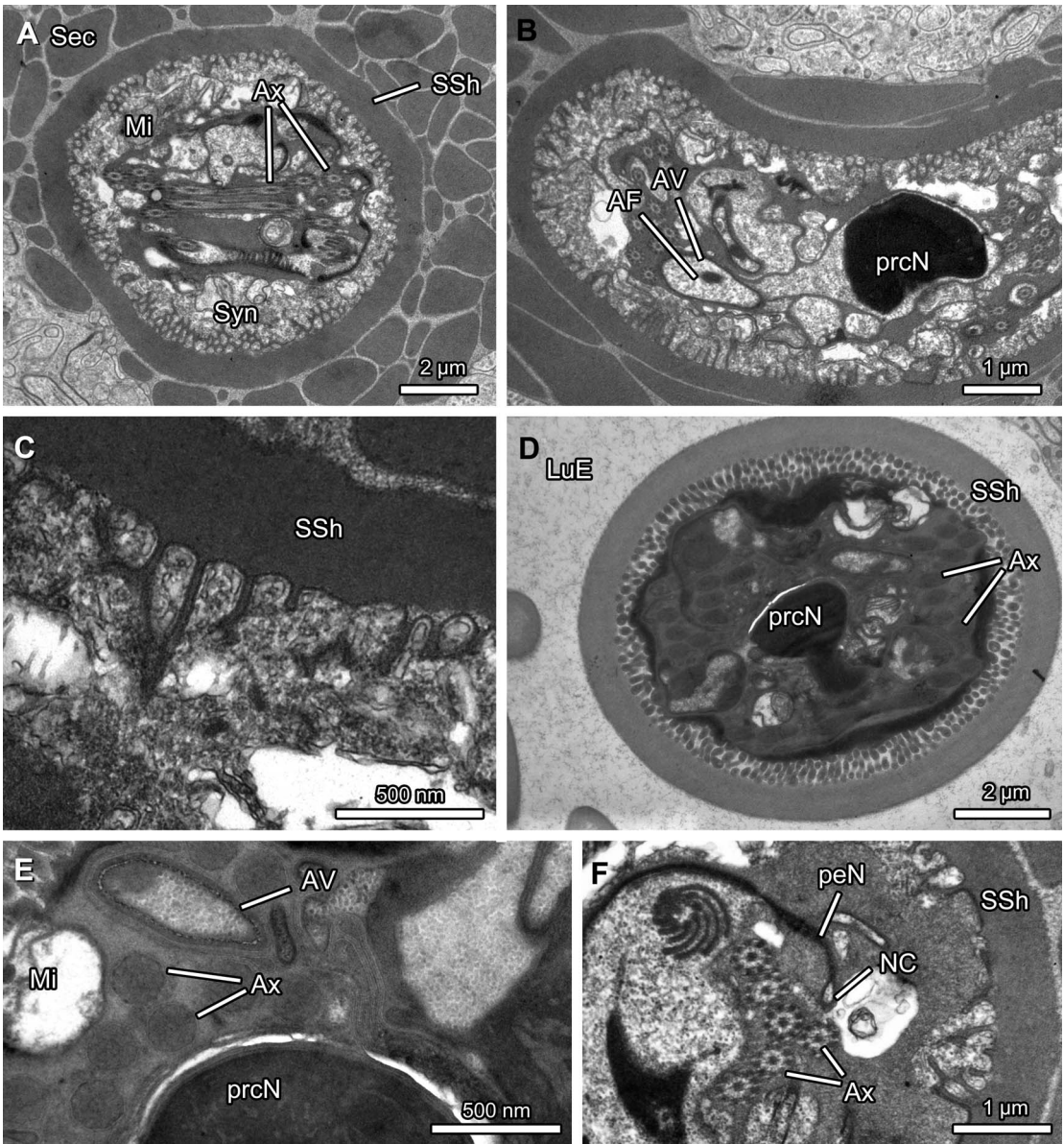


Fig. 16. Characteristics of synspermy and spermatozoa of *Neotrops waorani*. **A:** Sperm conjugates are surrounded by a distinct secretion sheath and characterized by heterogeneous cytoplasm, a distinct vesicular area, and numerous mitochondria. **B:** Longitudinal sections through sperm conjugates reveal the mainly oval shape of the synspermy. **C:** The membrane of the syncytium is constricted in the periphery. **D:** The subacrosomal space is widened. **E:** Due to the electron density of the vesicular area, axonemes are hardly visible. **F:** Within the ejaculatory duct, sperm conjugates further differentiate; this especially includes condensation of cytoplasm while peripheral constrictions recess.

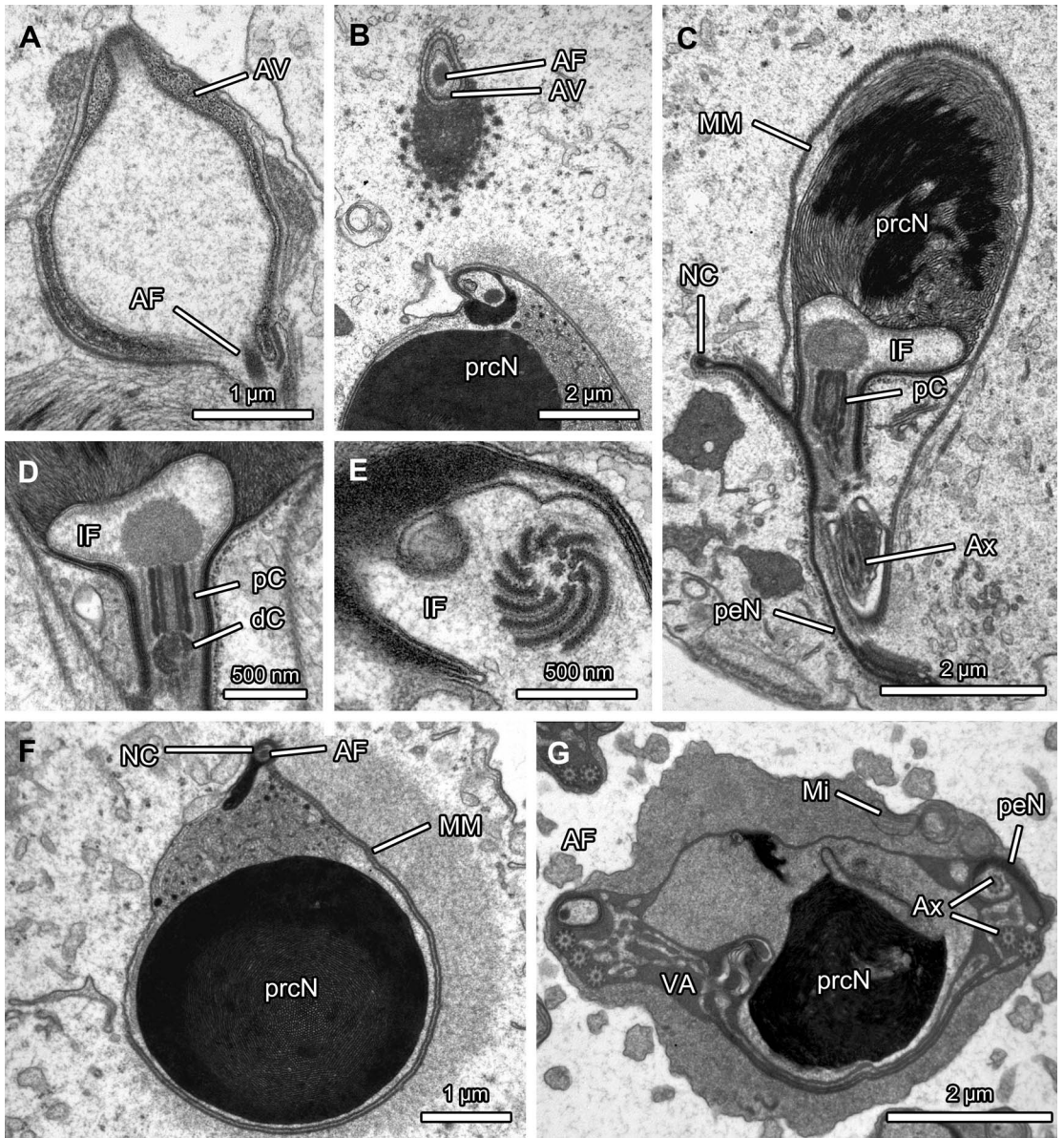


Fig. 17. Characteristics of spermiogenesis of *Neotrops waorani*. **A:** The posterior portion of AV is already deeply sunken into the anterior pole of the nucleus in early spermatids, the subacrosomal space is widened. **B:** The AV is surrounded by distinct electron-dense material. **C:** The chromatin appears fibrillar and shows dense streaks. **D:** The proximal centriole is enlarged. **E:** The base of the axoneme is surrounded by electron-dense secretions that arrange in plates. **F:** The NC runs in the periphery of the nucleus appears stalked because of the irregular chromatin-condensation pattern. **G:** At the end of spermiogenesis, a distinct electron-dense vesicular area is formed, while the main cell components coil within the cell.

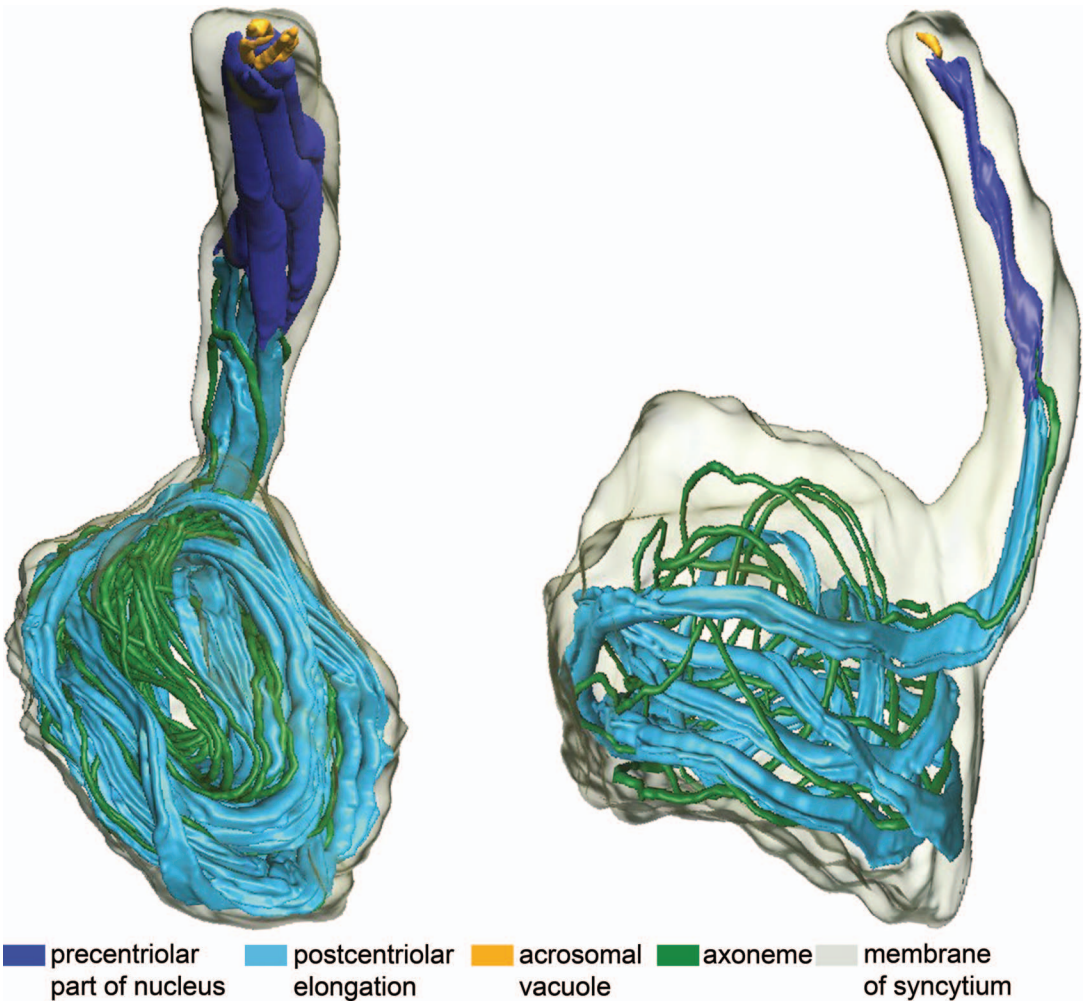


Fig. 18. Surface reconstruction of sperm transfer form of *Neoxyphinus termitophilus* illustrating the shape and arrangement of all four fused sperm, as well as the arrangement of an individual sperm within the deferent duct. Note the helically contorted preCN and the extremely elongated peN.

trioles are located (fig. 15D). The proximal centriole is nearly twice as long as the distal centriole (fig. 15D). A small collar of electron-dense, platelike secretions surrounds the base of the axoneme. At the end of spermiogenesis late spermatids that remained connected via cellular bridges (fig. 15E) start to fuse along their entire length, finally resulting in synspermia.

*Neotrops waorani* Grismado and Ramirez, 2013

**SPERM TRANSFER FORM** (fig. 16): Medium-sized (~9 μm), oval-shaped synspermia,

comprising four sperm. Within the deferent ducts, numerous mitochondria are visible in the periphery of sperm conjugates; the cytoplasm appears granular (fig. 16A, B). Cross sections of several, fingerlike constrictions of the peripheral cytoplasm are visible (fig. 16C). The cytoplasm and constrictions further condense (fig. 16D), finally a distinct peripheral ring of these cytoplasmic constrictions is formed (fig. 16E). Synspermia are surrounded by a thick (~200 nm), homogeneous secretion sheath (figs. 16E, F).

**SPERMATOOZOA** (fig. 16): **Acrosomal complex:** AV long, conical; wide subacrosomal

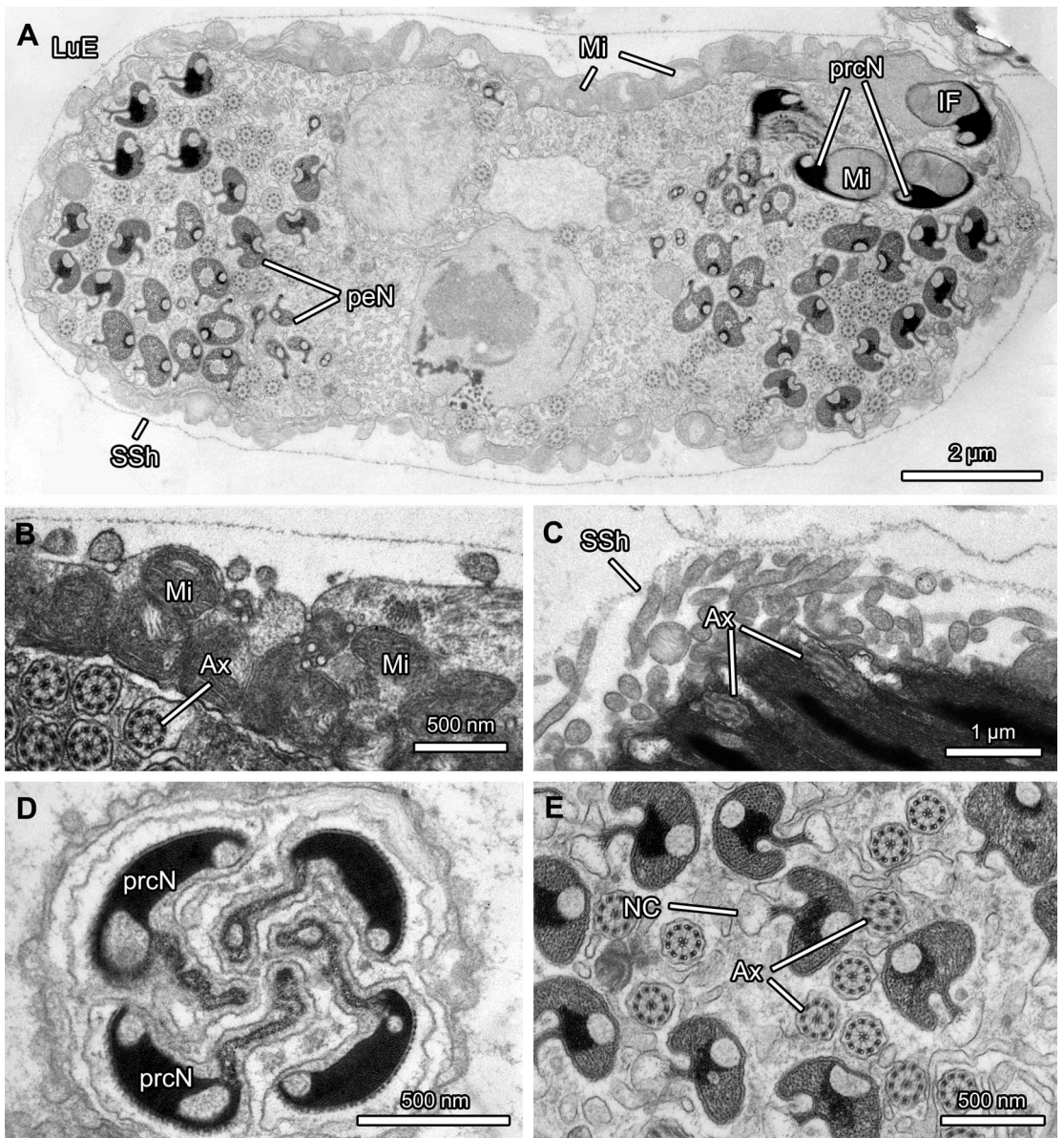


Fig. 19. Characteristics of synspermy and mature spermatozoa of *Neoxyphinus termitophilus*. **A:** The large oval-shaped sperm conjugate is surrounded by a very thin secretion sheath that is applied in the ejaculatory duct. **B:** The periphery of the sperm conjugate is composed of numerous mitochondria and small fingerlike constrictions of the membrane of the syncytium. **C:** These constrictions further deepen and surround the sperm conjugate. **D:** At the end of spermiogenesis four spermatids arrange closely attached to each other; they do not fuse, but instead cellular bridges (through which spermatids remain connected during spermiogenesis) widen and encase the spermatids, so that each sperm remains surrounded by its own cell membrane. **E:** The chromatin is irregularly condensed and possesses a distinct electron-lucent patch opposed to the NC, which is, although empty for the most part, partly enlarged.

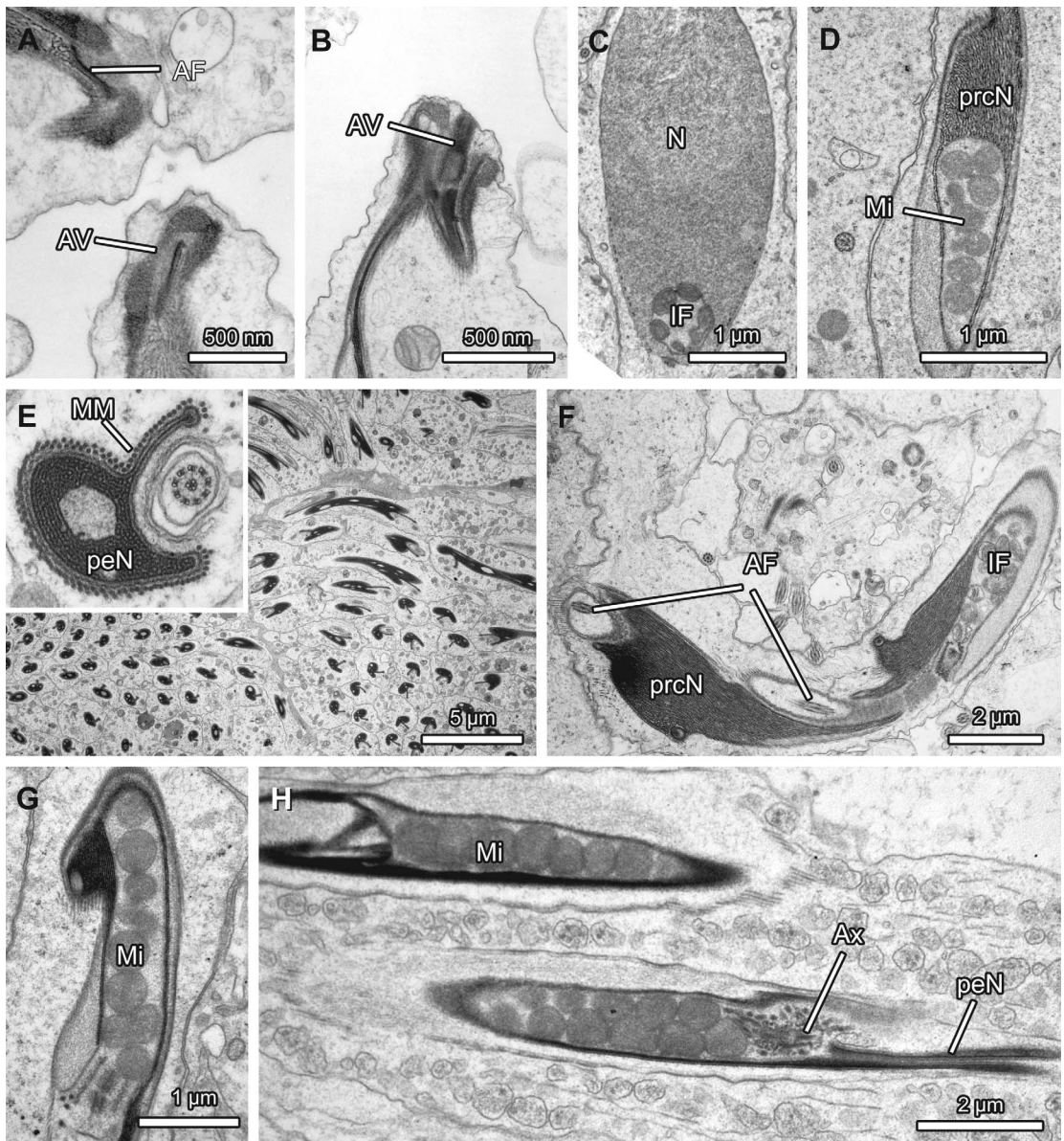


Fig. 20. Characteristics of spermiogenesis of *Neoxyphinius termitophilus*. **A:** Spermatids are characterized by a small AV. The anterior pole of the nucleus is extended at one side and the anterior pole of the AV is attached to the cell membrane. **B:** Mitochondria are present within the cytoplasm. **C:** During further development the chromatin starts condensation and appears fibrillar. **D:** At the posterior portion of the nucleus an IF, which is filled with numerous mitochondria, is formed. **E:** While the nucleus enormously elongates the characteristic chromatin-condensation pattern (central electron-lucent patch) is developed (inset). **F:** The axoneme curls around the nucleus. **G:** The two centrioles are arranged in tandem position. **H:** Besides the two centrioles and numerous mitochondria, a small amount of electron-dense secretions is present in the IF.

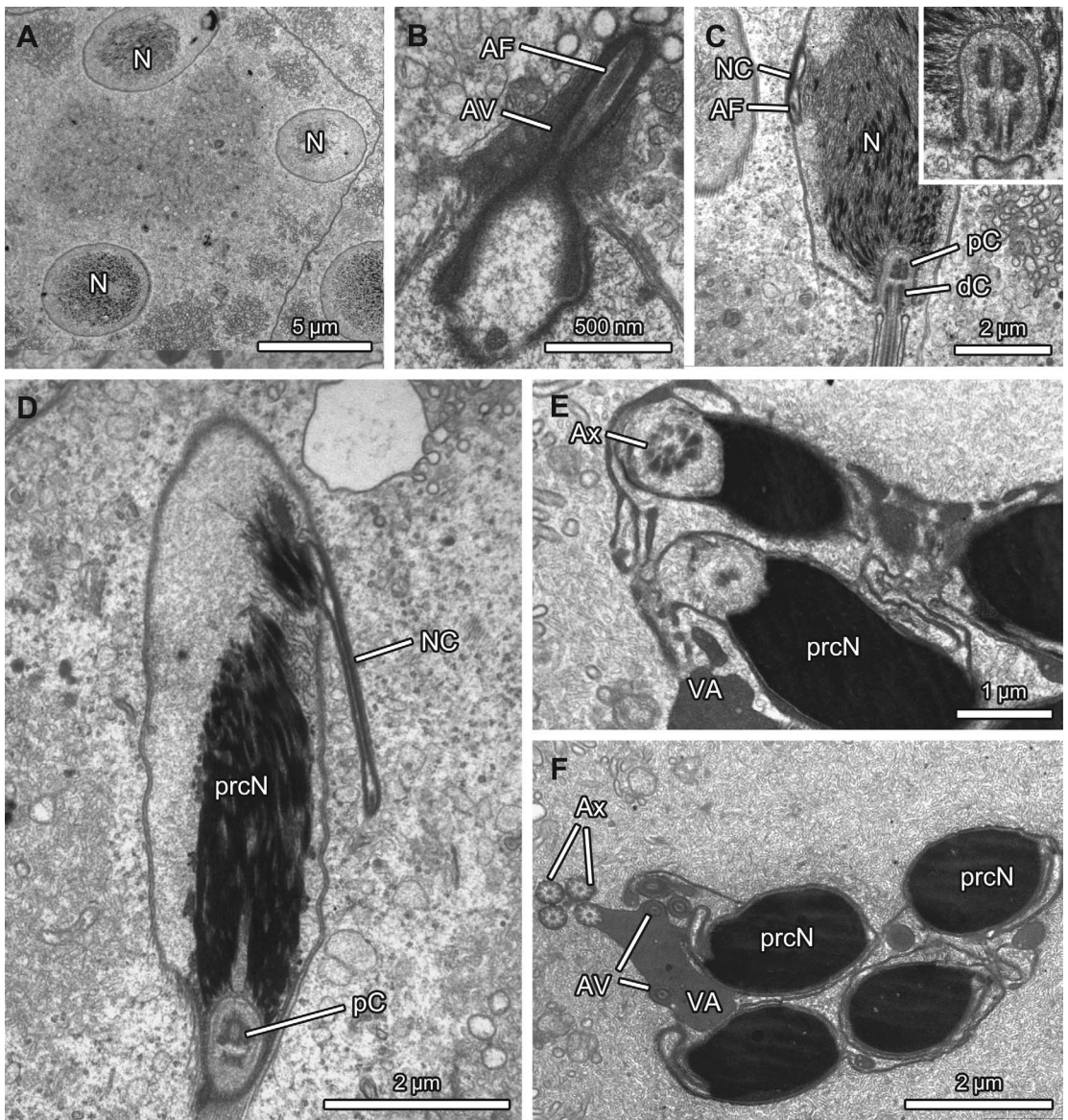


Fig. 21. Characteristics of spermiogenesis and mature spermatozoa of *Niarchos scutatus*. **A:** Early spermatids already fused entirely, thus all developing spermatids are surrounded by a common membrane. **B:** The posterior portion of the elongating AV is sunken into the anterior pole of the nucleus in early spermatids. **C:** Both centrioles (proximal and distal centriole) arrange in tandem position and migrate toward the posterior pole and thus induce the formation of the very small IF that comprises only the two centrioles (magnification in inset). **D:** The elongated NC is located in the periphery and usually bent toward the nucleus. **E:** The chromatin condenses irregularly and with distinct electron-lucent portions opposed to the portion in which the NC is running. **F:** At the end of spermiogenesis the four spermatids arrange closely attached to each other in the middle of the large sperm conjugate. The Ax of each spermatid coils within the cell membrane and a small, electron-dense VA that surrounds the main sperm cell components secondarily is formed.

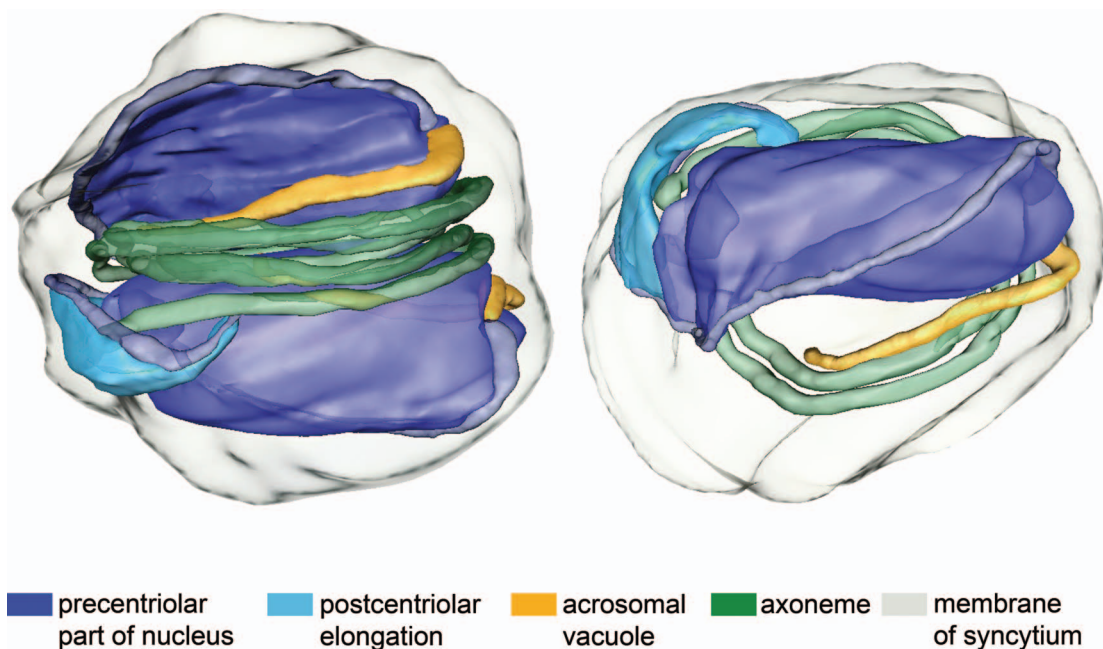


Fig. 22. Surface reconstruction of sperm transfer form of *Oonops* sp. (Ibiza) illustrating the shape and arrangement of two fused sperm, as well as the arrangement of an individual sperm. Note the very long AV, which is nearly as long as the prcN and the small peN.

space (fig. 16B, D). AF originates from the subacrosomal space, extends into the nuclear canal, but clearly ends before the base of the axoneme (fig. 16F). **Nucleus:** prcN indented at its anterior pole, irregularly condensed (fig. 16B), compact. peN flattened. NC located in the periphery, but empty for the most part. **Axoneme:** long, 9+3 microtubular pattern (fig. 16A, B, F).

**NOTES ON SPERMIOGENESIS** (fig. 17): All stages of spermiogenesis are present in the testis. Spermatids of the same developmental stage are arranged in cysts. The large AV possesses a wide subacrosomal space, is accompanied by a collar of electron-dense secretions and secretion droplets (fig. 17A), and is partially sunken into the anterior pole of the nucleus. The AF originates from the subacrosomal space (fig. 17A) and extends into the NC (fig. 17B, C). The nucleus is surrounded by a manchette of microtubules. The chromatin appears fibrillar in mid spermatids, but condenses irregularly (fig. 17C). Late spermatids retain this condensation pattern (fig. 17E–G). The implantation fossa contains a small amount

of spherical secretions (fig. 17D), the two centrioles (fig. 17C, D), and a collar of electron-dense plates that surround the base of the axoneme (fig. 17E). At the end of spermiogenesis main sperm cell components coil within the cell membrane and a loose vesicular area is formed, surrounding the latter (fig. 17G). Finally, four spermatids that still remained connected to each other via cellular bridges fuse.

*Neoxyphinus termitophilus* (Bristowe, 1938)

**SPERM TRANSFER FORM** (figs. 18, 19): Large (~25 μm), oval-shaped synspermia (within the ejaculatory duct) comprising four sperm (fig. 18). Synspermia, located in the deferent ducts, are bottle shaped (fig. 18). The bottleneck contains the acrosomal vacuoles, the short and helically contorted precentriolar parts of the nucleus and the base of the axonemes, as well as postcentriolar elongations of the nucleus, whereas the voluminous bulge is filled with the main parts of axonemes and postcentriolar elongations of nucleus that coil around each other.

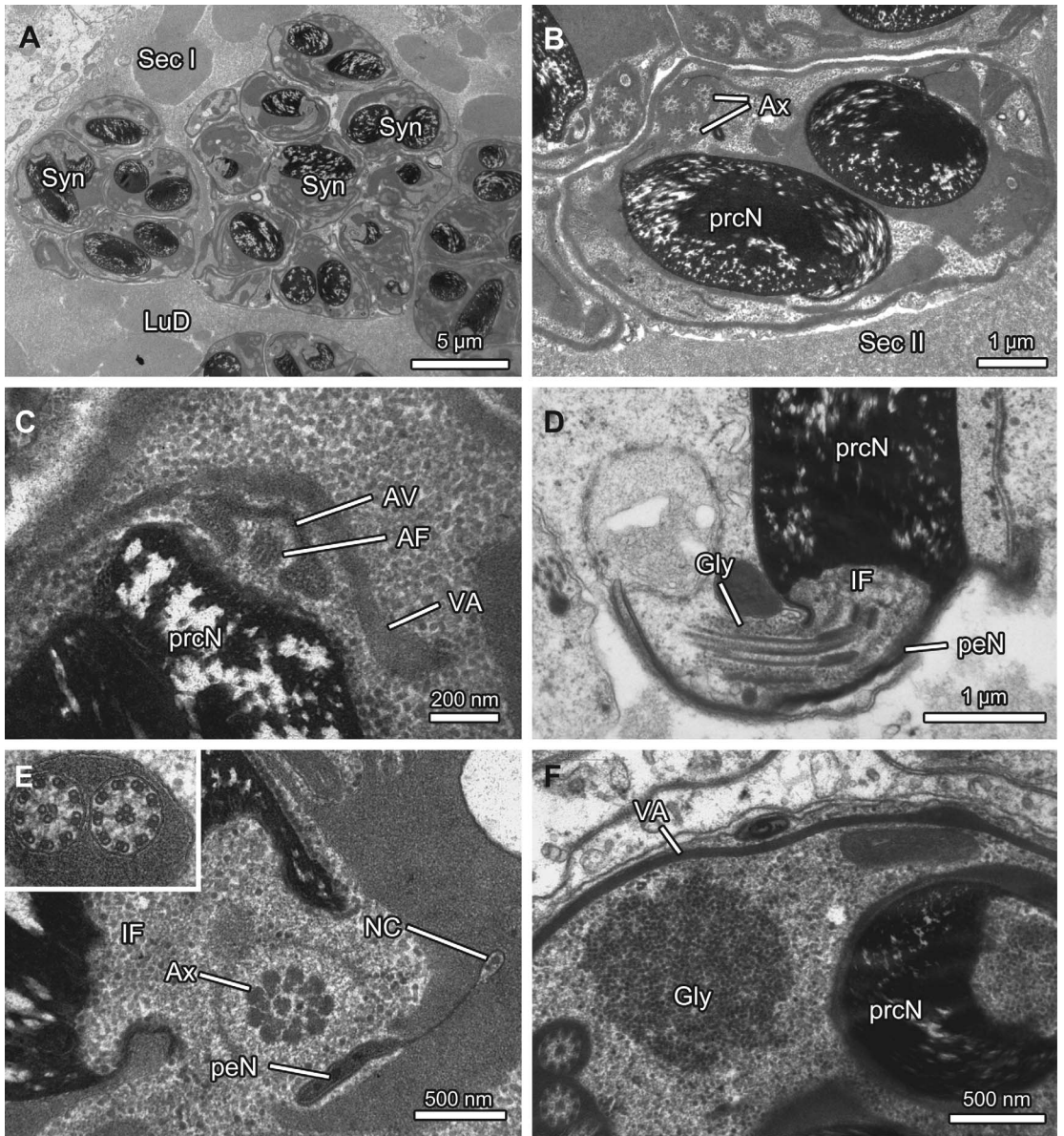


Fig. 23. Characteristics of synspermy of *Oonops* sp. (Ibiza). **A:** Sperm conjugates, which are composed of two sperm, arrange in cluster. **B:** Synspermy are not provided with a secretion sheath, but show a distinct electron-dense vesicular area. **C:** The condensed chromatin appears fibrillar, distinct electron-lucent stalks appear, and the cytoplasm appears granular in sperm conjugates. **D:** The NC is located on a distinct projection, running in the periphery of the nucleus; note mitochondria within the cytoplasm. **E:** The base of the axoneme, with a typical 9+3 microtubular pattern (inset), is associated with a little electron-dense material. **F:** Note a small amount of glycogen is present in the IF, as well as within the cytoplasm of the sperm conjugate. A thin ribbon originating from the vesicular area is located in the periphery of the sperm conjugate underneath the membrane of syncytium.

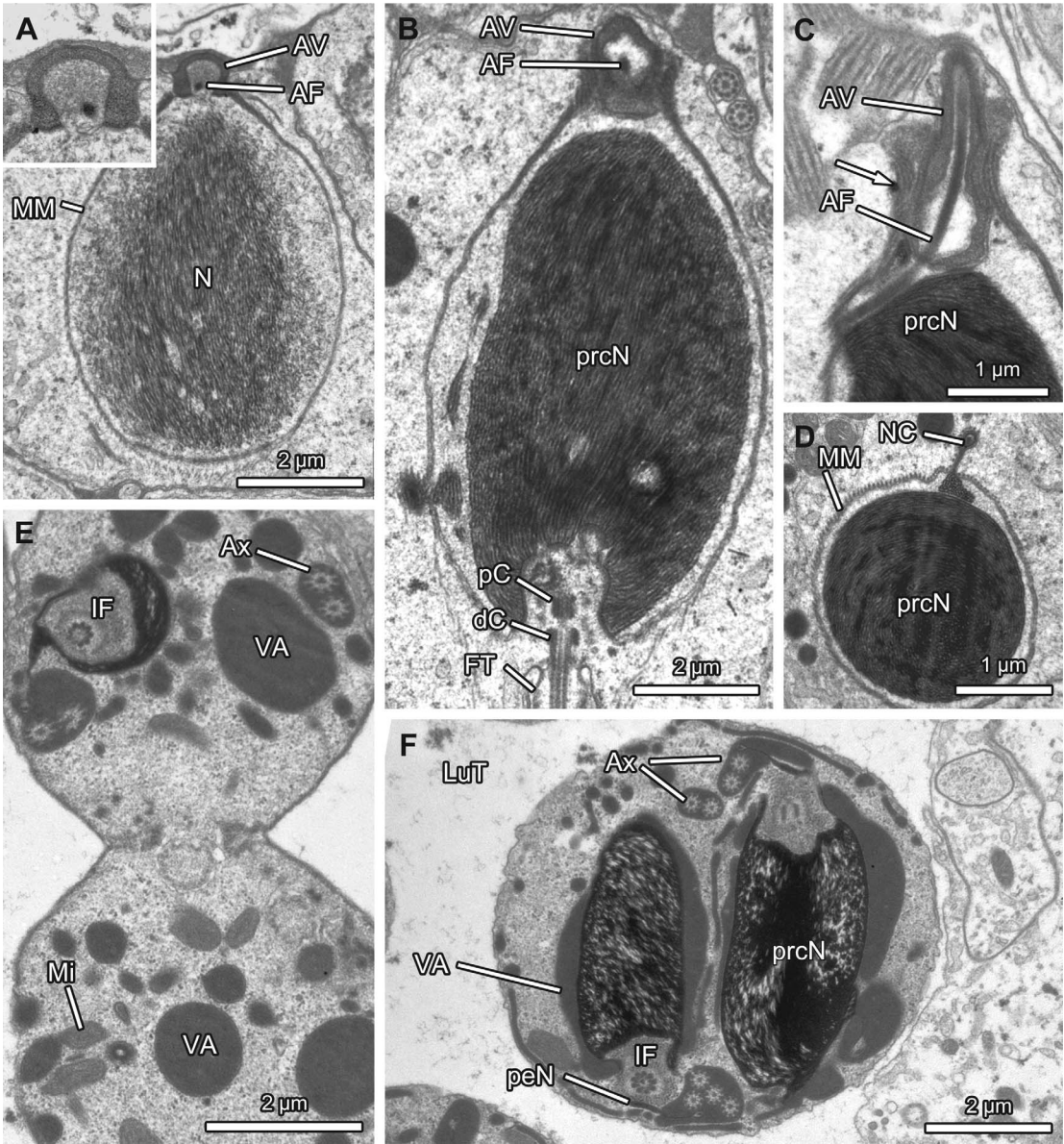


Fig. 24. Characteristics of spermiogenesis of *Oonops* sp. (Ibiza). **A:** The small developing AV is attached to the cell membrane anteriorly (magnification in inset); the nucleus is surrounded by a manchette of microtubules. **B:** The chromatin condenses irregularly and appears fibrillar in mid-spermatids. **C:** The elongated AV is surrounded by electron-dense material (arrow) at the anterior pole of the nucleus. **D:** The AF extends into the NC that is located on a distinct projection in the periphery of the nucleus. **E:** At the end of spermiogenesis, the main cell components coil within the cell membrane, while the spermatids remain connected with each other via cellular bridges. **F:** Finally, two spermatids fuse, forming a mainly spherical sperm conjugate.

Numerous mitochondria are located in the periphery of the sperm conjugate (fig. 19A, B). A very thin and loosely appearing secretion sheath (~30 nm), which is produced

in the ejaculatory duct, surrounds the sperm conjugates (fig. 19A–C).

**SPERMATOOZOA** (figs. 18, 19): **Acrosomal complex:** AV short (~1.2 μm) and cylindrical

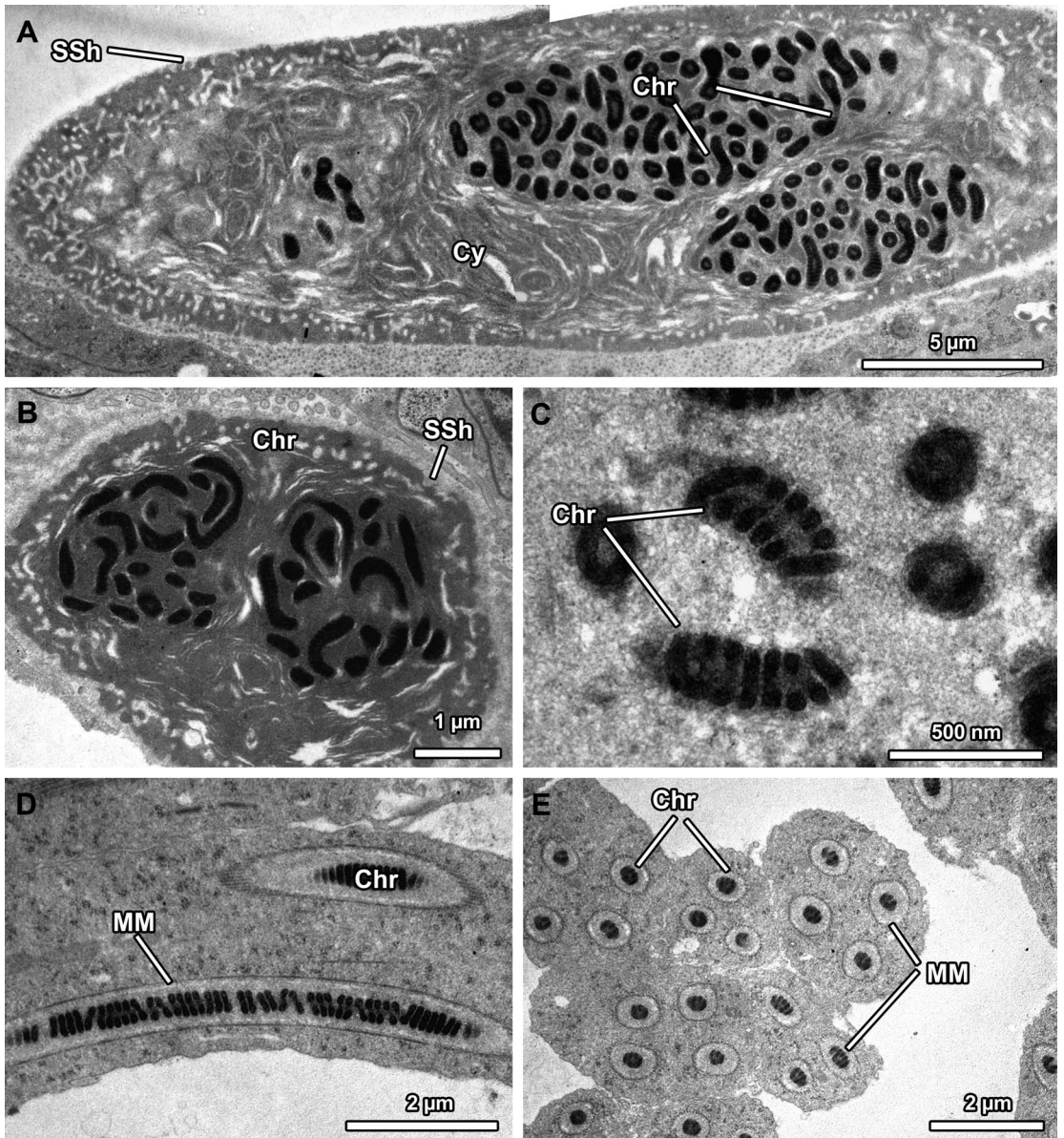


Fig. 25. Characteristics of the sperm transfer form of *Opopaea apicalis*. **A:** The STF is only composed of a condensed chromatin thread that is embedded in electron-dense cytoplasm and surrounded by a thin secretion sheath. **B:** Within the periphery of the STF distinct electron-lucent portions are visible. **C:** The chromatin thread is highly coiled, as is most obvious in late stages of spermiogenesis. **D:** The manchette of microtubules surrounds the chromatin thread. **E:** During the sperm development, the nucleus becomes extremely elongated, as indicated by numerous cross sections that are visible within one cell. Further cell components, such as an acrosomal complex, or an Ax are not developed.

(fig. 18). AF originates from the subacrosomal space and extends into the nuclear canal but ends clearly ends before the axonemal base. **Nucleus:** prcN short (~10.1 µm),

helically contorted with medium-sized implantation fossa that is filled with numerous mitochondria (fig. 19A), several spherical secretions, proximal and distal centriole, as

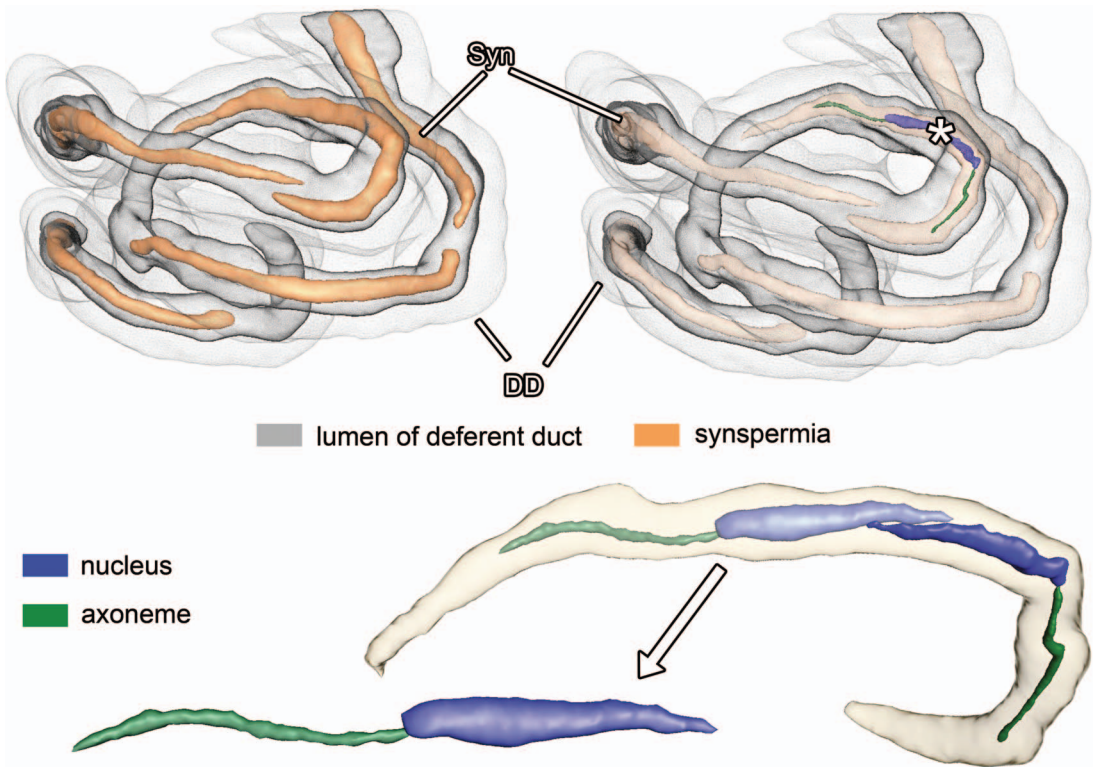


Fig. 26. Surface reconstruction of parts of the highly convoluted deferent ducts and sperm transfer forms of *Orchestina* sp. 1. (Chile), as based on serial light-microscopy images, illustrating the shape and arrangement of synspermia within the lumen of the deferent duct and the two fused sperm within one sperm conjugate. The axoneme is hypothetically reconstructed based on the presence of dense microtubular network within the cytoplasm of the sperm conjugate.

well as the base of the Ax. peN extremely elongated (~171.8 μm), oval in cross sections with distinct projection (fig. 19A, E). NC located within a distinct projection, twists around the peN (figs. 18, 19A, E) but is empty for the most part (fig. 19D). **Axoneme:** extremely long (~291.5 μm); centrioles arranged in tandem position; 9+3 axonemal pattern (fig. 19B, E).

**NOTES ON SPERMIOGENESIS:** Within the testis all stages of spermiogenesis are present, developing spermatids are arranged in cysts. Early spermatids are characterized by a large, oval nucleus that is surrounded by a manchette of microtubules. Mid spermatids are characterized by a small, cylindrical AV (fig. 20A, B) that is partly sunken into the anterior pole of the nucleus and accompanied by a small amount of electron-dense material (fig. 20B). Further development includes

condensation of chromatin that appears fibrillar in mid spermatids (fig. 20C, D). Mitochondria are always present within the implantation fossa (fig. 20D, F–H). Mid- and late spermatids show a characteristic chromatin-condensation pattern in which a small portion remains homogeneously electron lucent (fig. 20E, E inset). The axoneme is twisted around the postcentriolar elongation, thus both cell components seem to interact (fig. 20F). In late spermatids, both centrioles are arranged in tandem position (fig. 20G). The implantation fossa is filled with numerous mitochondria (figs. 20F–H). The two centrioles and the base of the Ax are surrounded by electron-dense secretion droplets and electron-dense secretion plates (fig. 20H). At the end of spermiogenesis four spermatids fuse and form large and voluminous synspermia. During early stages of this sperm conjugation,

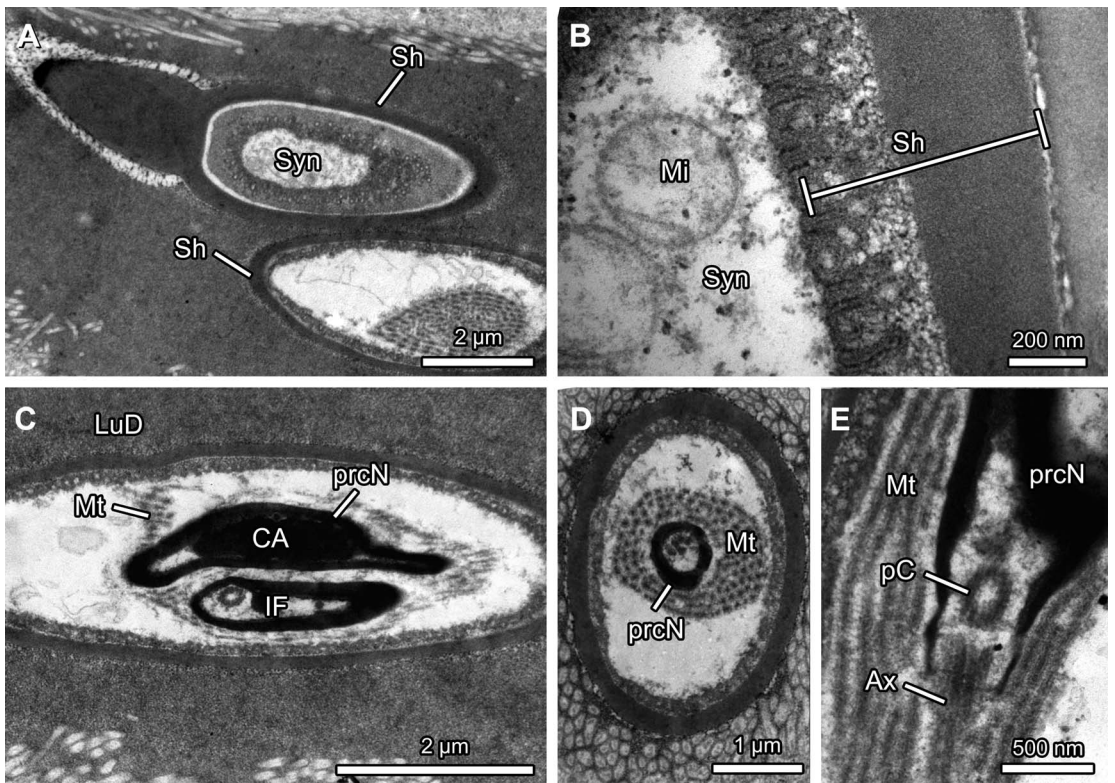


Fig. 27. Characteristics of synspermia of *Orchestina* sp. 1 (Chile). **A:** The synspermia are surrounded by a thin, electron-dense secretion sheath; a distinct cap is formed. **B:** The periphery of the membrane of syncytium is composed of several small constrictions. **C:** Sperm of one sperm conjugate are either located next to each other, or arranged in tandem position. **D:** The sperm cell components are not coiled and thus sprawled within the sperm conjugate. **E:** The two centrioles are arranged rectangularly.

four mainly individualized spermatids that remained connected to each other via cellular bridges arrange in close association. While the Ax's, as well as peN's coil, and form the massive bulge of early bottle-shaped synspermia, the cellular bridges widen posteriorly resulting in a large amount of common cytoplasm. Finally, the common cytoplasm, which contains numerous mitochondria, encases the spermatids secondarily during further differentiation of the sperm conjugate.

*Niarchos scutatus* Platnick and Dupérré, 2010

**SPERM TRANSFER FORM** (fig. 21): Synspermia comprising four sperm. Information on sperm transfer forms and sperm characteristics refer to sperm obtained from the testis. Within the lumen of the testis large

sperm conjugates are visible. Sperm are located in the center of the sperm conjugation, surrounded by an electron-dense vesicular area (fig. 21F) and large quantities of cytoplasm.

**SPERMATOZOA** (fig. 21): For the identification of sperm characters, only material from the testis was available, thus the following sperm characters refer to spermatogenic stages. **Acrosomal complex:** AV conical (fig. 21B), widened proximally, but narrow subacrosomal space for the most part (fig. 21 B). AF originates from the subacrosomal space and extends into the nuclear canal (fig. 21C, D), ends before the base of the axoneme. **Nucleus:** prcN compact with small implantation fossa that comprises only the two centrioles (fig. 21D). peN not identifiable. NC located in the periphery of the

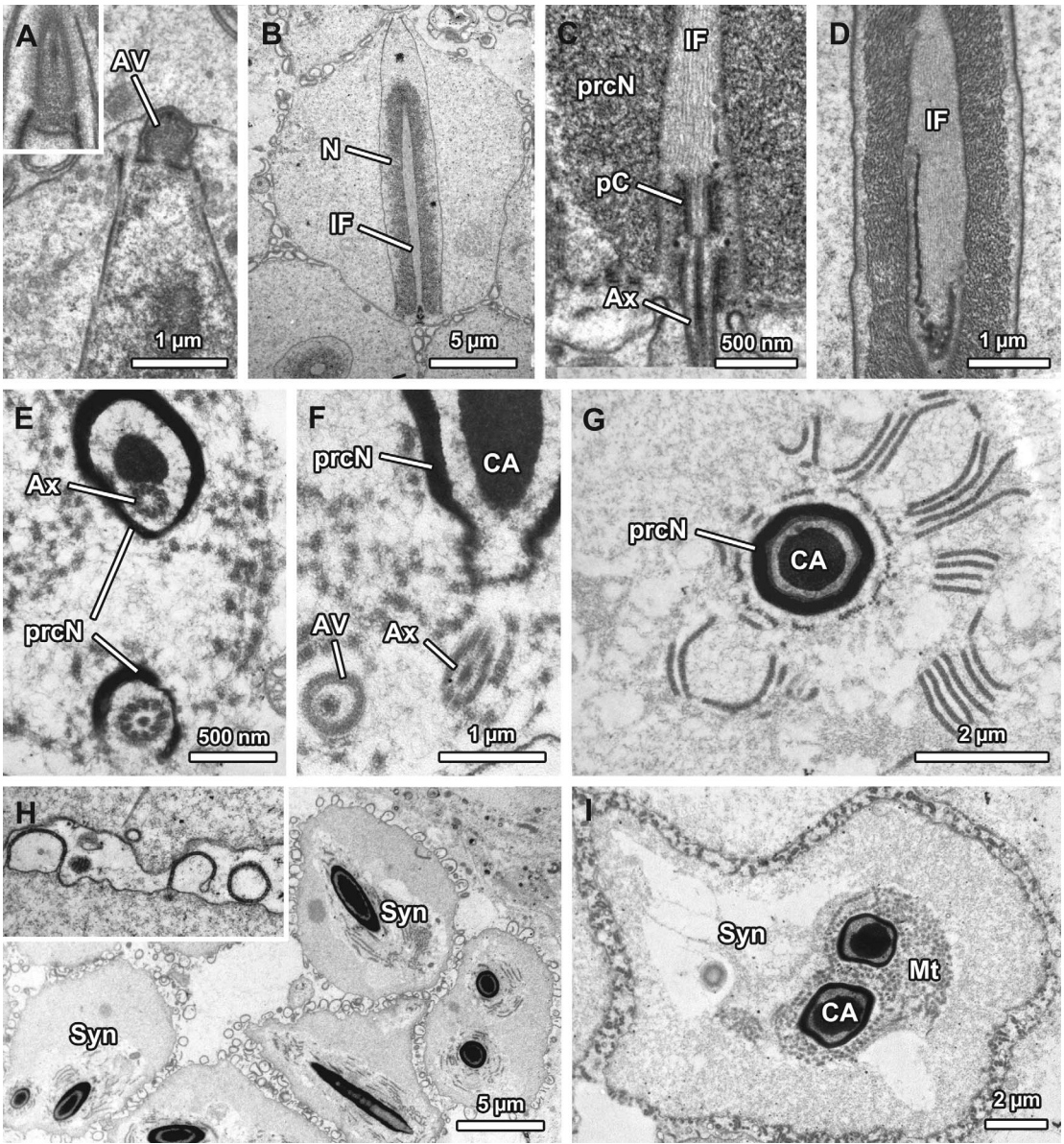


Fig. 28. Characteristics of spermiogenesis of *Orchestina* sp. 1 (Chile). **A:** At the anterior pole of the nucleus a small AV is formed, which is separated from the nucleus by a distinct, electron-dense plate. The AF originates from the subacrosomal space (inset). **B:** The chromatin starts condensation around the IF, which extends nearly as far as the anterior pole of the nucleus. **C:** The deep IF that contains the two centrioles is stabilized with microfilaments. **D:** These microfilaments are arranged in parallel. **E:** The axoneme originates from the distal centriole, a peN is not developed. **F:** In late spermatids a distinct centriolar adjunct is present in the IF. **G:** In addition to the manchette of microtubules, several microtubules arrange around the nucleus in late spermatids. **H:** The periphery of the spermatids possesses numerous looplike constrictions, which are obvious in higher magnification in (inset). **I:** Finally, two sperm fuse entirely and form large synspermia, the cytoplasm of which further compresses, while the sperm conjugates elongate.

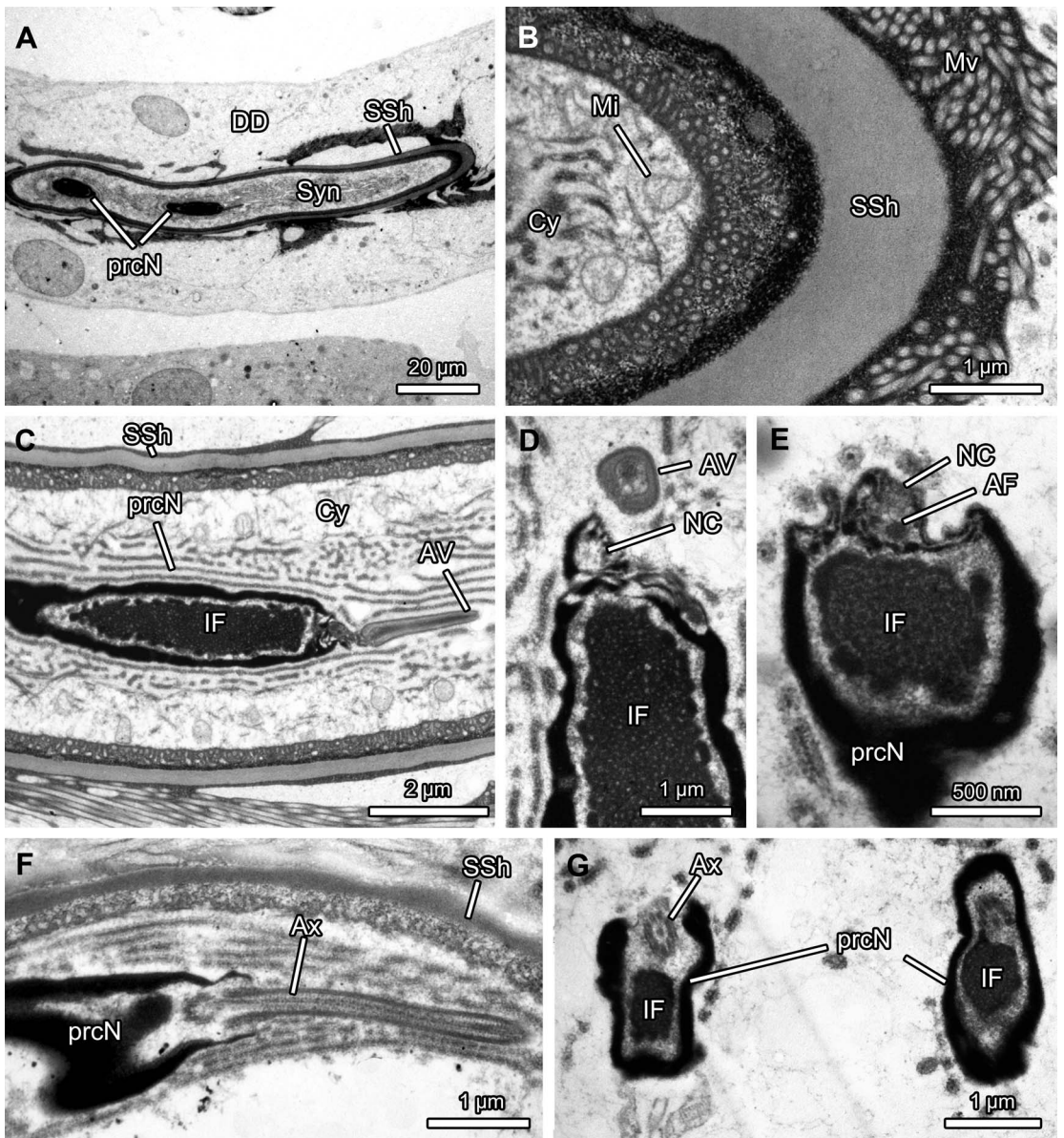


Fig. 29. Characteristics of synspermy and spermatozoa of *Orchestina* sp. 2 (Argentina). **A:** Sperm conjugates are elongated and tubelike. **B:** The secretion sheath that surrounds the synspermy is formed in the deferent ducts. **C:** The periphery of the cytoplasm of the syncytium is provided with numerous fingerlike constrictions. **D:** The IF is very large and filled with a distinct centriolar adjunct, the small NC is only visible near the anterior pole of the nucleus. **E:** The AV is small and provided with a narrow subacrosomal space. **F:** The axoneme extends from the posterior pole of the nucleus. **G:** A peN is not present.

nucleus (fig. 21C), elongated and bend toward the nucleus (fig. 21D, F). **Axoneme:** centrioles are arranged in tandem position (fig. 21D), 9+3 microtubular pattern (fig. 21E, F).

**NOTES ON SPERMIOGENESIS:** Within the testis early and late stages of spermiogenesis are present. Already early spermatids (four) fuse entirely, forming very large, developing

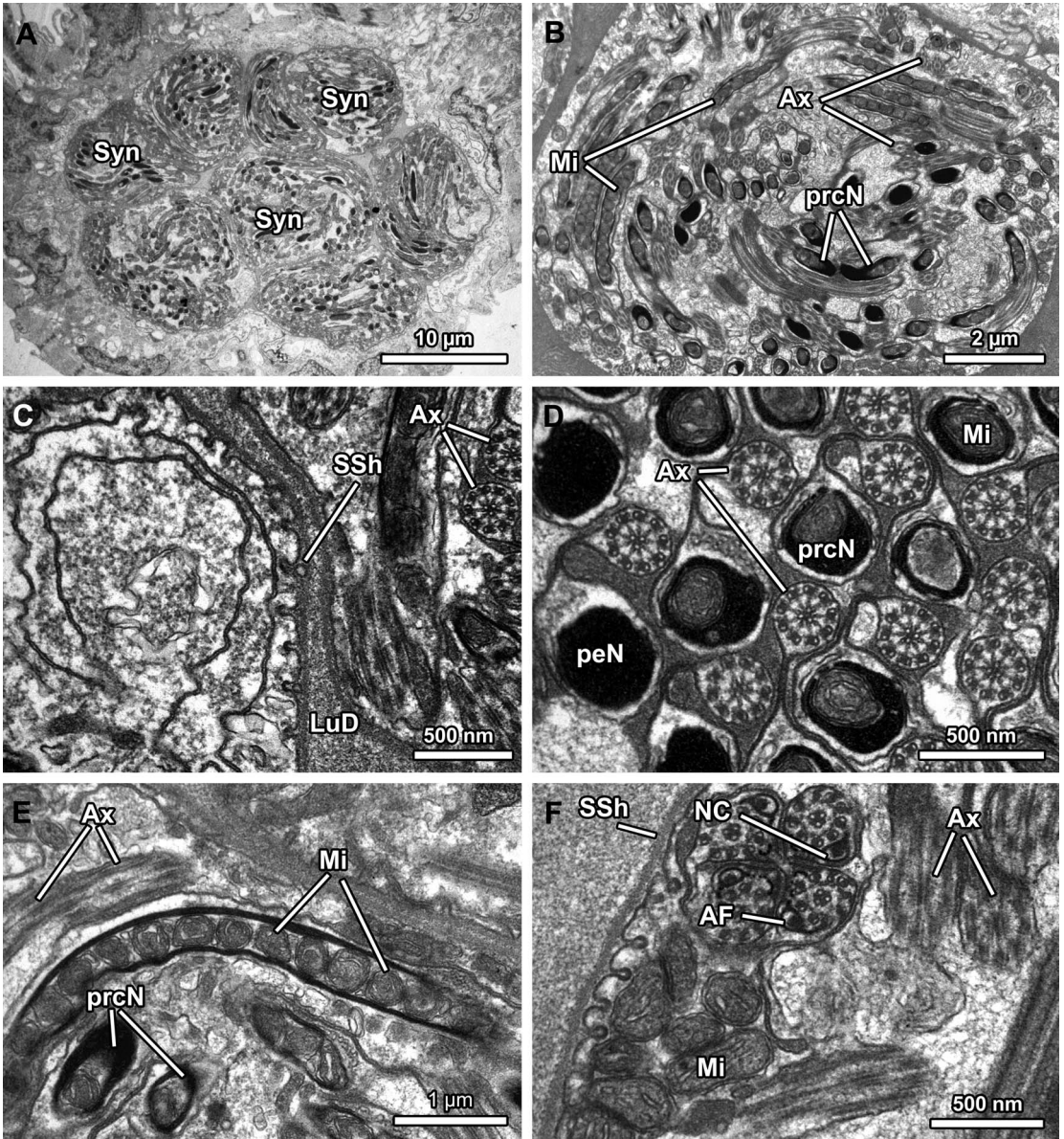


Fig. 30. Characteristics of synspermia of *Paradysderina fusiscuta*. **A:** The lumen of the deferent ducts is filled with large sperm conjugates. **B:** Sperm conjugates are composed of four sperm, which are randomly arranged and curled around each other. **C:** All sperm conjugates are surrounded by a very thin secretion sheath. Numerous membranes, as well as small folds are visible in the periphery. **D:** Sperm are not entirely fused, thus the main sperm cell components remain surrounded by their own membrane. **E:** The deep implantation fossa is filled with numerous mitochondria that are arranged in a row. **F:** Additional mitochondria are present in the periphery of the sperm conjugate.

synspermia (fig. 21A). The cytoplasm of this syncytium is characterized by large quantities of smooth endoplasmic reticulum. The AV is sunken into the anterior pole of the

nucleus (fig. 21B), which is surrounded by a manchette of microtubules. Two centrioles migrate toward the posterior pole of nucleus, inducing the formation of a

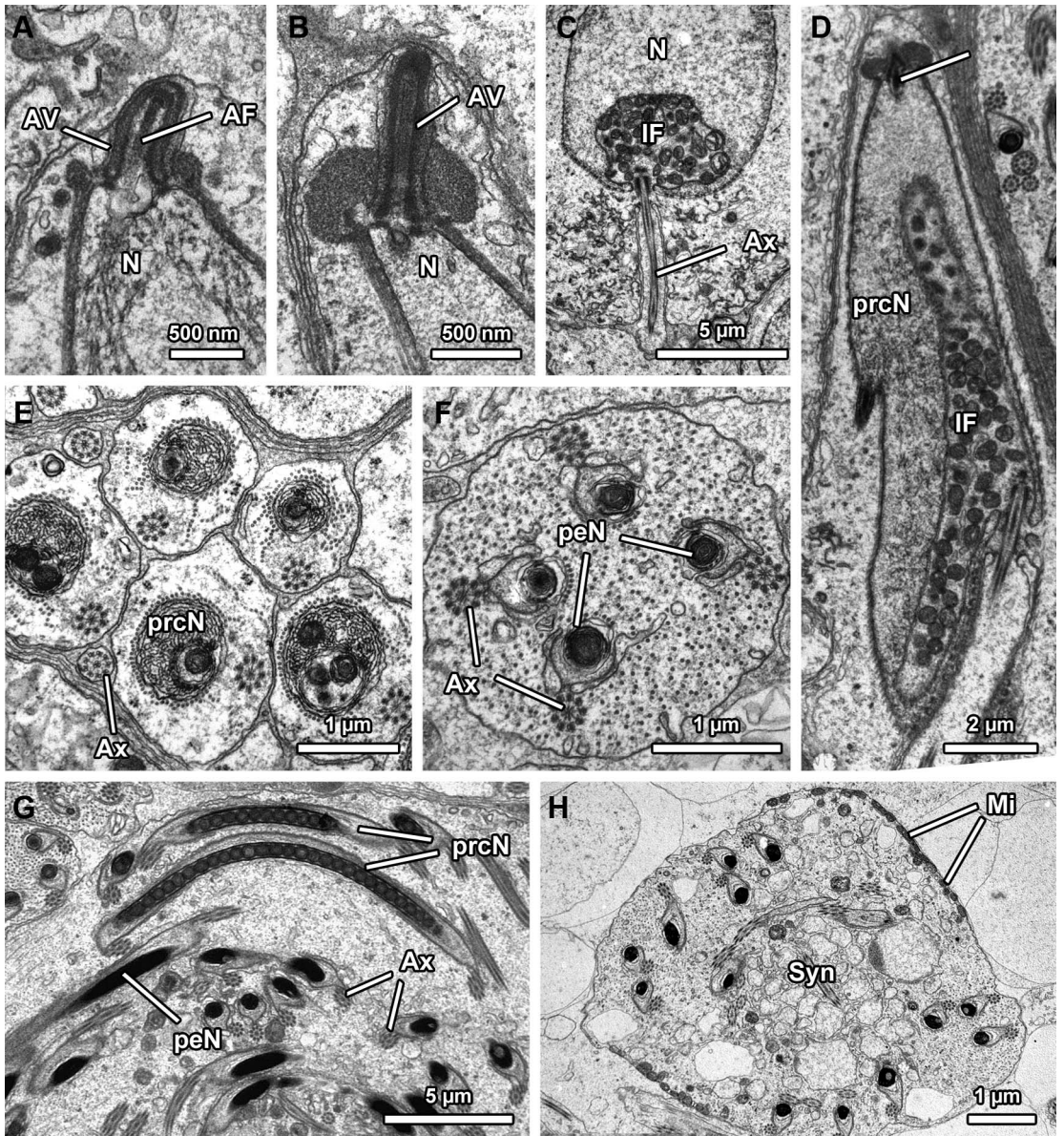
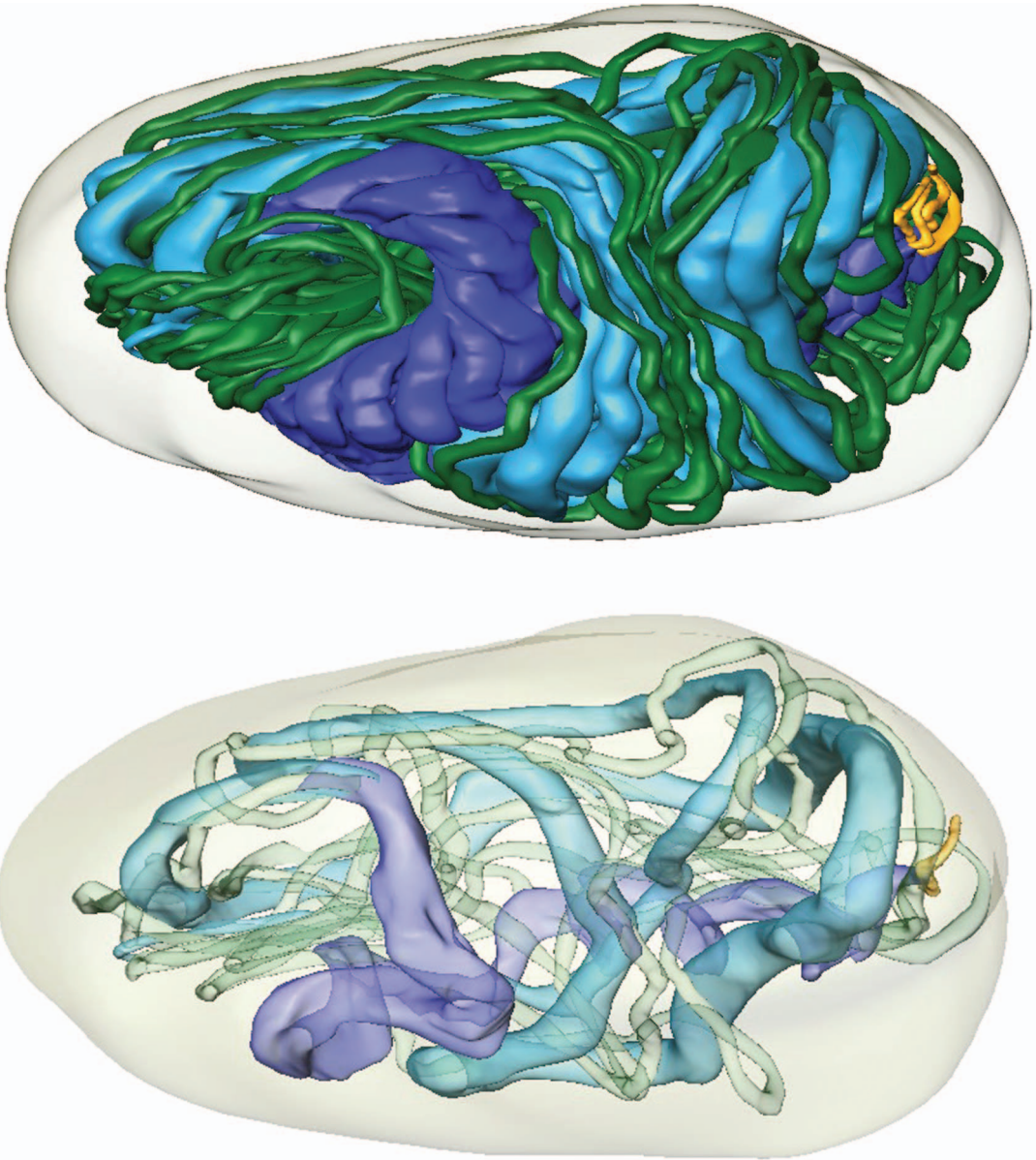


Fig. 31. Characteristics of spermiogenesis of *Paradyderina fuscicuta*. **A:** A small, fingerlike AV is formed at the anterior pole of the nucleus. **B:** The posterior portion of AV is accompanied by electron-dense material. **C:** At the posterior pole of nucleus a wide IF is formed. **D:** Numerous mitochondria are located in the IF. **E:** The chromatin appears fibrillar in mid spermatids. **F:** At the end of spermiogenesis four spermatids, which remained connected to each other via cellular bridges, arrange closely attached to each other and partly fuse. **G:** Finally, they form a large sperm conjugate, in which the main cell components of all spermatids coil. **H:** Additional mitochondria are located in the periphery of the sperm conjugate.

small implantation fossa (fig. 21D). The chromatin condenses heterogeneously (fig. 21C, D). The NC is extremely stretched, resembling a slender band in late spermatids

(fig. 21F). The peripheral microtubules of the two centrioles are surrounded by little electron-dense material (fig. 21E). Further development includes the complete



precentriolar part of nucleus    
  postcentriolar elongation    
  acrosomal vacuole    
  axoneme    
  membrane of syncytium

Fig. 32. Surface reconstruction of synsperma of *Paradysderina yanayacu*, illustrating the shape and arrangement of all four fused sperm, as well as the arrangement of an individual sperm. Note the very long peN and Ax, which coil around each other within the membrane of syncytium.

condensation of chromatin, resulting in a homogeneously electron-dense nucleus (fig. 21F) and formation of a vesicular area (fig. 21F).

*Oonops* sp. (Ibiza)

SPERM TRANSFER FORM (figs. 22, 23): Small (~5 μm), mainly oval-shaped synsper-

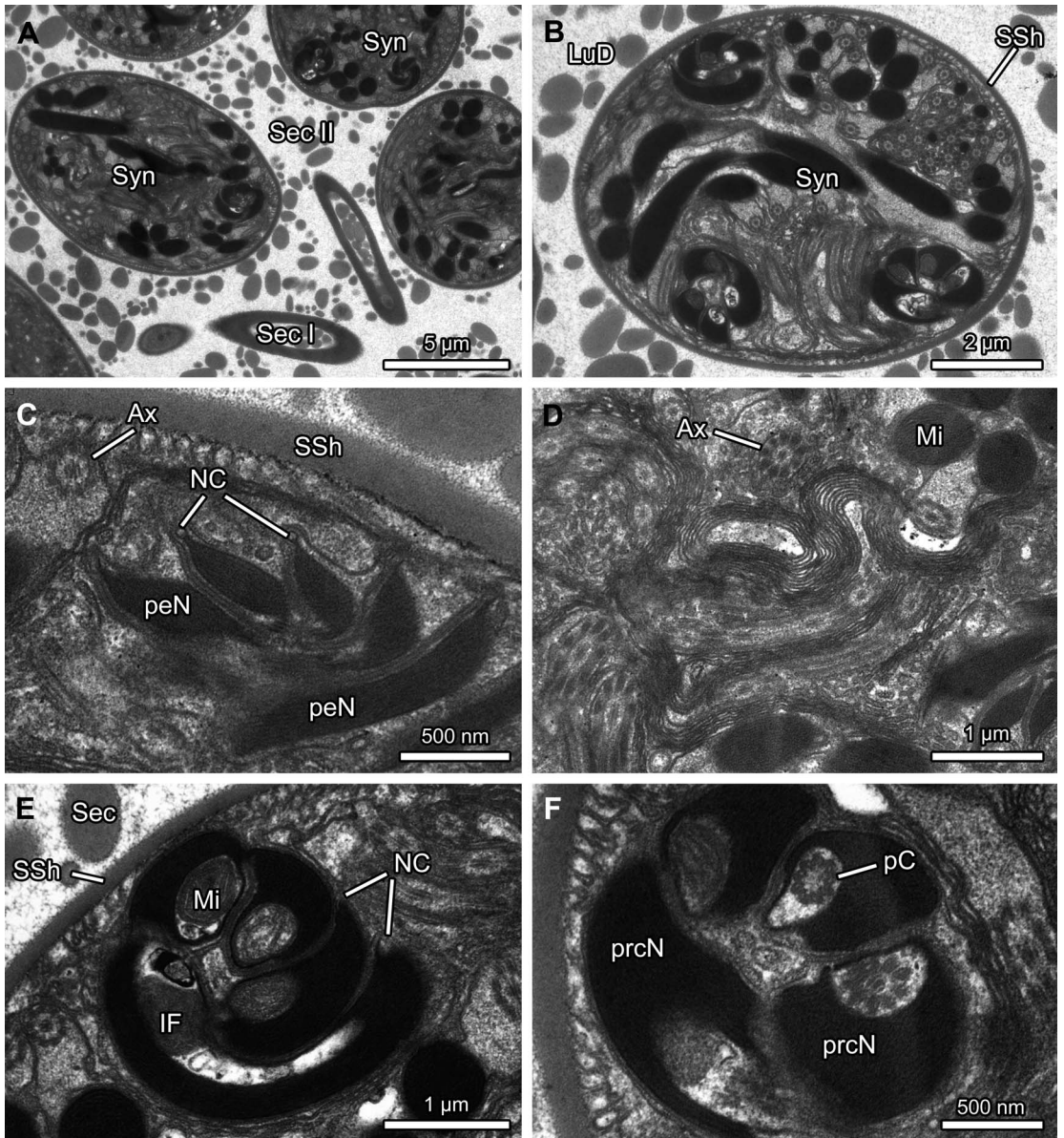


Fig. 33. Characteristics of synspermia of *Paradysderina yanayacu*. **A:** Within the lumen of the deferent ducts, numerous large, oval-shaped sperm conjugates and two types of secretion are visible. **B:** Cross sections through an entire sperm conjugate showing the arrangement of sperm cell components of all four sperm, which are beginning to coil around each other. **C:** Synspermia are surrounded by a thin secretion sheath. **D:** Numerous, densely packed membranes are visible. **E:** The four spermatids coil around each other, thus the prcN appears helically contorted. **F:** A small amount of electron-dense material surrounds the peripheral microtubules at the base of the axoneme.

mia (figs. 22, 23A) comprising two sperm (figs. 22, 23B). A distinct, electron-dense vesicular area surrounds all main cell components (fig. 23A–C). The cytoplasm appears

granular (fig. 23C, E). Synspermia are un-sheathed; instead, several sperm conjugates cluster in the distal deferent duct, embedded in a distinct secretion matrix (fig. 23A).

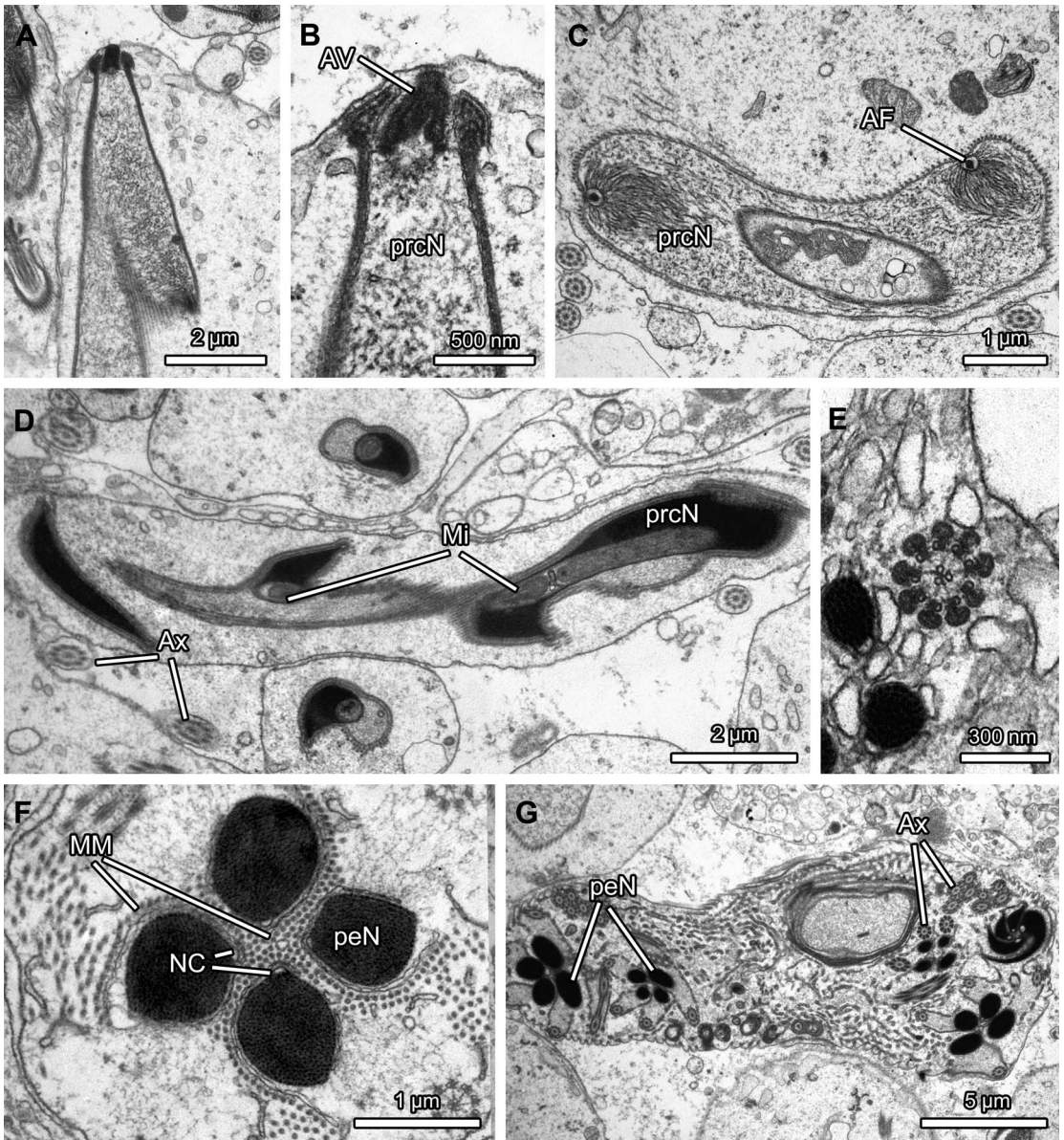


Fig. 34. Characteristics of spermiogenesis of *Paradysderina yanayacu*. **A:** A small AV that is attached to the cell membrane is formed at the anterior pole of nucleus. **B:** Little electron-dense material is associated with the posterior portion of the AV. **C:** The large IF contains numerous mitochondria. **D:** During the development of the spermatids the prcN extremely elongates and screws. **E:** Little electron-dense material is associated with the peripheral microtubules in the axoneme. **F:** At the end of spermiogenesis four spermatids arrange closely attached to each other and finally form a large synspermium. **G:** Large membrane whirls are visible within the sperm conjugate.

*Spermatozoa* (figs. 22, 23): **Acrosomal complex:** AV long (~3.9 μm), cylindrical; narrow subacrosomal space (fig. 23C). AF originates from the subacrosomal space, ends in the

region of the axonemal base. **Nucleus:** prcN compact (~4.3 μm) and tubelike (fig. 22) with a distinct crest, on which the nuclear canal is running (figs. 22, 23D, E). The

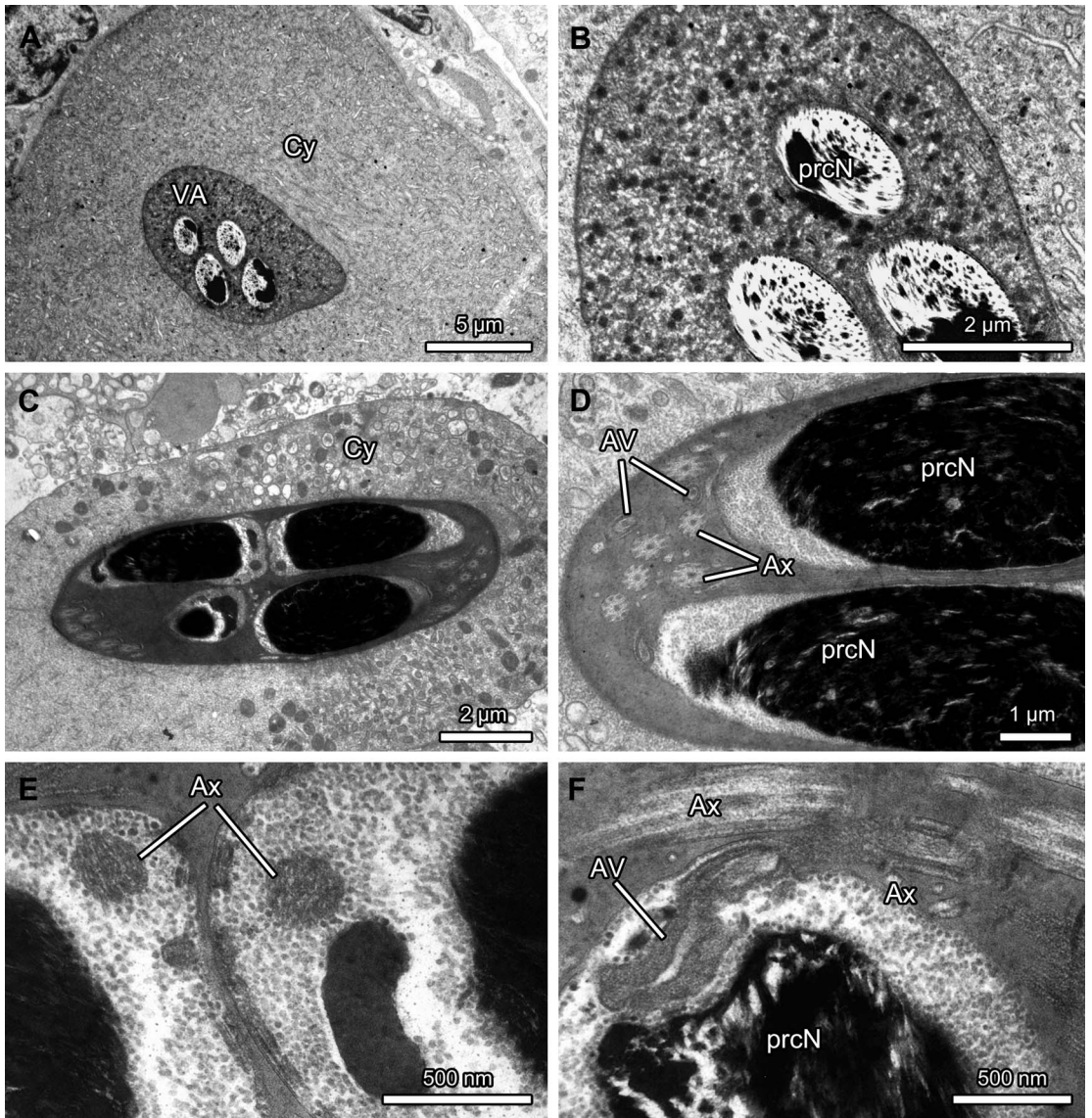


Fig. 35. Characteristics of synspermia of *Scaphios yanayacu*. **A:** Within the testis and proximal portion of the deferent ducts, the sperm conjugate is very voluminous, although the sperm cell components are restricted to a small portion that is located in the center of the synsperm. **B:** Furthermore, the vesicular area that surrounds the sperm cell components appears granular and the chromatin still looks spotty. **C:** Within the distal portion of the deferent ducts the cytoplasm of synspermia is compressed and numerous mitochondria are visible. **D:** Finally, the vesicular area is homogeneously electron dense. **E:** The microtubular pattern of the axoneme is hardly visible due to its electron density. The cytoplasm adjacent to the nuclei appears granular and presumably contains some glycogen. **F:** The anterior pole of nucleus is slightly indented.

implantation fossa is small but wide (fig. 23 D, E). Besides a little granular material, presumably glycogen (fig. 23D), the implantation fossa contains the two centrioles and

the base of the Ax (fig. 23E). peN nearly as long as prcN (~2.9 μm) and flattened (figs. 23, 24E). NC located in the periphery, on a distinct crest (fig. 23E). **Axoneme:** long

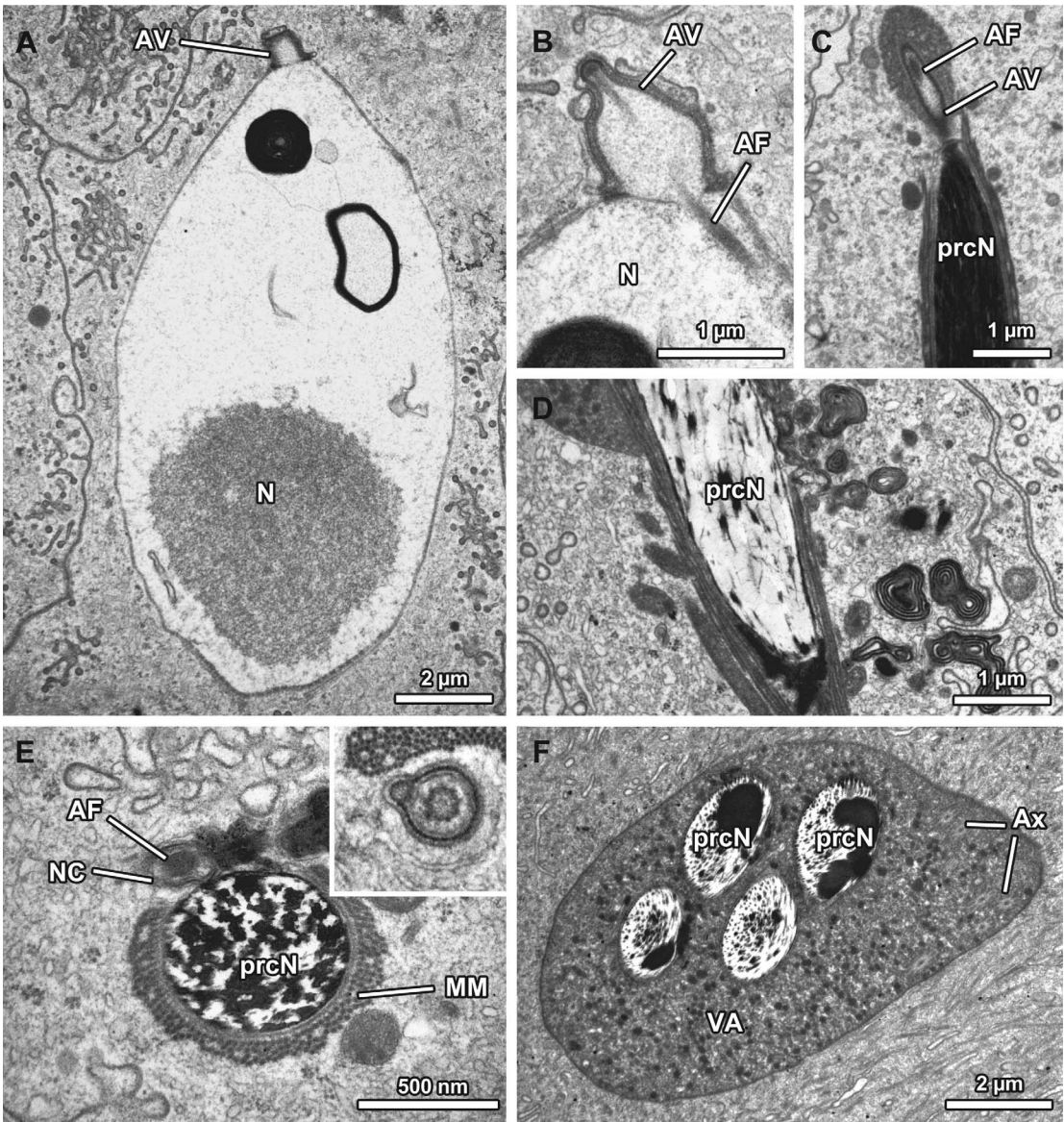


Fig. 36. Characteristics of spermiogenesis of *Scaphios yanayacu*. **A:** Early spermatids are characterized by a peculiar chromatin-condensation pattern. **B:** The acrosomal vacuole of early spermatids possesses an enlarged subacrosomal space. **C:** In midspermatids the AV is surrounded by electron-dense material. **D:** Numerous membrane whirls are visible in close association to the elongating nucleus in mid- and late spermatids. **E:** A multilayered manchette of microtubules surrounds the nucleus for its most part; the AF that runs inside the nuclear canal clearly ends before the axonemal base (inset). **F:** At the end of spermiogenesis four spermatids fuse completely and arrange in the middle of the voluminous sperm conjugate.

(~23.4 μm), 9+3 microtubular pattern (fig. 23E inset).

NOTES ON SPERMIOGENESIS (fig. 24): Within the testis all stages of spermiogenesis

are present; spermatids are arranged in cysts of the same developmental stage. Early spermatids are characterized by a large, mainly spherical nucleus that is surrounded

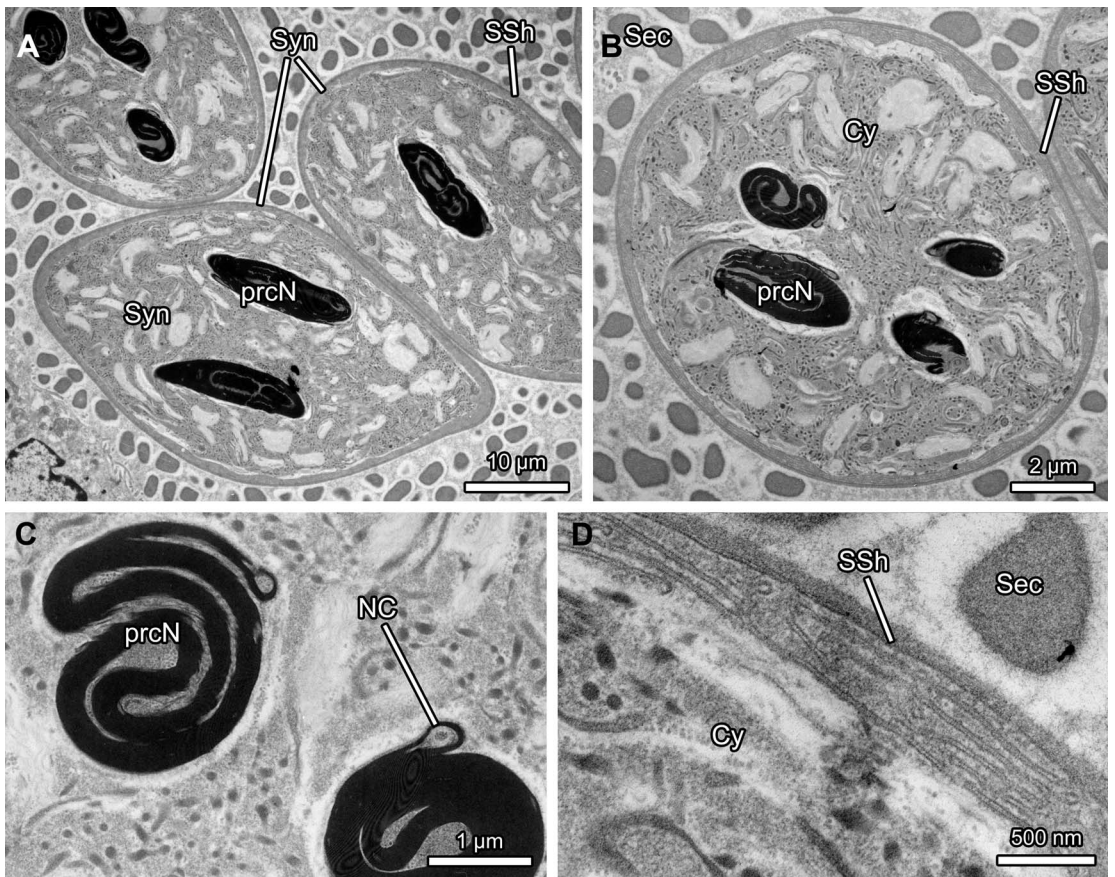


Fig. 37. Characteristics of synspermia of *Silhouettella loricatula*. **A**: Numerous sperm conjugates, as well as electron-dense secretions, are visible in the lumen of the deferent ducts. **B**: Section through sperm conjugates indicates the organization of sperm that are arranged in the center of synspermia, surrounded by heterogeneous cytoplasm. **C**: The nuclei show a peculiar chromatin-condensation pattern. **D**: The periphery of the sperm conjugate is composed of small membrane stacks. The entire sperm conjugate is surrounded by a thin secretion sheath.

by a manchette of microtubules (fig. 24A), and a developing acrosomal complex, which is attached to the anterior pole of the nucleus (fig. 24A). During further differentiation, the acrosomal vacuole sinks into the nucleus (fig. 24B, C). Simultaneously, the two centrioles migrate toward the posterior pole of the nucleus, consequently forming an implantation fossa (fig. 24B). The posterior portion of nucleus is constricted, resulting in a small neck. Chromatin condensation occurs heterogeneously and shows a specific pattern, in which a distinct crest of dense chromatin is separated from the remaining, tubelike condensing chromatin of the nucleus (fig. 24B). The NC that contains

the AF is located in the periphery of this crest (fig. 24B, D). At the end of spermiogenesis, the Ax is retracted and coils within the cell membrane (fig. 24E). At the same time, several electron-dense vesicles fuse, initiating formation of a distinct vesicular area that surrounds all main sperm cell components (fig. 24E, F). Finally, two spermatids that are still connected via cellular bridges fuse, forming synspermia (fig. 24E, F).

*Opopaea apicalis*

SPERM TRANSFER FORM (fig. 25):  
Large sperm transfer forms (>25 µm),

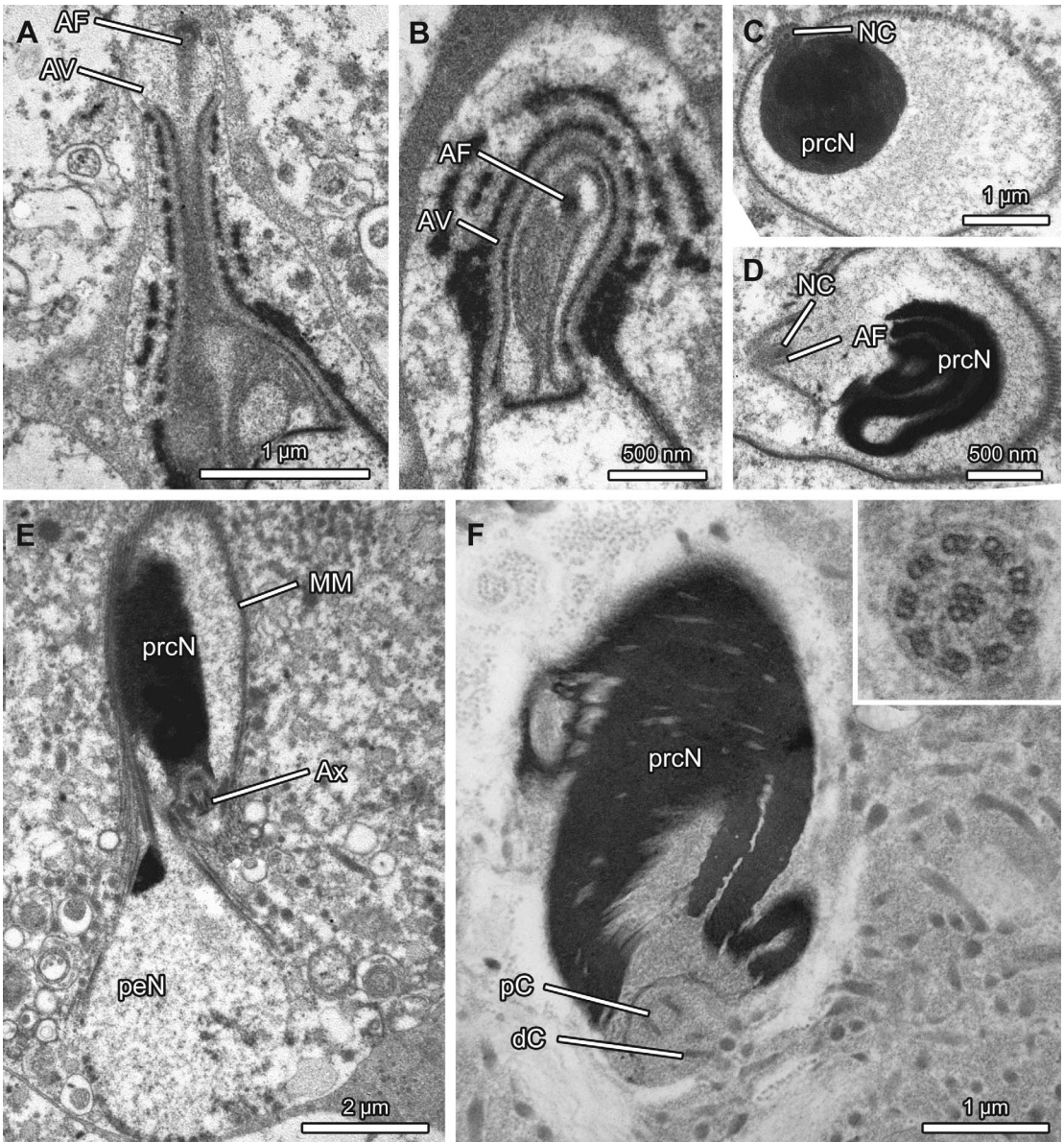


Fig. 38. Characteristics of spermiogenesis of *Silhouettella loricaatula*. **A:** The AV is separated from the nucleus by distinct electron-dense plate. **B:** Higher magnifications reveal little granular material inside the subacrosomal space, in addition to the acrosomal filament. **C:** The manchette of microtubules and the NC indicate the actual dimensions of the nucleus. **D:** The NC runs in the periphery of the nucleus and contains the AF. **E:** While the nucleus elongates a small, droplike peN is formed, which disappears in further development. **F:** The very small implantation fossa contains only the two centrioles; the axoneme, which possesses the typical microtubular pattern, originates from the distal centriole (inset).

composed of only a chromatin thread that is embedded in an electron-dense matrix and surrounded by a thin (~70 nm) homogeneous secretion sheath (fig. 25A, B).

*Spermatozoa* (fig. 25): **Acrosomal complex:** AV absent. AF absent. **Nucleus:** prcN condensed chromatin thread that is tightly screwed (fig. 25C). peN absent. NC inapplicable (due to missing AF). **Axoneme:** absent.

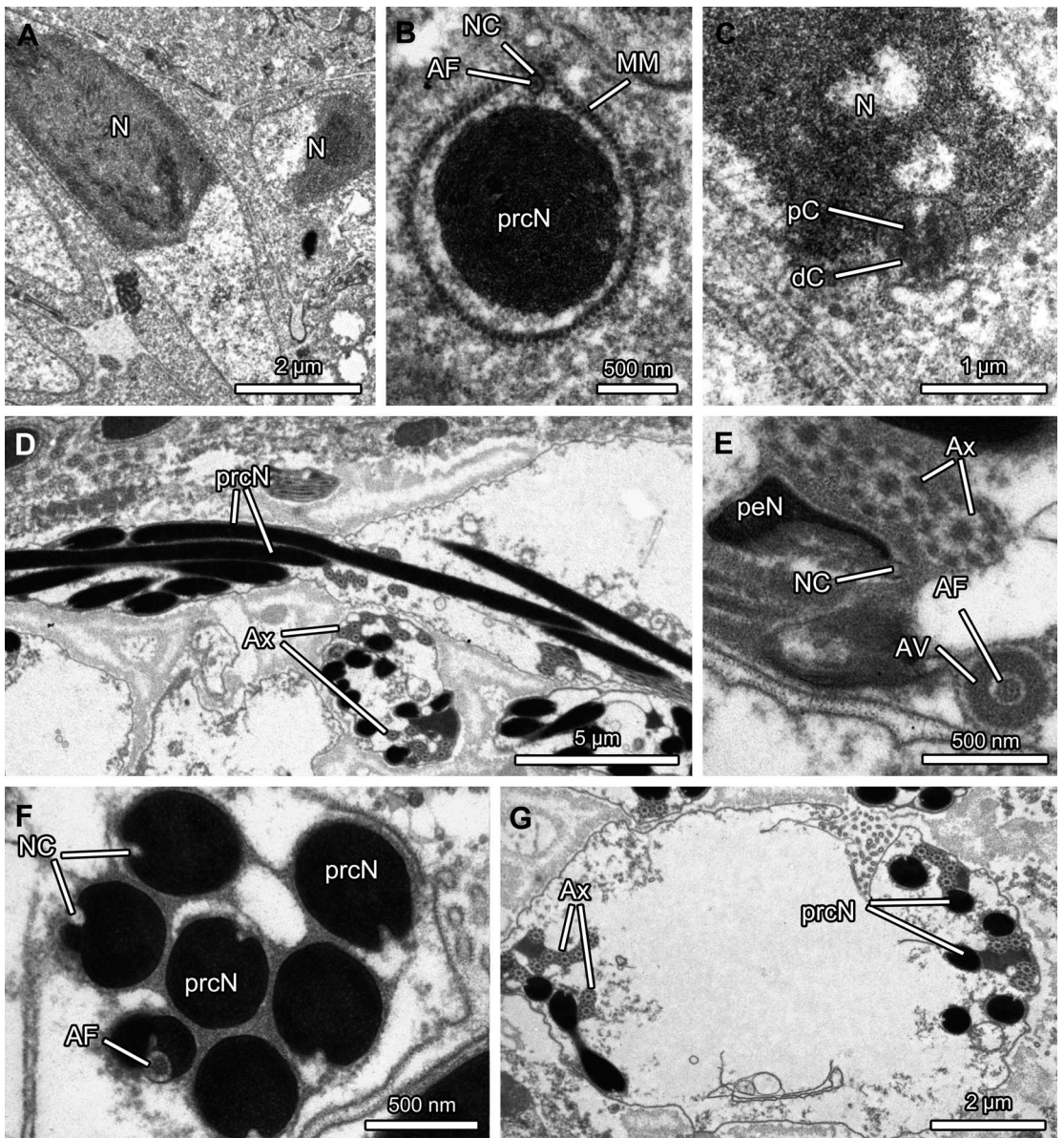


Fig. 39. Characteristics of sperm and spermiogenesis of *Stenoconops peckorum*. **A:** The chromatin condenses irregularly in developing spermatids and appears fibrillar. **B:** A single-layered manchette of microtubules surrounds the nucleus. **C:** The IF is very small and contains only the two centrioles. **D:** During further development, the nucleus extremely elongates. **E:** The short peN is thin and flag shaped. **F:** The AF, which originates from the subacrosomal space, clearly ends before the base of the axoneme. **G:** At the end of spermiogenesis, the main sperm cell components coil.

NOTES ON SPERMIOGENESIS (fig. 25): The chromatin is highly condensed and appears threadlike (fig. 25C–E). Moreover, the chromatin thread is helically contorted. Some

mitochondria are visible. At the end of spermiogenesis, the manchette of microtubules, which surround the developing nucleus (fig. 25E), disintegrates.

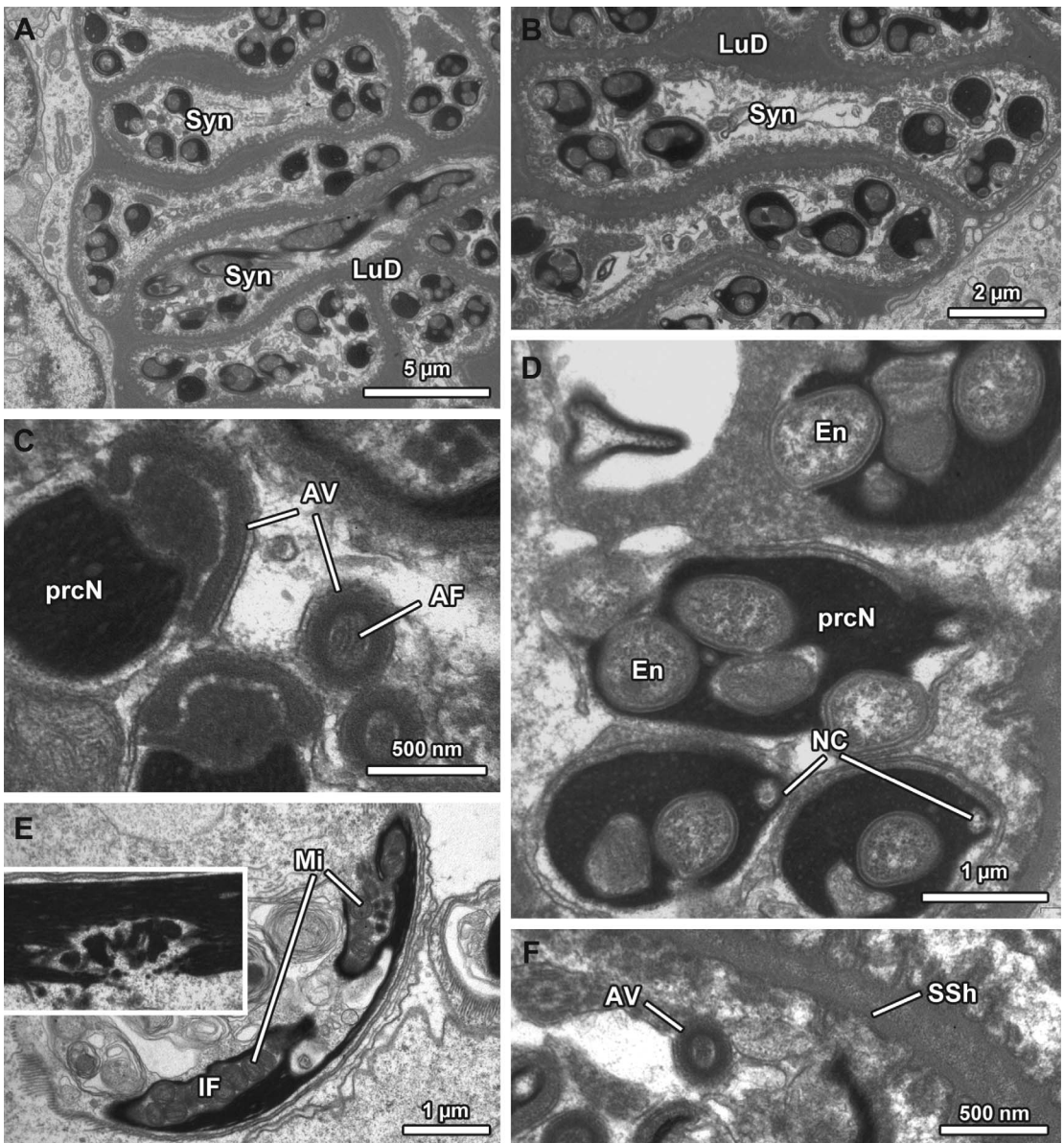


Fig. 40. Characteristics of synspermy of *Tinadysderina otonga*. **A**: Numerous synspermy are located in the lumen of the deferent ducts, additional secretions are not detectable. **B**: Sperm conjugates are disclike, thus they resemble a dumbbell in cross sections. **C**: The subacrosomal space is widened toward the anterior pole of nucleus, resulting in a conical shape of the AV. **D**: Numerous endosymbionts occur within the nucleus of the sperm. **E**: The nucleus appears torn in some sperm, which is probably related to the endosymbiont infection and might affect the chromatin condensation (inset). **F**: The irregularly folded membrane of syncytium is surrounded by a thin secretion sheath.

*Orchestina* sp. 1 (Chile)

SPERM TRANSFER FORM (figs. 26, 27):  
 Long (>80 µm), tubelike synspermy (fig. 26),

comprising two sperm (fig. 26) that are arranged consecutively to each other (fig. 26). A thick electron-dense secretion sheath (~800 nm) surrounds the sperm conjugates

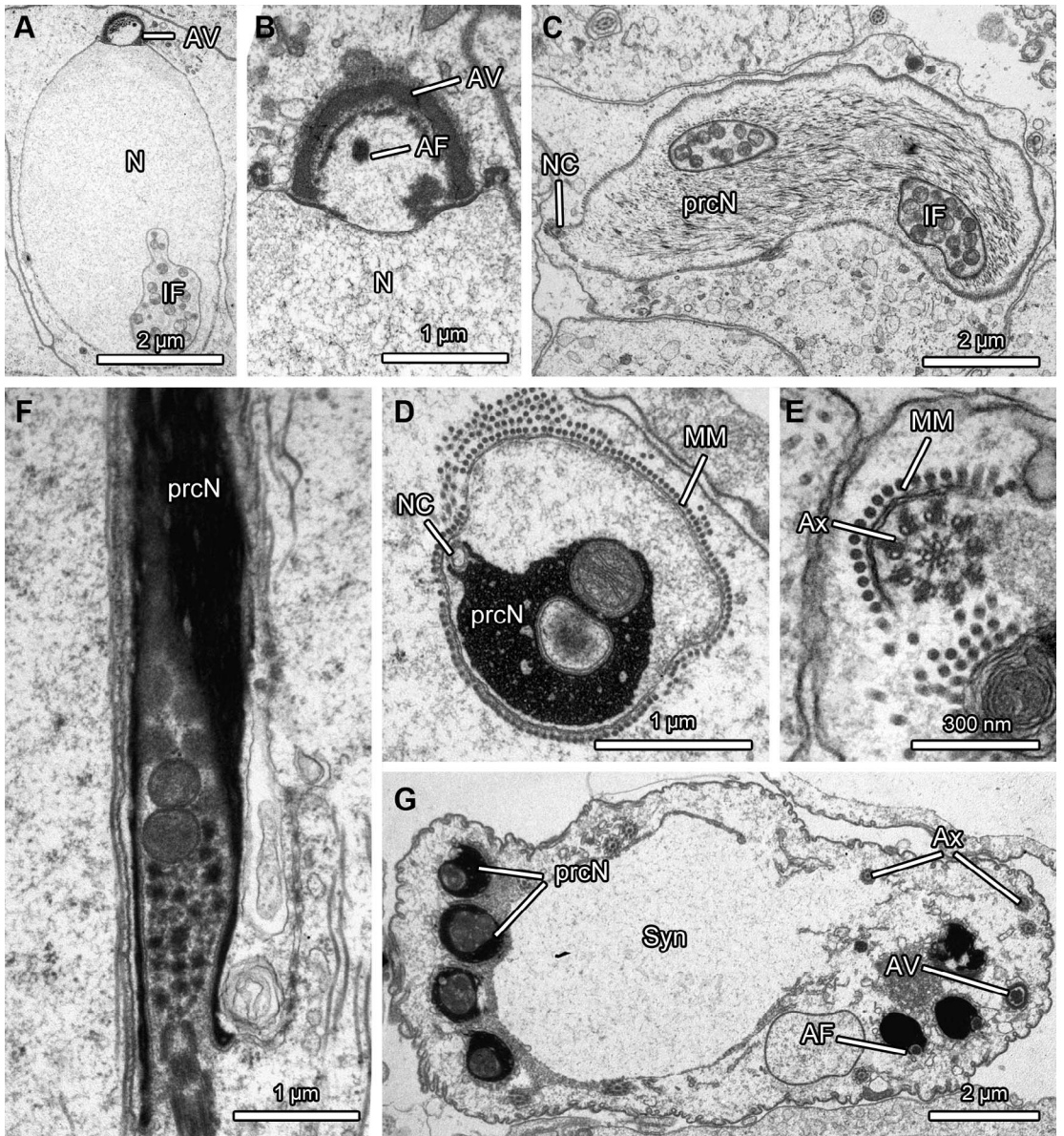


Fig. 41. Characteristics of spermiogenesis of *Tinadysderina otonga*. **A:** The implantation fossa of early spermatids is already filled with a large amount of mitochondria. **B:** The subacrosomal space is enlarged toward the anterior pole of nucleus. **C:** The chromatin appears fibrillar in mid spermatids. **D:** During further development, the chromatin condenses irregularly as indicated by the manchette of microtubules, which illustrates the actual dimensions of the nucleus. **E:** Little electron-dense material surrounds the microtubules of the axoneme. **F:** In addition to mitochondria, small electron-dense secretions are located in the IF. **G:** At the end of spermiogenesis four spermatids fuse to form synsperma.

(fig. 27A–D). Sperm cell components are uncoiled (fig. 26) and surrounded by a small amount of conspicuous electron-dense fibrils, mitochondria are present (fig. 27B).

**SPERMATOZOA** (fig. 27): **Acrosomal complex:** AV small, cylindrical. AF originates from the subacrosomal space and extend into the nuclear canal. **Nucleus:** prcN tubelike and

elongated (~19.2  $\mu\text{m}$ ) with deep implantation fossa that extends as far as the anterior pole of the nucleus and is filled with a distinct, electron-dense centriolar adjunct (fig. 27C). peN absent (fig. 27E). NC located in the periphery. **Axoneme:** short (~19.2  $\mu\text{m}$ ); 9+3 microtubular pattern.

**NOTES ON SPERMIOGENESIS** (fig. 28): Within the testis all stages of spermiogenesis are visible. A small, developing AV is attached to the cell membrane (fig. 28A, inset) and extends toward the anterior pole of nucleus, from which it is separated by a distinct electron-dense plate (fig. 28A). The AF originates from the subacrosomal space. During development of the spermatids the chromatin condenses and appears fibrillar in midspermatids (fig. 28B–D). The deep implantation fossa of early and midspermatids is filled with numerous microfilaments (fig. 28 C, D) and few electron-dense secretions (fig. 28C, D) that form a distinct centriolar adjunct in late spermatids, which completely covers the proximal centriole (fig. 28E–G). In the periphery of the developing spermatids numerous looplike constrictions are visible (fig. 28H inset), resulting in a fringed appearance of the latter (fig. 28H, I).

*Orchestina* sp. 2 (Argentina)

**SPERM TRANSFER FORM** (fig. 29): Long, tubelike synspermia (fig. 29A), comprising two spermatozoa. The sheath that surrounds the sperm conjugates (~1  $\mu\text{m}$ ) is formed in the deferent ducts (fig. 29B, C) and further condenses during the passage of the sperm conjugates toward the ejaculatory duct. Early sperm conjugates are oval shaped and further compress and elongate within the long deferent ducts. Fused sperm of a sperm conjugate are not coiled (fig. 29 E). Mitochondria are always present within the cytoplasm of the syncytium (fig. 29E).

**SPERMATOOZOA** (fig. 29): **Acrosomal complex:** AV small, cylindrical (fig. 29E), and provided with a narrow subacrosomal space. AF originates from the subacrosomal space and extends into the NC (fig. 29D). **Nucleus:** prcN tubelike (fig. 29E) and provided with a very deep implantation fossa that extends as far as the anterior pole of the nucleus. The implantation fossa is filled with a large

amount of an electron-dense centriolar adjunct (fig. 29D–F). peN not developed (fig. 29F). NC located in the periphery of the prcN (fig. 29D). **Axoneme:** 9+3 microtubular pattern.

**NOTES ON SPERMIOGENESIS:** Information on spermiogenesis were not obtained due to missing material from the testis.

*Paradysderina fusiscuta* Platnick and Duperré, 2011

**SPERM TRANSFER FORM** (fig. 30): Large (~12  $\mu\text{m}$ ), mainly oval synspermia (fig. 30A, B) comprising four sperm. Numerous membranes are located in the periphery (fig. 30C), as well as among all sperm components (fig. 30E). Thus, although fused, each sperm remains surrounded by its own membrane (fig. 30D). The deep implantation fossa is completely filled with mitochondria (fig. 30 E). In addition, there are numerous mitochondria located in the peripheral cytoplasm (fig. 30F). A thin, homogeneous secretion sheath (~50 nm) surrounds the sperm transfer forms (fig. 30F).

**SPERMATOOZOA** (fig. 30): **Acrosomal complex:** AV small, cylindrical with narrow subacrosomal space. AF originates from the subacrosomal space and extends into the nuclear canal, clearly ends after the axonemal base (fig. 30F). **Nucleus:** prcN extremely elongated, providing a deep implantation fossa that is completely filled with mitochondria (fig. 30D–F). peN long and oval shaped (fig. 30D), contains parts of the implantation fossa. NC located in the periphery. **Axoneme:** very long, always in close association with the nucleus (fig. 30D); 9+3 microtubular pattern (fig. 30D, F).

**NOTES ON SPERMIOGENESIS** (fig. 31): Within the testis all stages of spermiogenesis are present. Spermatids of the same developmental stage are arranged in cysts. Early spermatids are characterized by a large, mainly spherical nucleus that is surrounded by a manchette of microtubules. The acrosomal complex, which is composed of a small, cylindrical AV and the AF, is formed at the anterior pole of the nucleus (fig. 31A). The AV is attached to the cell membrane (fig. 31 A, B); proximally it is surrounded by some electron-dense material (fig. 31B). The wide

implantation fossa at the posterior pole of the nucleus is filled with numerous, small mitochondria (fig. 31C, D). It extends toward the prcN, as well as into the peN (fig. 31D). Further differentiation of the spermatid includes chromatin condensation that consequently appears fibrillar (fig. 31E) and an enormous elongation of the nucleus. The Ax curls around the latter (fig. 31E, F). The chromatin of late spermatids is highly condensed (fig. 31G). At the end of spermiogenesis, four slender spermatids arrange closely attached to each other. The main cell components coil within the cell membrane, while the cellular bridges widen and secondarily surround the main sperm cell components. The fused sperm are the subject to several differentiations including partial restriction of common cytoplasm and further coiling processes, before large sperm conjugates are released into the lumen of the testis (fig. 31H).

*Paradysderina yanayacu* Platnick and Dupérré, 2011

**SPERM TRANSFER FORM** (figs. 32, 33): Large (~12  $\mu\text{m}$ ), oval-shaped synspermia (fig. 33A, B) comprising four sperm (fig. 32). Numerous membrane stacks are visible (fig. 33 C, D). Sperm are coiled and curled around each other (figs. 32, 33E, F). A homogeneous secretion sheath (~250 nm) surrounds the sperm transfer forms (fig. 33A–C).

*Spermatozoa* (figs. 32, 33): **Acrosomal complex:** AV small (~1.5  $\mu\text{m}$ ), cylindrical (fig. 32), with narrow subacrosomal space. AF originates from the narrow subacrosomal space and extends into the nuclear canal but clearly ends before the axonemal base. **Nucleus:** prcN elongated (~22.9  $\mu\text{m}$ ) and helically contorted (fig. 33E, F). Surface reconstructions reveal a tubelike shape (fig. 32). peN long (~61.9  $\mu\text{m}$ ) and mainly oval in cross sections (fig. 33B, C). NC located in the periphery (fig. 33C) but empty for the most part (fig. 33C). **Axoneme:** long (~160.3  $\mu\text{m}$ ). 9+3 microtubular pattern (fig. 33C–F). Little centriolar adjunct surrounds both centrioles, as well as the base of the Ax (fig. 33F). Moreover, the peripheral microtubules of the central portion of Ax are surrounded by electron-dense material (fig. 33D).

**NOTES ON SPERMIOGENESIS** (fig. 34): Within the testis all stages of spermiogenesis are visible. Developing spermatids are arranged in cysts. Early spermatids are characterized by, e.g., a large, mainly spherical nucleus and a developing acrosomal complex. While the chromatin starts to condense it appears fibrillar (fig. 34A–C). The proximal portion of the small, cylindrical AV is enclosed by a little electron-dense material (fig. 34A, B). The nucleus is surrounded by a manchette of microtubules (fig. 34C, F). The deep and wide implantation fossa is filled with numerous mitochondria (fig. 34C, D). While the nucleus elongates the chromatin further condenses (fig. 34D). Dense chromatin of the precentriolar part of nucleus appears helically contorted around the implantation fossa (fig. 34D). Little electron-dense material is attached to the peripheral microtubules of the central Ax (fig. 34E). At the end of spermiogenesis four spermatids group closely attached and initiate curling around each other (fig. 34F, G). This process is certainly supported by microtubules that originate from the disintegrating manchette of microtubules and show a distinct arrangement (fig. 34F). The cytoplasm condenses and enlarged, widened cell membranes fold between the sperm, resulting in numerous membrane stacks and one prominent membrane whorl in the center of the sperm conjugate (fig. 34G).

*Scaphios yanayacu* Platnick and Dupérré, 2010

**SPERM TRANSFER FORM** (fig. 35): Synspermia that comprise four sperm. The entire sperm conjugate is rather large and un-sheathed. Within the lumen of the proximal deferent ducts, the nuclei of sperm of one sperm conjugate appear still spotted (fig. 35A, B), while a distinct vesicular area that is composed of numerous electron-dense vesicles surrounds the main sperm cell components (fig. 35A, B). In the distal deferent ducts this vesicular area is homogeneously electron dense (fig. 35C, D). The periphery of the sperm conjugate is built by large quantities of granular cytoplasm of the syncytium, which contains numerous mitochondria and vesicles

(fig. 35C). Only the axonemes coil within the membrane of the syncytium (fig. 35D–E).

**SPERMATOZOA** (fig. 35): **Acrosomal complex:** AV conical with moderately widened subacrosomal space (fig. 35F). AF originates from the subacrosomal space and extends into the nuclear canal but clearly ends before the base of the axoneme. **Nucleus:** prcN elongated, compact, and tubelike (fig. 35C) with a small implantation fossa that comprises only the two centrioles. peN not identifiable. NC located in the periphery, in late spermatids not identifiable. **Axoneme:** 9+3 microtubular pattern (fig. 35D, E).

**NOTES ON SPERMIOGENESIS** (fig. 36): The periphery of spermatids of all developmental stages is frequently invaginated and folded, resulting in a loose and spongy appearance (fig. 36A). Early spermatids are characterized by a large, oval nucleus with already irregularly condensed chromatin (fig. 36A). The subacrosomal space of the developing AV is enlarged (fig. 36B). The AF extends into the NC (fig. 36B) but clearly ends before the end of the axonemal base (fig. 36B, E inset). The AV is surrounded by electron-dense material in mid spermatids (fig. 36C). The chromatin condenses irregularly, resulting in a spotted appearance of the nucleus of mid- and late spermatids (fig. 36D, E). Conspicuous membrane whorls, as well as electron-dense vesicles are in close association to the nucleus (fig. 36D). At the end of spermiogenesis, four spermatids fuse, while the main sperm cell components arrange in the center of the developing sperm conjugate (fig. 36F).

*Silhouettella loricatula* (Roewer, 1942)

**SPERM TRANSFER FORM** (fig. 37): Large, cone-shaped synspermia comprising four sperm. The cytoplasm of the syncytium is heterogeneous and numerous electron-dense plates and droplets, as well as electron-lucent gaps occur (fig. 37A, B). The most obvious characteristic is the distinct, irregular chromatin-condensation pattern (fig. 37B, C). Numerous platelike membrane stacks are visible in the periphery of the sperm conjugate (fig. 37D). A thin homogeneous secretion sheath (<100 nm) surrounds each sperm conjugate (fig. 37A, B, D).

**SPERMATOZOA** (fig. 37): **Acrosomal complex:** AV cylindrical. AF originates from the subacrosomal space and extends into the nuclear canal. **Nucleus:** prcN elongated, characterized by a conspicuous irregular chromatin-condensation pattern (fig. 37A–C) and a very small implantation fossa that contains only the two centrioles (fig. 37B). peN not visible in mature sperm; NC located in the periphery (fig. 37C), but empty for the most part (fig. 37C). **Axoneme:** 9+3 microtubular pattern.

**NOTES ON SPERMIOGENESIS** (fig. 38): The anterior portion of the prcN is deeply indented and surrounds the AV (fig. 38A, B) in addition to a little electron-dense material (fig. 38B). Besides the AF the subacrosomal space contains some granular material (fig. 38B). The chromatin starts condensation around the nuclear canal (fig. 38C, D) before the characteristic chromatin-condensation pattern is formed (fig. 38F). While the nucleus elongates and the chromatin starts to condense, a small dropletlike elongation of the nucleus is formed (fig. 38E). This peN probably disintegrates in further development. The implantation fossa is very small and contains only the two centrioles (fig. 38F). Neither the centrioles nor the axoneme (fig. 38F inset) are surrounded by electron-dense material.

*Stenoonops peckorum* Platnick and Dupérré, 2010

**SPERM TRANSFER FORM** (fig. 39): Synspermia (fig. 39G); refers to data obtained from sperm conjugates in the lumen of the testis, because the deferent ducts were empty. The number of sperm that are fused within synspermia is uncertain.

**SPERMATOZOA** (fig. 39): **Acrosomal complex:** AV cylindrical, narrow subacrosomal space (fig. 39E). AF originates from the subacrosomal space and extends into the nuclear canal (fig. 39B, F) but clearly ends before the axonemal base (fig. 39E). **Nucleus:** prcN extremely elongated and tubelike (fig. 39D). The chromatin is homogeneously condensed, the surface appears smooth (fig. 39D, F). IF very small, comprising only the two centrioles. peN very short, thin, and flag shaped (fig. 39E). NC located in the

periphery (fig. 39F). **Axoneme:** 9+3 microtubular pattern (fig. 39E).

**NOTES ON SPERMIOGENESIS** (fig. 39): Within the testis, cysts of developing spermatids of different developmental stages occur. In early spermatids the chromatin starts condensation in the center of the developing nucleus (fig. 39A). A manchette of microtubules surrounds the nucleus (fig. 39B) and parts of the Ax. It appears fibrillar in mid spermatids (fig. 39C). The nucleus enormously elongates in midspermatids and finally becomes tubelike in late spermatids (fig. 39D). At the end of spermiogenesis the main sperm cell components coil within the cell (fig. 39G).

*Tinadysderina otonga* Platnick, Berniker and Bonaldo, 2013

**SPERM TRANSFER FORM** (fig. 40): Large (~12  $\mu\text{m}$ ), dislike synspermia (fig. 40A, B) comprising four spermatozoa. Sperm conjugates are flattened, dislike and resemble a dumbbell in cross sections (fig. 40A, B). All sperm conjugates show numerous bacteria occupying the nuclei (fig. 40, D, E). Infected sperm are already visible in the testis, where the spermatid development is likely influenced by means of, e.g., a partially deficient chromatin condensation (fig. 40E inset). A thin, homogeneous secretion sheath (~80 nm) surrounds the sperm conjugates (fig. 40 F).

**SPERMATOZOA** (fig. 40): **Acrosomal complex:** AV conical, thus widened posteriorly (fig. 40C), possessing a narrow subacrosomal space (fig. 40C). AF originates from the subacrosomal space and extends into the nuclear canal, but clearly ends before the base of the Ax. **Nucleus:** prcN elongated, tubelike with deep implantation fossa that contains numerous mitochondria (fig. 40E), as well as electron-dense secretions. peN long, oval shaped. NC located in the periphery, empty for the most part (fig. 40D). **Axoneme:** 9+3 microtubular pattern.

**NOTES ON SPERMIOGENESIS** (fig. 41): Within the testis, all stages of spermiogenesis are visible. Spermatids develop in large cysts. Early spermatids are characterized by, e.g., a large, oval nucleus, and a developing acrosomal complex (fig. 41A, B). Besides

the AF the subacrosomal space possesses little electron-dense material (fig. 41B). The nucleus of early spermatids is slightly indented at its anterior pole (fig. 41B). At its posterior pole, a large implantation fossa, containing numerous small mitochondria, is formed (fig. 41C). Further spermatid development includes chromatin condensation, which appears fibrillar in mid spermatids (fig. 41C). As a consequence, the nucleus elongates extremely and involves certain shape changes, finally resulting in a tubelike appearance. The nucleus is always surrounded by a manchette of microtubules (fig. 41D), which disintegrates after sperm conjugation. Additional microtubules located near other cell components are visible in all developmental stages (fig. 41E). The implantation fossa contains little electron-dense secretions, in addition to numerous mitochondria. The two centrioles are arranged in tandem position in late spermatids (41F). At the end of spermiogenesis four spermatids fuse (fig. 41G). These large, early sperm conjugates are characterized by a large, electron-lucent cytoplasm in the center (fig. 41G), and numerous membranes, as well as Golgi derivatives (fig. 41G). The cell membrane of the syncytium is irregularly folded in the periphery (fig. 41G). Further development includes condensation of cytoplasm.

## DISCUSSION

The present study provides the first comparative analysis of the primary male genital system and spermatozoa of the highly diverse spider family Oonopidae. A total of 18 species corresponding to 13 genera were investigated and analyzed with respect to evolutionary and functional implications.

## EVOLUTIONARY AND FUNCTIONAL IMPLICATIONS

**EVOLUTIONARY MORPHOLOGY OF SPERM TRAITS:** Most female spiders mate with more than one male, thus spider sperm are suggested to show a remarkable structural diversity, due to postcopulatory sexual selection and sperm competition (Michalik and Ramírez, 2014). Compared to all other spider

TABLE 1

**Length of the Axoneme and Nucleus based on Measurements Obtained from Surface Reconstructions**

Note: the axoneme is always shorter, or as long as the nucleus (precentriolar part of nucleus and postcentriolar elongation of nucleus) in species with a very short postcentriolar elongation of nucleus.

|                    | Source                           | Length<br>of Ax<br>( $\mu\text{m}$ ) | Length<br>of prcN<br>( $\mu\text{m}$ ) | Length<br>of peN<br>( $\mu\text{m}$ ) | Length<br>of N<br>( $\mu\text{m}$ ) | Relation<br>Ax:N |        |
|--------------------|----------------------------------|--------------------------------------|--|---------------------------------------|-------------------------------------|------------------|--------|
| <b>Caponiidae</b>  | <i>Caponina alegre</i>           | Lipke and<br>Michalik, 2012          | 51.9                                   | 2.5                                   | 73.7                                | 76.2             | Ax < N |
| <b>Orsolobidae</b> | <i>Hickmanolobus mollipes</i>    | Lipke et al., 2014                   | 28.4                                   | 5.8                                   | 4.7                                 | 10.5             | Ax > N |
|                    | <i>Osornolobus</i> sp. 1         |                                      | 51.9                                   | 5.6                                   | 9.8                                 | 15.4             | Ax > N |
|                    | <i>Osornolobus</i> sp. 2         |                                      | 34.6                                   | 6.5                                   | 6.5                                 | 13               | Ax > N |
|                    | <i>Tasmanoonops alipes</i>       |                                      | 25.1                                   | 3.2                                   | 5.2                                 | 8.4              | Ax > N |
|                    | <i>Tasmanoonops</i> sp. 1        |                                      | 19.5                                   | 3.6                                   | 2.9                                 | 6.5              | Ax > N |
|                    | <i>Tasmanoonops</i> sp. 2        |                                      | 20.9                                   | 4.6                                   | 4                                   | 8.6              | Ax > N |
| <b>Oonopidae</b>   | <i>Escaphiella ramirezi</i>      | present study                        | 58.4                                   | 1.3                                   | 126                                 | 127.3            | Ax < N |
|                    | <i>Orchestina</i> sp. 1 (Chile)  |                                      | 19.2                                   | –                                     | 19.2                                | 19.2             | Ax = N |
|                    | <i>Neotrops pombero</i>          |                                      | >55                                    | 5.4                                   | 11.7                                | 17.1             | Ax > N |
|                    | <i>Neoxyphinus termitophilus</i> |                                      | 291.5                                  | 171.8                                 | 10.13                               | 181.93           | Ax > N |
|                    | <i>Oonops</i> sp. (Ibiza)        |                                      | 23.4                                   | 2.9                                   | 4.3                                 | 7.2              | Ax > N |
|                    | <i>Paradysderina yanayacu</i>    |                                      | 160.3                                  | 61.9                                  | 22.9                                | 84.8             | Ax > N |

taxa studied to date, such diversity is most evident in Oonopidae. We identified certain morphological characteristics that are likely influencing specific functions of the sperm, e.g., sperm movement. Furthermore, the relative size of the nucleus compared to the axoneme, for example, was proposed to be a good predictor of sperm velocity (Calhim et al., 2011). It has been shown in mammals that proportions between individual sperm cell components, i.e., the ratio of the nucleus to the flagellum, influence the swimming velocity (e.g., Gage, 1998; Malo et al., 2006; Humphries et al., 2008; Lüpold et al., 2009). To our knowledge, there is no study relating the actual efficiency of spider sperm movements with the form and shape of specific sperm cell components. However, we assume the size and shape of, for example, the postcentriolar elongation are likely influencing the efficiency to move. The absence of a postcentriolar elongation of nucleus, for example, in *Gamasomorpha* cf. *vianai*, *Cinetomorpha* sp. (Iguazú), *Orchestina* sp. 1 (Chile), *Orchestina* sp. 2 (Argentina), and *Silhouettella loricatula*, as well as the reduction of the latter to a very tiny flag-shaped appendix in *Escaphiella ramirezi* and *Stenoonops peckorum*, is particularly obvious and opposed to the extreme long postcentriolar elongation (compared to the pre-

triolar part of nucleus) of, e.g., *Neoxyphinus termitophilus* (see table 1). Interestingly, the length of the postcentriolar elongation is likely correlated with the length of the axoneme. Michalik and Ramirez (2014) suggested that the length of the postcentriolar elongation is best estimated in relation to the precentriolar part of nucleus (char. 22) based on sections of the latter within sperm transfer forms, whereas the length of the axoneme is indicated based on the number of coils of the axoneme within the sperm transfer form (char. 29). As shown in figure 42, based on these measures there is a trend toward a shorter axoneme in species with a very short postcentriolar elongation. However, the number of coils is probably only a valid measure in cleistospermia and highly dependent on the overall compactness of the STF. Moreover, virtually all estimates of the length of sperm cell components are based on 2D TEM images, which particularly hinder specification in large and complex primary sperm conjugates. However, this limitation can be circumvented with the help of surface reconstruction.

Within spiders, Lipke and Michalik (2012) provided the first surface reconstruction of sperm conjugates of *Caponina alegre* Platnick, 1994 (Caponiidae), and depicted the extremely short postcentriolar elongation

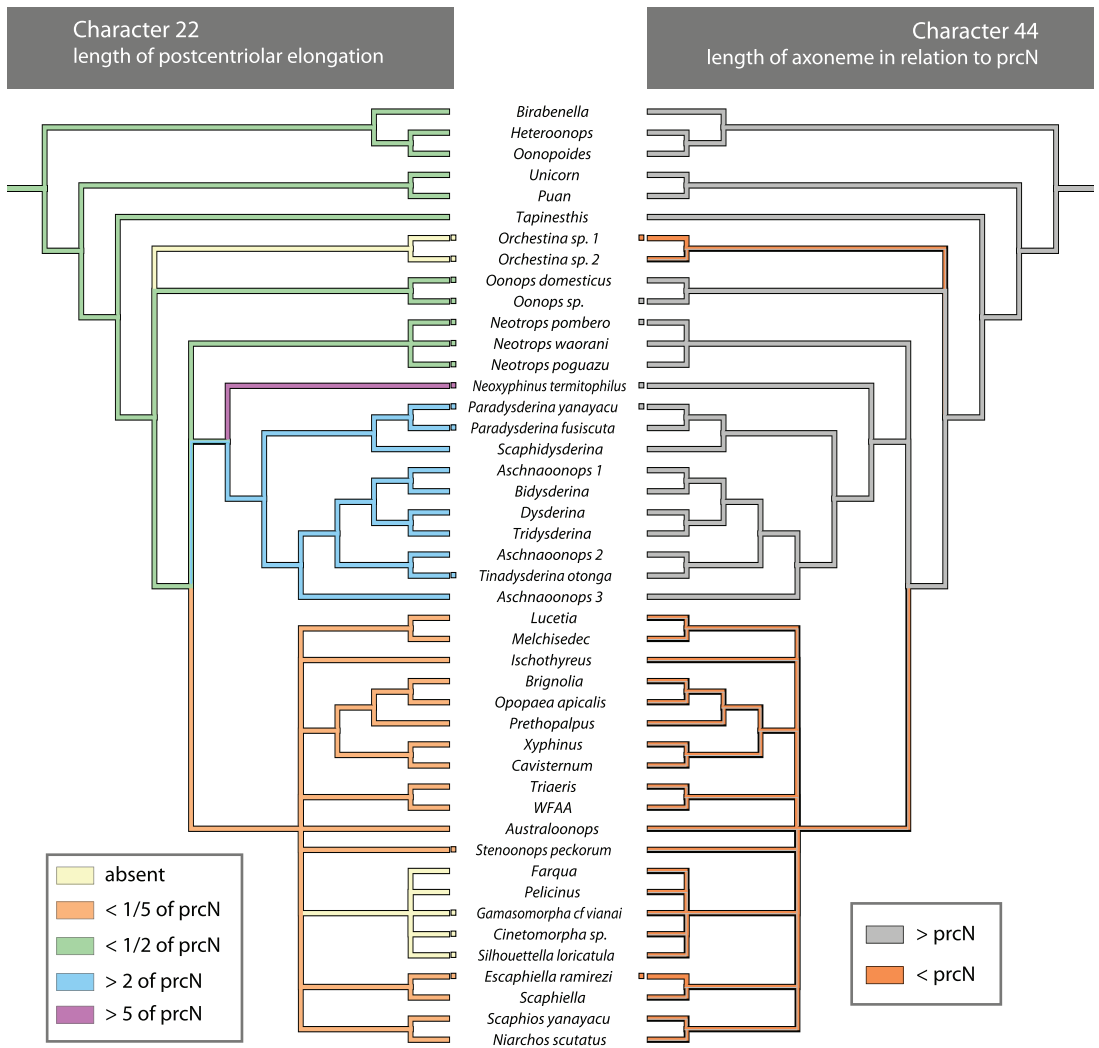


Fig. 42. Scenario of the evolution of the length of peN and length of axoneme. Note, that the axoneme is shorter than the prcN in species with a very small postcentriolar elongation, and in those species that lack the latter as e.g., *Orchestina* sp. 1 (Chile). Although the ratio of length of the axoneme in relation to the nucleus could be precisely measured only from a surface reconstruction, the number of coils of the axoneme (char. 29) in 2D images allows similar conclusions. Phylogeny based on Bayesian tree as given in de Busschere et al. (2014).

(~2.5 μm), as well as an axoneme (~52 μm), which is shorter than the precentriolar part of nucleus (~74 μm). Recently, Lipke et al. (2014) analyzed several representatives of Orsolobidae and revealed postcentriolar elongations having a similar length as the precentriolar part of nucleus, while the axoneme is longer than the precentriolar part of nucleus. The present study further complements knowledge on this issue (see

table 1). In *Escaphiella ramirezi*, for example, the postcentriolar elongation is very short (~1.3 μm) while the axoneme (~58.4 μm) is shorter than the precentriolar part of nucleus (~126 μm). On the other hand, the postcentriolar elongation is very long in, e.g., *Neoxyphinus termitophilus* (~171.8 μm), while its axoneme is also extremely long (~291.5 μm) and much longer than the precentriolar part of the nucleus (~10.1 μm). Thus, there is likely

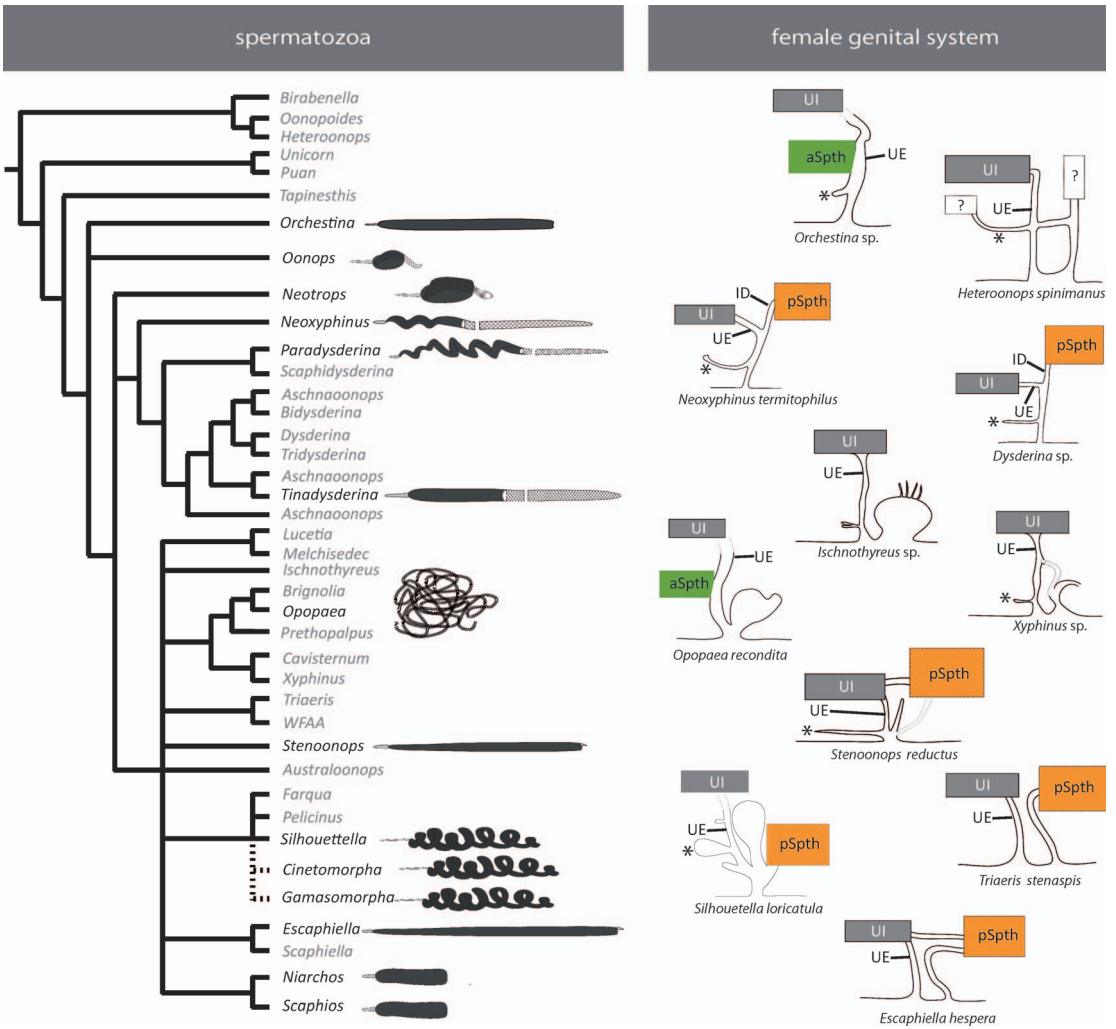


Fig. 43. Schematic drawings of sperm (virtually uncoiled) of all investigated Oonopidae and simplified schematic drawings of the female genital system based on the detailed descriptions of Burger (2007, 2009, 2010, 2011) and Burger et al. (2003, 2006, 2010a). Implications on the actual shape and size of sperm storage sites and specific components of the female genital system are not represented to facilitate the understanding on the relationship of individual parts of the female genital system. Phylogeny based on Bayesian tree as given in de Busschere et al. (2014). Dashed lines indicate additional taxa analyzed in the present study, which were placed according to their sperm morphology. The asterisks indicate the position of the anterior sclerite.

a positive correlation between the length of the axoneme and the length of the postcentriolar elongation of the nucleus. Species provided with a very short or missing postcentriolar elongation have a short axoneme, whereas a long axoneme always cooccurs with a prominent postcentriolar elongation (table 1).

In a comparative study on diving beetles, Higginson et al. (2012) suggested that the evolution of sperm morphology is likely driven by the complexity of the female reproductive tract. However, according to our results, such a correlation is not evident in Oonopidae. Although the female reproductive tract is astonishingly diverse in Oonopi-

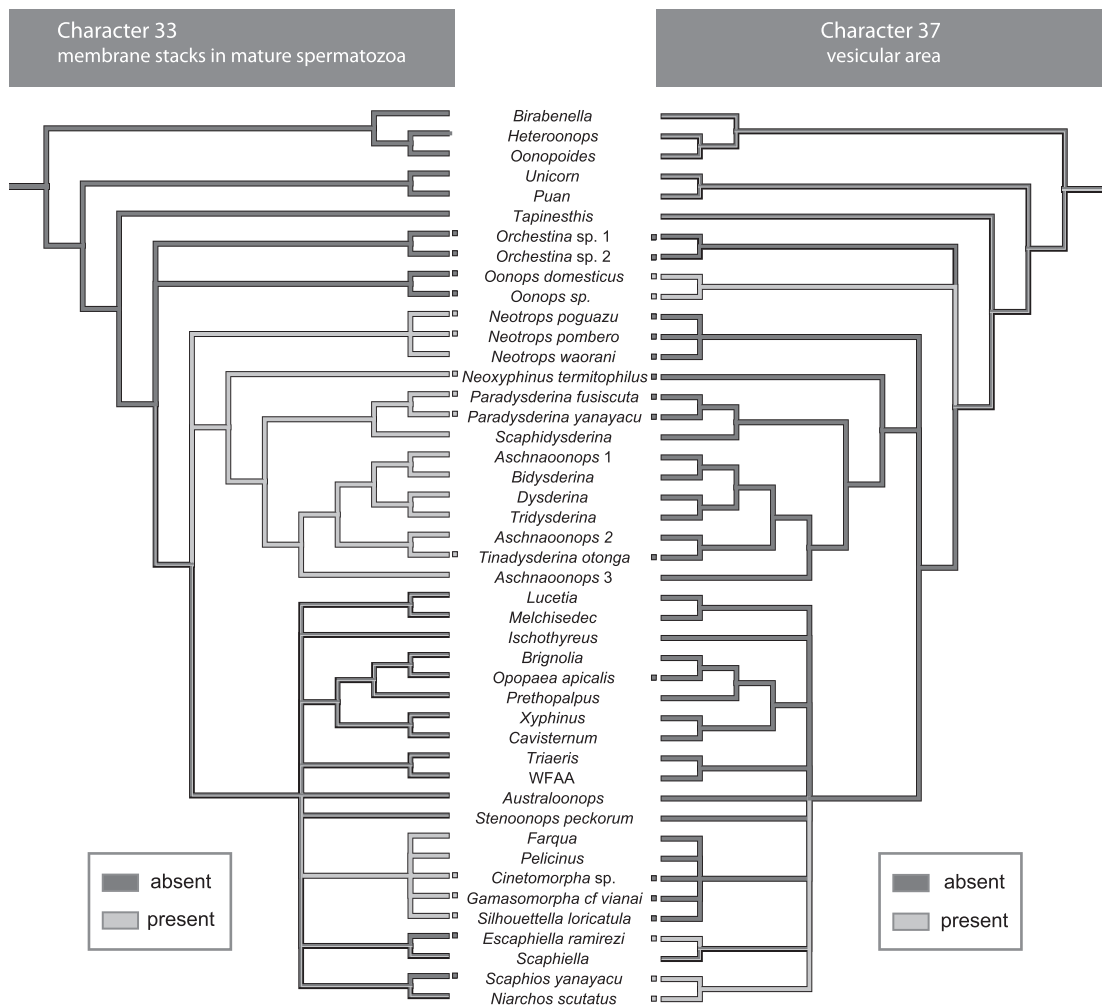


Fig. 44. Evolutionary scenario illustrating the occurrence of a distinct vesicular area and membrane stacks in mature spermatozoa. Within sperm transfer forms of the investigated Oonopidae, only one type of these additional membrane reservoirs is present. Phylogeny based on Bayesian tree as given in de Busschere et al. (2014).

dae and highly complex in certain species (Burger, 2007, 2009, 2010a, 2011; Burger et al., 2003, 2006, 2010), this diversity has no apparent correlation in sperm morphology. Females of *Silhouettella loricatula* and *Neoxyphinus termitophilus*, for example, share a very similar organization with respect to their reproductive tracts, but sperm morphology is exceptionally different in these species (fig. 43).

**AFLAGELLATE SPIDER SPERM—THE CASE OF *OPOPAEA APICALIS*:** In general, a sperm is composed of a head (haploid genetic materi-

al), a midpiece (composed of mitochondria that surround the base of the axoneme) and a flagellum (Morrow, 2004). However, in spiders a distinct midpiece is known only from Mesothelae (Ōsaki, 1969; Michalik et al., 2004a; Michalik, 2007). Mitochondria, if present at all, are nonspecifically distributed within the cytoplasm of the sperm transfer forms. Spider sperm are further characterized by a 9+3 axonemal pattern; thus the axoneme possesses three central tubuli (Ōsaki, 1969; Baccetti et al., 1970; Alberti, 1990), although some taxa within Orbiculariae lost the central

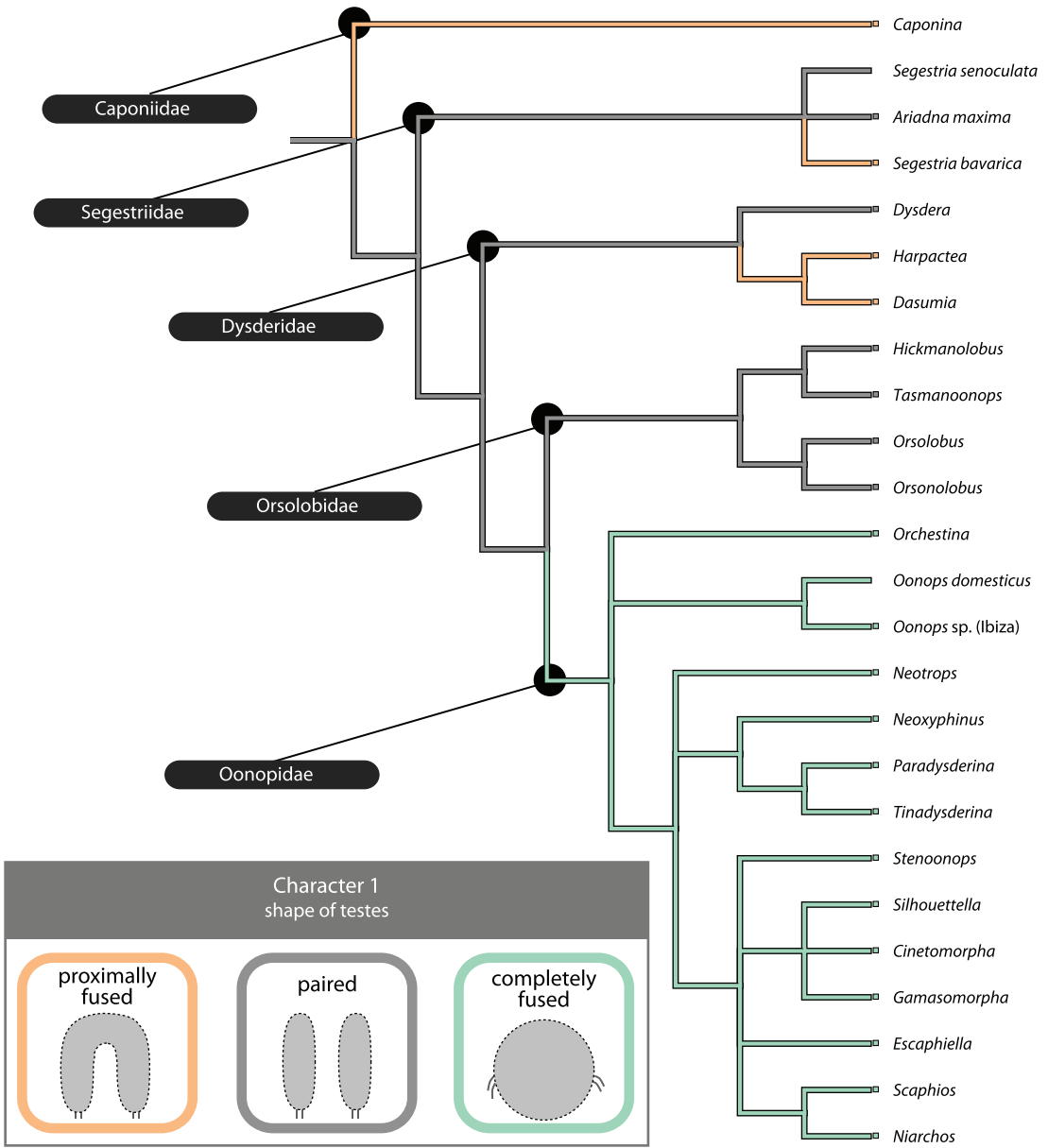


Fig. 45. One potential evolutionary scenario illustrating the diversity of testis organization in Dysderoidea. Data of Caponiidae, Segestriidae, Dysderidae, and Orsolobidae were obtained from the literature (Michalik et al., 2004b; Michalik, 2009; Lipke and Michalik, 2012; Lipke et al., 2014; Michalik and Ramírez, 2014).

tubuli exhibiting a derived 9+0 (Linyphiidae, Pimoidae) or 12+0 (Synotaxidae) axonemal pattern (Alberti, 1990; 2000; Michalik and Alberti, 2005; Michalik and Hormiga, 2010; Michalik and Ramírez, 2014). However, aside from the above-mentioned exceptions con-

cerning the microtubular pattern, all spider sperm described to date are flagellated. In contrast, in *Opopaea apicalis* neither an axoneme nor centrioles can be identified within spermatids, or mature sperm. Thus, this species possesses aflagellate sperm, which

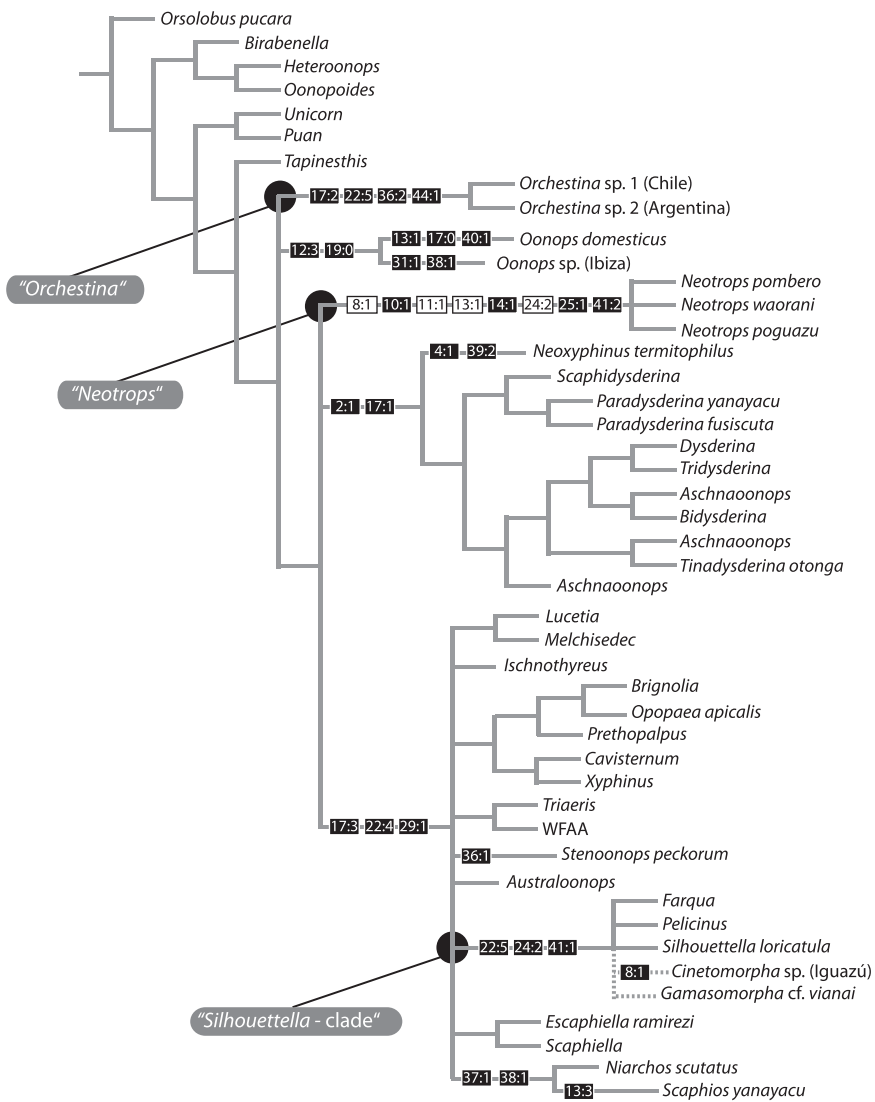


Fig. 46. Synapomorphies from the male reproductive system and sperm of Oonopidae (char. number:state number). Black boxes indicate unambiguous synapomorphies; dashed lines are used for two additional species investigated in the present study that were placed according to their sperm morphological traits. Phylogeny based on Bayesian tree as given in de Busschere et al. (2014).

is the first reported case of this condition for spiders. Although unique for spiders, the loss of a flagellum is known throughout all animal groups and has evolved independently in at least 36 taxonomic groups (Morrow, 2004). This structural loss usually involves a loss of motility (Pitnick et al., 2009), but production of such sperm is suggested to be less time-consuming and less expensive (Pitnick, 1996; Morrow, 2004). In a comparative approach

using sister groups for which the level of sperm competition was unambiguously known, Morrow (2004) suggested that the absence of a flagellum, and thus the loss of motility, is favored when sperm competition is low or absent. Whether this holds true for the spermatozoa of *O. apicalis* remains unclear, as detailed information on the mating behavior and postcopulatory processes of oonopids (i.e., sperm dumping, which is

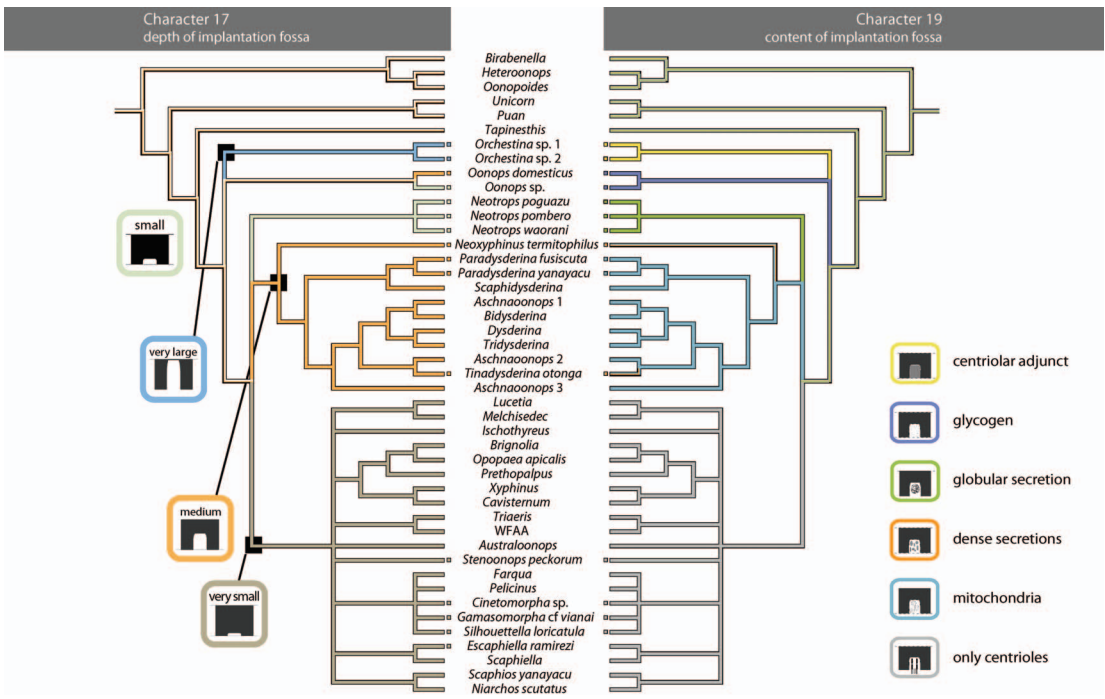


Fig. 47. Depth of IF and its content. The deep implantation fossa of both *Orchestina* species is filled with a distinct centriolar adjunct. In general there is only one type of content present in the IF. In contrast, the implantation fossa of *Neoxyphinus termitophilus* and *Tinadysderina otonga* are filled with mitochondria, as well as additional dense secretions. The very small IF of, e.g., *Escaphiella ramirezi*, contains only the two centrioles. Phylogeny based on Bayesian tree as given in de Busschere et al. (2014).

reported in, e.g., *Silhouettella loricatula* Burger, 2007; 2010a) are mostly missing.

The peculiar sperm of *O. apicalis* provide further features that are not known from any other spider taxon to date. Spermatozoa of this species are composed only of a condensed chromatin thread within an irregularly electron-dense cytoplasm surrounded by a thin, electron-lucent secretion sheath. Whether only one or several chromatin threads are transferred remains unclear.

**INTRANUCLEAR ENDOSYMBIONTS—THE CASE OF *TINADYSDERINA OTONGA*:** Bacterial endosymbionts, especially those of the reproductive system, are extremely widespread in nature (Metcalf and Bordenstein, 2012) and *Wolbachia* is probably the most common endosymbiont, infecting an estimate of more than two thirds of arthropod species (Darby et al., 2007; Hilgenboecker et al., 2008). Most important, *Wolbachia* is known to affect the reproductive biology, i.e., forcing asexuality

of the host species and feminizing the host species by means of a strongly biased sex ratio, as well as inducing male killing and incompatibility (reviewed in Werren et al., 2008). Arthropod endosymbionts are in general transmitted maternally and thus involve an evolutionary conflict, which might affect the reproduction of infected species. However, so far, only a few spiders (including at least two oonopid taxa) are known to be parthenogenetic (Platnick et al., 2012a).

In spiders, besides *Wolbachia* there are only few other endosymbionts (e.g., *Rickettsia*, *Spiroplasma*, *Cardinium*) recognized (Afzelius et al., 1989; Goodacre et al., 2006; Duron et al., 2008; Martin and Goodacre, 2009; Vanthournout et al., 2011). In general, most of these endosymbionts are maternally inherited and thus common in females, especially within the female germ line (Duron and Hurst, 2013). Alberti et al. (1986) described *Rickettsia*-infected sperm conju-

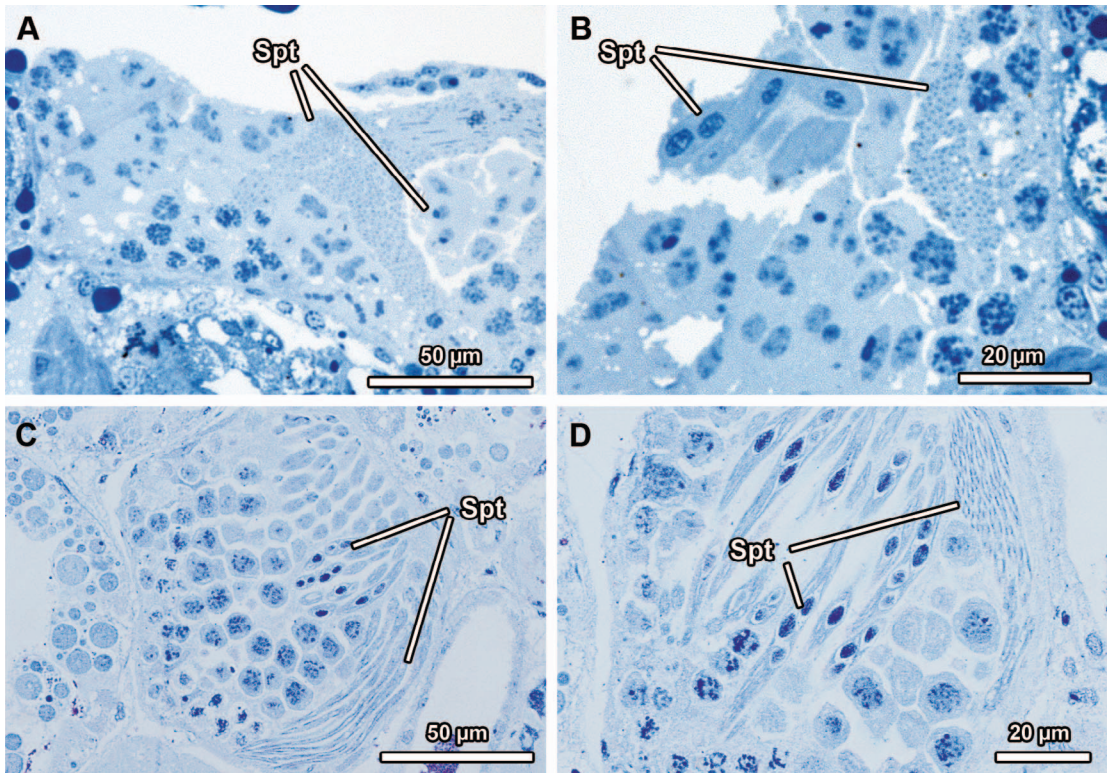


Fig. 48. Characteristics of sperm developmental stages of *Opopaea apicalis* (A, B) and *Brignolia parumpunctata* (C, D) as revealed by light microscopy. Note the similar organization of spermatogenic stages in both species, as well as the appearance of condensed chromatin, accordingly. (C and D, courtesy of M. Burger)

gates (coenospermia) of one specimen of the bird spider *Pamphobeteus* sp. (Theraphosidae), thus suggesting the occurrence of paternal transmission. This first evidence of infected spider sperm was subsequently followed by a screening of sperm of 35 spider taxa (theraphosid and araneomorph spiders) for these endosymbionts, revealing no further indications of an infection (Afzelius et al., 1989). Although numerous subsequent studies addressed the fine structure of spider spermatozoa (e.g., Alberti, 1990; Michalik et al., 2003; 2004a, 2004b, 2005a, 2005b; Michalik and Uhl, 2005) another evidence of endosymbionts within spermatids and sperm was given only 20 years later by Michalik et al. (2006) for a tetragnathid (*Tetragnatha boydi* O. P.-Cambridge, 1898). Hence, our study, which revealed the presence of endosymbionts within developing and mature sperm of the goblin spider *Tinadysderina otonga*, is

the third description of endosymbionts in spiders in general and the first description within Synspermiata to date. However, in contrast to the sparsely distributed endosymbionts in sperm conjugates of the bird spider (compare Afzelius et al., 1989), almost all sperm were infected in *Tinadysderina*. We analyzed the reproductive system of two specimens, both of which showed high infestation rates. Moreover, in contrast to the infected tetragnathid spider, where endosymbionts were apparently present only in spermatids (Michalik et al., 2006), we observed large quantities of endosymbionts in both, developing spermatids and mature sperm. Thus, intranuclear endosymbionts are likely transferred and the influence on the reproductive biology of this species should be addressed in future studies.

A recent study (Watanabe et al., 2014) illustrated extensive intranuclear *Rickettsia*

infections of sperm of a leafhopper (*Nephotettix cincticeps* (Uhler, 1896)). The authors furthermore demonstrated for the first time that these endosymbionts are efficiently transmitted paternally via an intrasperm passage, without depressing sperm function. This mode of transmission might also apply for endosymbionts of *Tinadysderina otonga*, because infections were not thought to interfere with spermatid development or sperm conjugation, although there are indications on locally deficient chromatin condensation. However, the actual effect of endosymbiont infections should be addressed in further studies focusing on the efficacy and longevity of sperm in this species.

**SPERM CONJUGATION:** Within spiders, Haplogynae are particularly diverse with respect to sperm transfer forms (Alberti, 1990; Michalik and Lipke, 2013; Michalik and Ramírez, 2014). Besides individual sperm (cleistospermia), sperm are transferred as sperm conjugates (two or more sperm that are physically united). Based on developmental mechanisms, two types of sperm conjugation, primary and secondary, can be distinguished (Higginson and Pitnick, 2011). Sperm of primary sperm conjugates originate from a common spermatogonium and remain associated with each other. In contrast, secondary sperm conjugates are formed after separation of spermatids. In spiders, coenospermia that are described for Filistatidae (Alberti and Weinmann, 1985; Michalik et al., 2003) as well as the so-called rouleaux, which are known from Telemidae (e.g., Legendre and Lopez, 1978; Juberthie et al., 1981), represent secondary sperm conjugates, whereas synspermia are classified as primary sperm conjugates (reviewed in Michalik and Ramírez, 2014). Synspermia are present in a wide range of ecribellate Haplogynae families including Caponiidae, Dysderidae, Segestriidae, Scytodidae, and Sicariidae (Alberti and Weinmann, 1985; Michalik et al., 2004b), and this STF was recently recovered as synapomorphy for ecribellate Haplogynae. Thus, this heterogeneous large clade of araneomorph spiders was named Synspermata accordingly (Michalik and Ramírez, 2014).

In oonopids, both cleistospermia and synspermia have been reported (Alberti and

Weinmann, 1985; Michalik and Ramírez, 2014; present study). However, the mechanism of the formation of STF varies remarkably. For example, the spermatids of *Niarchos scutatus* already fuse entirely during early spermatid development and remain conjugated. Moreover, a fusion of developing spermatids is also detectable in *Oonops domesticus* (see Alberti and Weinmann, 1985: fig. 10a). Nevertheless, spermatids of the latter species finally separate at the end of spermiogenesis, forming cleistospermia. Thus, fusion of spermatids during spermiogenesis is not necessarily associated to a specific sperm transfer form. However, synspermia of *Loxosceles intermedia* Mello-Leitão, 1934, a representative of the Sicariidae, do not originate from an entire fusion of spermatids (Costa-Ayub and Faraco, 2007). Although spermatids are connected to each other via cellular bridges, the main sperm cell components remain separated from each other. The cellular bridges widen and enclose the connected spermatids secondarily during formation of the sperm conjugate (Costa-Ayub and Faraco, 2007). This organization is also present in three oonopid taxa studied herein (*Neoxyphinus termitophilus*, *Paradysderina yanayacu*, and *Paradysderina fusiscuta*).

Sperm conjugates are often extensively equipped with membranes, which is of particular interest with regard to their capacitation within the female reproductive system. Spider sperm are transferred coiled and inactive (i.e., immotile), and thus need to uncoil to gain motility (Herberstein et al., 2011a). Consequently, membranes that are retained in sperm transfer forms are useful during capacitation, which usually entails uncoiling of sperm (Alberti and Weinmann, 1985). Thus, the occurrence of additional membranes should be especially advantageous in synspermia. Alberti and Weinmann (1985) already hypothesized the function of additional membranes as sort of “precapacitation” process. In Oonopidae, these membranes either originate from retained membranes or a vesicular area (fig. 44). The presence of a vesicular area is common in arachnids and described for various spiders (Alberti and Weinmann, 1985; Lipke and Michalik, 2012; Michalik

TABLE 2

**Dimensions of Sperm Transfer Forms, Number of Included Sperm in Sperm Conjugates, Thickness of The Secretion Sheath, if Present, and Body Size of Male and Female**

Although the variation of body size is low, the dimensions of sperm transfer forms are highly variable. Note most sperm conjugates are composed of four sperm.

|                                      | Diameter of STF<br>(longest stretch)<br>( $\mu\text{m}$ ) | Thickness of<br>secretion<br>sheath (nm) | Sperm in<br>syngamia<br>(number) | Total body<br>length $\delta^*$<br>(mm) | Total body<br>length $\text{♀}^*$<br>(mm) |
|--------------------------------------|---|--|----------------------------------|---|---|
| <i>Cinetomorpha</i> sp. (Iguazú)     | ~25   | ~80                                      | 4                                | –                                       | –   |
| <i>Escaphiella ramirezi</i>          | ~70   | ~50                                      | 4                                | 1.39                                    | 1.18                                      |
| <i>Gamasomorpha</i> cf <i>vianai</i> | >30   | ~80                                      | 4 (?)                            | –                                       | –   |
| <i>Neotrops poguazu</i>              | ~10   | ~80                                      | 4                                | 2.04                                    | 2.34                                      |
| <i>Neotrops pombero</i>              | ~10   | ~250                                     | 4                                | 1.4                                     | 1.85                                      |
| <i>Neotrops waorani</i>              | ~9  | ~200                                     | 4                                | 1.52                                    | 1.76                                      |
| <i>Neoxyphinus termitophilus</i>     | ~25   | ~30                                      | 4                                | 2.05                                    | 2.37                                      |
| <i>Niarchos scutatus</i>             | ?   | –  | 4                                | 1.41                                    | 1.76                                      |
| <i>Oonops</i> sp. (Ibiza)            | ~5  | –  | 2                                | –                                       | –   |
| <i>Opopaea apicalis</i>              | >25   | ~70                                      | –                                | –                                       | –   |
| <i>Orchestina</i> sp. 1 (Chile)      | >80   | ~800                                     | 2                                | –                                       | –   |
| <i>Orchestina</i> sp. 2 (Argentina)  | >80   | ~1000                                    | 2                                | –                                       | –   |
| <i>Paradysderina fusiscuta</i>       | ~12   | ~50                                      | 4                                | 1.54                                    | 1.61                                      |
| <i>Paradysderina yanayacu</i>        | ~12   | ~250                                     | 4                                | 1.60                                    | 1.86                                      |
| <i>Scaphios yanayacu</i>             | ~12   | –  | 4                                | 1.36                                    | 1.76                                      |
| <i>Silhouettella loricatea</i>       | >25   | ~80                                      | 4 (?)                            | 1.5–2**                                 | 1.5–2**                                   |
| <i>Stenoonops peckorum</i>           | ?   | ?  | 4                                | 1.19                                    | 1.22                                      |
| <i>Tinadysderina otonga</i>          | ~20   | ~80                                      | 4                                | 1.83                                    | 2.11                                      |

\*Total body length as specified in Abraham et al. (2012), Grismado and Ramirez (2013), Platnick and Dupérré (2009a, 2010a, 2010b, 2011) and Platnick et al. (2013).

\*\*Range of body length as given in Wiehle (1953).

et al, 2004b; Michalik and Huber, 2006), as well as Acari, Amblypygi, Palpigradi, Pseudoscorpions, Ricinulei, and Uropygi (Alberti, 1979; Alberti and Coons, 1999; Alberti and Palacios-Vargas, 1987; Talarico et al., 2008, Tripepi and Saita, 1985). However, the actual function, as well as evolution of these additional membrane reservoirs is not yet clear. In Oonopidae, these additional membrane reservoirs never occur in conjunction. Thus, the presence of either membrane stacks or a vesicular area might reflect an independent evolution of this character based on specific reproductive strategies. Primary sperm conjugates consist of several spermatozoa, which need to dissociate within the female reproductive system (Higginson and Henn, 2012). Thus, sperm conjugation without concomitantly entire fusion of cell membranes as is realized in *Neoxyphinus termitophilus* and both *Paradysderina* species might reflect an adaptive state that is related to the activation (capacitation) process. Sperm that retain their own membrane likely

accelerate as the capacitation process. However, further studies focusing on the dissociation of sperm, as well as activation processes of syngamia in the female genital tract are needed to reveal the function of those additional membranes.

**SECRETION SHEATH:** In general, spider spermatozoa are transferred encapsulated, that is, surrounded by a sheath of variable thickness (reviewed in Alberti, 1990, 2000; Michalik and Lipke, 2013; Michalik and Ramirez, 2014). The sheath is either applied in the testes or in the deferent ducts (Michalik and Ramirez, 2014). In contrast, in *Neoxyphinus termitophilus*, the very thin, loosely appearing sheath is not applied until they reach the ejaculatory duct. However, un-sheathed STF (sensu Lipke et al., 2014) have been described for representatives of Caponiidae (Lipke and Michalik, 2012) and Orsolobidae (Lipke et al., 2014), as well as one theridiid, *Phoroncidia* sp. (Lopez and Boissin, 1975). The function of the secretion sheath is still unknown, although tradition-

ally a putative protective function during sperm induction (sperm uptake into male pedipalps) and transfer into the female genital system (Bertkau, 1877; Alberti, 1990), as well as storage within the female's spermathecae (Michalik et al., 2013), was suggested. Thus, a thick secretion sheath is likely correlated with a long residency time, while a thin secretion sheath might indicate short storage times within the female spermatheca (Michalik et al., 2013). The present study revealed various thicknesses in Oonopidae, ranging from a very thin and loosely appearing secretion sheath in *Neoxyphinus termitophilus* to the compact and thick secretion sheath that surrounds sperm conjugates of both *Orchestina* species (table 2). However, data on mating and postcopulatory processes in Oonopidae are sparse; thus, a correlation of the thickness of the secretion sheath with the residency time in females is not obvious. In addition to the previous described variability of the surrounding secretion sheaths, STF of three oonopids of the present study are not provided with a secretion sheath. These unshathed STF might reflect a male strategy. Spider sperm need to be activated within the female reproductive system by female secretory products (Uhl, 1993; 2000; Herberstein et al., 2011b; Vöcking et al., 2013). Consequently, unshathed sperm might bypass an initial triggering and avoid a direct female choice, as suggested by Lipke et al. (2014). However, in this case the putative protective function during sperm induction and transfer into the female genital system should be correlated with additional secretions that achieve a protection during sperm induction and transfer (Lipke et al., 2014).

Our findings provide (1) new insights into putative adaptations of unshathed STF, and (2) support the suggestion of Lipke et al. (2014) that STFs without a sheath are likely more common in spiders. Prior to sperm uptake, unshathed sperm conjugates of *Oonops* sp. (Ibiza), for example, are arranged in a cluster embedded in a dense matrix of fibrillar secretions that originate from the deferent ducts. STFs are wrapped in these secretions and thus likely protected during sperm uptake and transfer into the female genital system, although they are not pro-

vided with an individual sheath. STFs in general are transferred along with a large amount of secretions (Michalik, 2009), and thus the function of the distinct arrangement of synspermia of *Oonops* sp. (Ibiza) remains speculative.

We found unshathed sperm conjugates in *Scaphios yanayacu*. Moreover, we assume sperm conjugates of *Niarchos scutatus* are transferred without a sheath. Although we could analyze only the testis of the latter species, sperm conjugates resemble those of *Scaphios yanayacu* to a great extent. Both species show a characteristic organization of STF, in which four fused sperm that are located in the center of the very large sperm conjugates are enclosed by a distinct vesicular area and a large amount of cytoplasm. In general, sperm transfer forms of spiders tend to be especially compact and cell components are often densely packed, while most of the cytoplasm is discarded at the end of spermiogenesis. However, in both species sperm conjugates retain large quantities of cytoplasm. Thus, a thick cytoplasmic layer shields the sperm, which are arranged in the center of the sperm conjugate. This implies either a protective function or maintains viability during sperm storage inside the female genitalia.

**SIZE DEPENDENT VARIABILITY OF STF:** Sperm transfer forms of Oonopidae show remarkable size differences as summarized in table 2. Oval-shaped sperm conjugates of *Oonops* sp., for example, are rather small with approximately 5  $\mu\text{m}$  in their largest dimension. In contrast, oval-shaped STFs of *Cinetomorpha* sp. (Iguazú) and *Neoxyphinus termitophilus* are approximately 25  $\mu\text{m}$  long. Moreover, the tubelike synspermia of both *Orchestina* species and the bonelike sperm conjugates of *Escaphiella ramirezi*, although slender, are extremely long and extend to more than 70  $\mu\text{m}$ . However, this variety is not reflected in the body size of oonopids (table 2). *Neoxyphinus termitophilus* and *Neotrops poguazu*, for example, are the largest oonopids investigated in the present study (2.04 mm, and 2.05 mm total body length of the male). The STFs, however, of these species are medium sized (*Neotrops poguazu*) and large (*Neoxyphinus termitophilus*), but

certainly not the largest compared with the remaining oonopid species (table 2).

In a recent study that aimed at analyzing the fine structure of spermatozoa and STFs of Orsolobidae, Lipke et al. (2014) investigated a putative correlation of sperm transfer forms and thinnest portion of the spermophor inside the male pedipalp, which was previously suggested by Alberti and Coyle (1991) and Michalik et al. (2004a). Although the size of sperm transfer form as well as the diameter at the thinnest portion of the spermophor varies within Orsolobidae, a correlation was not evident. However, female genital traits and postcopulatory sexual selection might affect the evolution in size of sperm transfer forms. The female genital system of Oonopidae is highly diverse and remarkably complex. Moreover, distinct sperm-storage sites, or spermatheca, for example, are missing in some oonopid species (e.g., Burger, 2010a; 2010b; Burger, 2011; Watanabe et al., 2014). Females of *Orchestina* sp. for example mate with multiple males and store sperm in a single bulgelike anterior spermatheca (fig. 43), in which sperm competition likely occurs through sperm mixing (Burger et al., 2010). We found extremely long and thin sperm transfer forms in both *Orchestina* species (STFs >80  $\mu\text{m}$ ), which possibly evolved to reduce the risk of sperm competition by minimizing the available space and thus block access to the spermatheca for sperm from subsequent males.

Sperm conjugates of *Escaphiella ramirezi* are also extremely long (STF >70  $\mu\text{m}$ ). The female genital system of *Escaphiella hespera* (Chamberlin, 1924), however, resembles the organization known from entelegyne spiders, in which an independent copulatory duct connects the spermatheca with the uterus internus (Burger, 2009). Furthermore, in *E. hespera* sperm have to pass a very narrow insertion duct before they can be stored in the spermatheca. Thus, the organization of the female genitalia might have affected the evolution of very long and thin STFs in *Escaphiella* by means of coevolution of male and female genital traits, as was already shown for some nephilids by Kuntner et al. (2009). However, the diversity of size and shape of STFs in Oonopidae is remarkably high and the responsible selective pressures

that drove the evolution of the STF remains speculative.

#### PHYLOGENETIC IMPLICATIONS

**DYSDEROIDEA:** In general, the primary male reproductive system is composed of paired tubular testes, thin deferent ducts and an unpaired ejaculatory duct, as recognized by Bertkau (1875). Since then, a variety of studies has revealed a remarkable diversity in the gross morphology of the male reproductive system (Michalik, 2009). The monophyly of Oonopidae, for example, was first convincingly supported based on the completely fused testis (Burger and Michalik, 2010). This finding was later corroborated by investigations of the tarsal organ morphology (Platnick et al., 2012b) and only recently supported by molecular data (de Busschere et al., 2014). Our study corroborates the occurrence of completely fused testes in further members of Oonopidae. However, the testis of *Oonops* sp. (Ibiza) is partly different in its organization as it is distally indented (figs. 1E, 2). In spiders, besides completely fused testes, partly fused testes are known. The superfamily Dysderoidea, which consists of the four families Segestriidae, Dysderidae, Orsolobidae, and Oonopidae, was first suggested by Forster and Platnick (1985) based on morphological characteristics concerning the respiratory and female genital systems. An evolutionary scenario on the shape of the testes in Dysderoidea is summarized in figure 45. Within dysderoids, proximally fused testes are described for some Dysderidae and Segestriidae (Michalik et al., 2004b; Michalik and Ramirez, 2014). Moreover, the testes of a few Dysderidae (Michalik et al., 2004b) and a segestriid, *Ariadna maxima* (Nicolet, 1849), are paired (Michalik and Ramirez, 2014). The testes of all investigated Orsolobidae, which are the suggested sister group of Oonopidae (Forster and Platnick, 1985; Platnick et al., 1991; Ramirez, 2000), are paired (Burger and Michalik, 2010; Lipke et al. 2014). We favor the more parsimonious scenario in which completely fused testes is a synapomorphy of Oonopidae (fig. 45). However, we could not identify an additional synapomorphy for Oonopidae, with respect

to the primary male genital system, STF, and sperm traits.

OONOPIDAE: Even though our taxon sampling covers the main lineages of Oonopidae, information is still sparse and fragmentary due to the extremely high variation of sperm characters. Nevertheless, based on the present study several unambiguous synapomorphies could be recovered (fig. 46). *Orchestina* is suggested to split relatively basal within Oonopidae (Platnick et al., 2012b; de Busschere et al., 2014). The sperm of both investigated *Orchestina* species are highly derived and possess unique characteristics not yet known from any other oonopid taxon. However, sperm traits of *Orchestina* are likely conserved within the genus. Sperm of *Orchestina* are extremely long ( $>80 \mu\text{m}$ ), which might be correlated with an extremely long spermophor inside the male copulatory organ (Matías Izquierdo, personal communication). Sperm of *Orchestina* are, e.g., provided with a very deep implantation fossa (char. 17:2), which extends as far as the anterior pole of the nucleus and contains numerous microfilaments (char. 20:1) that are replaced by a distinct centriolar adjunct in mature spermatozoa (figs. 47). Moreover, sperm of both investigated *Orchestina* species do not coil at the end of spermatogenesis (char. 36:2) and have an axoneme, which is shorter or equal in length compared with the nucleus (char. 44:1). However, *Orchestina* sperm lack a postcentriolar elongation (char. 22:5), which is not known from any other spider family so far.

This absence (char. 22:5) is also characteristic for the “*Silhouettella*-clade”. Our data also suggest a close relationship of *Cinetomorphia* sp. (Iguazú), *Gamasomorpha* cf. *vianai*, and *Silhouettella loricatula*. This close relationship is well defined based on the specific organization of STF, the peculiar, irregular chromatin-condensation pattern (char. 24:2), and helically contorted nuclei (char. 41:1).

The spermatozoa of *Opopaea* (based on the evidence of *O. apicalis*) are not comparable to any other spider genus, because these spermatozoa only consist of a chromatin thread (char. 40:4), which is highly contorted. Moreover, as shown in figure 48, spermatozoa of *Brignolia parumpunctata* (Simon,

1893) (courtesy of M. Burger) likely possess chromatin threads as well. The aberrant organization of these spermatozoa involves functional constraints because additional cell organelles, such as a flagellum are not developed at all. Aflagellate spermatozoa are capable of an amoeboid or crawling movement, as was shown for a variety of taxa (reviewed in White-Cooper and Bausek, 2010). These spermatozoa, however, are probably prevented from directional movement and therefore likely depend on female-controlled guidance and passively performed movement. Thus, aflagellate spermatozoa likely evolved under low sperm competition (Morrow, 2004). However, the spermatozoa of *O. apicalis* lack any additional cell organelles, which seem to be also unique among spiders. Besides the axoneme and the nucleus that contains condensed chromatin, spider spermatozoa, in general, exhibit an acrosomal complex, which is composed of an acrosomal vacuole and an acrosomal filament (Alberti, 1990; Michalik and Lipke, 2013). The acrosomal vacuole initiates the acrosome reaction and thus facilitates the fertilization process. Thus, the loss of the acrosomal complex involves alternative mechanisms to ensure fertilization. Further studies should therefore scrutinize whether these spermatozoa that lack any additional organelles have evolved multiple times independently or characterize a specific clade of goblin spiders.

Furthermore, we could recover numerous synapomorphies for the genus *Neotrops*. This genus is characterized by, e.g., a long proximal centriole (char. 25:1) and distinct electron-dense lamellae that surround the base of the axoneme. Moreover, these spermatozoa possess an acrosomal vacuole that is deeply sunken into the anterior pole of the nucleus (char. 10:1), while the subacrosomal space is enlarged (char. 11:1). Further characteristics are the irregular chromatin-condensation pattern (char. 24:2), as well as an irregular shape of the precentriolar part of nucleus in mature spermatozoa (char. 41:2).

*Neoxyphinus* was suggested to be the sister to the remaining taxa that are included in a “*Dysderina* clade”; within this clade *Paradysderina* and *Scaphidysderina* are the supposed sister to *Dysderina*, *Aschnaonops*,

*Bidysderina*, *Tridysderina*, and *Tinadysderina* (de Busschere et al., 2014). Our data also corroborate a relationship of *Neoxyphinus*, *Paradysderina*, and *Tinadysderina*, since this “*Dysderina* clade” + *Neoxyphinus* exhibits a medium-sized implantation fossa (char. 17:1) that contains numerous mitochondria, a well-developed postcentriolar elongation, and an apparent long axoneme. The presence of mitochondria within the implantation fossa seems especially remarkable as it has not been reported outside this group and thus represents a potential synapomorphy for these taxa.

The proposed sister relationship between *Niarchos* and *Scaphios* (Platnick and Dupérré 2010b; de Busschere et al., 2014) can also be confirmed based on the sperm morphological characters, the presence of a distinct vesicular area (char. 37:1), and the peculiar organization of unsheathed STF (char. 38:1) that contain four spermatozoa, which are located in the center of the STF and shielded by a voluminous layer composed of cytoplasm and numerous mitochondria.

### CONCLUSIONS

The present study highlights morphological features of the primary male reproductive system and sperm characters of 18 species of Oonopidae. All investigated oonopids of the present study transfer synspermia, which further corroborates the suggestion of Michalik and Ramírez (2014) that this STF is characteristic for Synspermiata. Our study recovered 30 unambiguous synapomorphies for different oonopid taxa, which permit the postulation of several specific clades, such as a *Neotrops* clade (chars. 10:1; 14:1; 25:1; 41:2) and a *Silhouettella* clade (chars. 22:5; 24:2; 41:1). In addition, we highlighted several characteristics that are best explained as functional adaptations. The formation of synspermia in *Neoxyphinus termitophilus* and both *Paradysderina* species, in which sperm retain their individual membrane for the most part, is likely associated with postcopulatory mechanisms, although its significance is not yet understood. We furthermore suggest that the reduction in size (e.g., *Escaphiella ramirezi*, *Stenoonops peckorum*), as well as the loss

(e.g., *Orchestina*) of a postcentriolar elongation has likely evolved several times independently. However, the first evidence of an aflagellate spider sperm (*Opopaea apicalis*), as well as the occurrence of the longest sperm conjugates (sperm conjugates of *Orchestina*) and longest sperm (*Neoxyphinus termitophilus*, ~300  $\mu\text{m}$ ) within spiders corroborate the enormous variability of sperm traits, features likely driven by postcopulatory sexual selection.

### ACKNOWLEDGMENTS

The authors thank Matias A. Izquierdo, Cristian Grismado, Facundo Labarque, and Martín J. Ramírez (Museo Argentino de Ciencias Naturales, Buenos Aires, Argentina), Petra Sierwald (Field Museum, Chicago), Norman Platnick (American Museum of Natural History, New York) and the whole PBI team in Ecuador for collecting specimens, who made this study possible. Furthermore, Cristian Grismado, Matias Izquierdo as well as Norman Platnick are gratefully acknowledged for determining species. We are very grateful to Matthias Burger (Hawai'i) for kindly providing a specimen of *Silhouettella loricaula* and light-microscopic images of the male genital system of additional goblin spiders that significantly supplemented our analysis. We thank Gerd Alberti (University of Greifswald) for very helpful discussion and comments, as well as continuous support. Furthermore, we are indebted to Gabriele Uhl (University of Greifswald) for her support. We thank Martín J. Ramírez and one anonymous reviewer for comments on an earlier version of the manuscript.

For sharing a fantastic and productive time P.M. is indebted to the whole team of the Niarchos expedition to Ecuador, and is especially grateful to Norman Platnick for his support of this study. Furthermore, P.M. thanks Carsten Müller (University of Greifswald, Germany) for an inspiring field excursion to Ibiza Island.

Funding for this research has been provided by the German Research Foundation to P.M. (DFG Mi 1255/5-1). Furthermore, this study is part of the PBI project supported by the U.S. National Science Foundation

(NSF DEB-0613754) and we are especially grateful to the funder of the Niarchos expedition to Ecuador.

#### REFERENCES

- Abraham, N., et al. 2012. A revision of the Neotropical goblin spider genus *Neoxyphinus* Birabén, 1953 (Araneae, Oonopidae). *American Museum Novitates* 3743: 1–75.
- Afzelius, B.A., G. Alberti, R. Dallai, J. Godula, and W. Witalinski. 1989. Virus- and *Rickettsia*-infected sperm cells in arthropods. *Journal of Invertebrate Pathology* 53: 365–377.
- Alberti, G. 1979. Zur Feinstruktur der Spermien und Spermiocytenogenese von *Prokoenia wheeleri* (Rucker, 1901) (Palpigradi, Arachnida). *Zoomorphology* 94: 111–120.
- Alberti, G. 1990. Comparative spermatology of Araneae. *Acta Zoologica Fennica* 190: 17–34.
- Alberti, G. 2000. Chelicerata. In K.G. Adiyodi, and R.G. Adiyodi (editors), *Reproductive biology of invertebrates*, 311–388, Oxford: Queensland.
- Alberti, G., and L.B. Coons. 1999. Acari: mites. In F.W. Harrison, and R.F. Foelix (editors), *Chelicerata, Arthropoda*, 515–1265, Wiley-Liss: New York.
- Alberti, G., and F.A. Coyle. 1991. Ultrastructure of the primary male genital system, spermatozoa, and spermiogenesis of *Hypochilus pococki* (Araneae, Hypochilidae). *Journal of Arachnology* 19: 136–149.
- Alberti, G., and J.G. Palacios-Vargas. 1987. Fine structure of spermatozoa and spermatogenesis of *Schizomus palaciosi*, Redell and Cockendolpher, 1986 (Arachnida: Uropygi, Schizomida). *Protoplasma* 137: 1–14.
- Alberti, G., and C. Weinmann. 1985. Fine structure of spermatozoa of some labidognath spiders (Filistidae, Segestriidae, Dysderidae, Oonopidae, Scytodidae, Pholcidae; Araneae; Arachnida) with remarks on spermiogenesis. *Journal of Morphology* 185: 1–35.
- Alberti, G., B.A. Afzelius, and S.M. Lucas. 1986. Ultrastructure of spermatozoa and spermatogenesis in bird spiders (Theraphosidae, Mygalomorphae, Araneae). *Journal of Submicroscopic Cytology* 18: 739–753.
- Baccetti, B., R. Dallai, and F. Rosati. 1970. The spermatozoon of arthropoda. 8. The 9+3 flagellum of spider sperm cells. *Journal of Cell Biology* 44: 681–682.
- Baehr, B.C., and M.S. Harvey. 2013. The first goblin spiders of the genus *Camptoscaphiella* (Araneae: Oonopidae) from new caledonia. *Australian Journal of Entomology* 52: 144–150.
- Baehr, B.C., M.S. Harvey, M. Burger, and M. Thoma. 2012. The new Australasian goblin spider genus *Prethopalpus* (Araneae, Oonopidae). *Bulletin of the American Museum of Natural History* 369: 1–113.
- Bertkau, P. 1875. Über den Generationsapparat der Araneiden. *Archiv für Naturgeschichte* 41: 235–262.
- Bertkau, P. 1877. Über die Übertragungsorgane und die Spermatozoen der Spinnen. *Verhandlungen des Naturhistorischen Vereins der Preussischen Rheinlande* 34: 28–32.
- Birabén, M. 1954. Nuevas Gamasomorphinae de la Argentina (Araneae, Oonopidae). *Notas del Museo de la Plata* 17: 181–212.
- Bristowe, W.S. 1938. Some new termitophilous spiders from Brazil. *Annals and Magazine of Natural History* (11) 2: 67–73.
- Burger, M. 2007. Sperm dumping in a haplogyne spider. *Journal of Zoology* 273: 74–81.
- Burger, M. 2009. Female genitalia of goblin spiders (Arachnida: Araneae: Oonopidae): A morphological study with functional implications. *Invertebrate Biology* 128: 340–358.
- Burger, M. 2010a. Complex female genitalia indicate sperm dumping in armored goblin spiders (Arachnida, Araneae, Oonopidae). *Zoology (Jena)* 113: 19–32.
- Burger, M. 2010b. Goblin spiders without distinct receptacula seminis (Arachnida: Araneae: Oonopidae). *Journal of Morphology* 271: 1110–1118.
- Burger, M. 2011. Functional morphology of female goblin spider genitalia (Arachnida: Araneae: Oonopidae) with notes on fertilization in spiders. *Zoologischer Anzeiger* 250: 123–133.
- Burger, M., and P. Michalik. 2010. The male genital system of goblin spiders: evidence for the monophyly of Oonopidae (Arachnida: Araneae). *American Museum Novitates* 3675: 1–13.
- Burger, M., W. Nentwig, and C. Kropf. 2003. Complex genital structures indicate cryptic female choice in a haplogyne spider (Arachnida, Araneae, Oonopidae, Gamasomorphinae). *Journal of Morphology* 255: 80–93.
- Burger, M., W. Graber, P. Michalik, and C. Kropf. 2006. *Silhouettella loricatula* (Arachnida, Araneae, Oonopidae): a haplogyne spider with complex female genitalia. *Journal of Morphology* 267: 663–677.
- Burger, M., M.A. Izquierdo, and P. Carrera. 2010. Female genital morphology and mating behavior of *Orchestina* (Arachnida: Araneae: Oonopidae). *Zoology* 113: 100–109.
- Calhim, S., M.C. Double, N. Margraf, T.R. Birkhead, and A. Cockburn. 2011. Maintenance of sperm variation in a highly promiscuous wild

- bird. PLoS ONE 6: e28809. [doi: 10.1371/journal.pone.0028809].
- Chamberlin, R.V. 1924. The spider fauna of the shores and islands of the Gulf of California. Proceedings of the California Academy of Sciences 12: 561–694.
- Costa-Ayub, C.L.S., and C.D. Faraco. 2007. Ultrastructural aspects of spermiogenesis and synspermy in the brown spider *Loxosceles intermedia* (Araneae: Sicariidae). Arthropod Structure and Development 36: 41–51.
- Darby, A.C., N.H. Cho, H.H. Fuxelius, J. Westberg, and S.G. Andersson. 2007. Intracellular pathogens go extreme: genome evolution in the Rickettsiales. Trends in Genetics 23: 511–520.
- de Busschere, C., et al. 2014. Unravelling the goblin spider puzzle: rDNA phylogeny (Araneae: Oonopidae). Arthropod Systematics and Phylogeny 72: 177–192.
- Dunlop, J., D. Penney, and D. Jekel. 2015. A summary list of fossil spiders and their relatives. The World Spider Catalog. Natural History Museum Bern, version 16.0. Online resource (<http://wsc.nmbe.ch>).
- Duron, O., and G.D. Hurst. 2013. Arthropods and inherited bacteria: from counting the symbionts to understanding how symbionts count. BMC Biology 11: 45.
- Duron, O., et al. 2008. The diversity of reproductive parasites among arthropods: *Wolbachia* do not walk alone. BMC Biology 6: 27.
- Edward, K.L., and M.S. Harvey. 2009. A new species of *Ichnothyreus* (Araneae: Oonopidae) from monsoon rainforest of northern Australia. Records of the Western Australian Museum 25: 287–293.
- Fannes, W., D. De Bakker, K. Loosveldt, and R. Jocqué. 2008. Estimating the diversity of arboreal oonopid spider assemblages (Araneae, Oonopidae) at afrotropical sites. Journal of Arachnology 36: 322–330.
- Forster, R.R., and N.I. Platnick. 1985. A review of the austral spider family Orsolobidae (Arachnida, Araneae), with notes on the superfamily Dysderoidea. Bulletin of the American Museum of Natural History 181 (1): 1–230.
- Gage, M. 1998. Mammalian sperm morphometry. Proceedings of the Royal Society of London B, Biological Sciences 265: 97–103.
- Giribet, G., G.D. Edgecombe, W.C. Wheeler, and C. Babbitt. 2002. Phylogeny and systematic position of opiliones: a combined analysis of chelicerate relationships using morphological and molecular data. Cladistics 18: 5–70.
- Goodacre, S.L., O.Y. Martin, C.F. Thomas, and G.M. Hewitt. 2006. *Wolbachia* and other endosymbiont infections in spiders. Molecular Ecology 15: 517–527.
- Grismado, C.J., and M.J. Ramírez. 2013. The New World goblin spiders of the genus *Neotrops* (Araneae: Oonopidae), part I. Bulletin of the American Museum of Natural History, 383: 1–150.
- Grismado, C.J., C. Deeleman, L.N. Piacentini, M.A. Izquierdo, and M.J. Ramírez. 2014. Taxonomic review of the goblin spiders of the genus *Dysderoides* Fage and their Himalayan relatives of the genera *Trilacuna* Tong and Li and *Himalayana*, new genus (Araneae: Oonopidae). Bulletin of the American Museum of Natural History 387: 1–108.
- Herberstein, M.E., J.M. Schneider, G. Uhl, and P. Michalik. 2011a. Sperm dynamics in spiders. Behavioral Ecology 22: 692–695.
- Herberstein, M.E., et al. 2011b. Sperm storage and copulation duration in a sexually cannibalistic spider. Journal of Ethology 29: 9–15.
- Higginson, D.M., and K.R. Henn. 2012. Effects of sperm conjugation and dissociation on sperm viability in vitro. PLoS ONE 7: e34190. [doi: 10.1371/journal.pone.0034190].
- Higginson, D.M., and S. Pitnick. 2011. Evolution of intra-ejaculate sperm interactions: do sperm cooperate? Biological Reviews, 86: 249–270.
- Higginson, D.M., K.B. Miller, K.A. Segraves, and S. Pitnick. 2012. Female reproductive tract form drives the evolution of complex sperm morphology. Proceedings of the National Academy of Sciences of the United States of America 109: 4538–4543.
- Hilgenboecker, K., K. Hammerstein, P. Schlattmann, A. Telschow, and J.H. Werren. 2008. How many species are infected with *Wolbachia*? A statistical analysis of current data. FEMS Microbiological Letters 281: 215–220.
- Humphries, S., J.P. Evans, and L.W. Simmons. 2008. Sperm competition: linking form to function. BMC Evolutionary Biology 8: 319.
- Jamieson, B.G.M., R. Dallai, and B.A. Afzelius. 1999. Insects—their spermatozoa and phylogeny, Science Publishers: Enfield, NH
- Juberthie, C., A. Lopez, and J. Kovoov. 1981. Spermiogenesis and spermatophore in *Telematenella* Simon (Araneae: Telemidae)—an ultrastructural study. International Journal of Invertebrate Reproduction 3: 181–191.
- Kuntner, M., J.A. Coddington, and J.M. Schneider. 2009. Intersexual arms race? Genital coevolution in Nephilid spiders (Araneae, Nephilidae). Evolution 63: 1451–1463.
- Legendre, R., and A. Lopez. 1978. Présence d'un spermatophore dans le genre *Apneumonella* (Araneae, Telemidae): valeur systématique et problèmes de biologie sexuelle. Bulletin de la Société Zoologique de France 103: 35–41.

- Lipke, E., and P. Michalik. 2012. Formation of primary sperm conjugates in a haplogyne spider (Caponiidae, Araneae) with remarks on the evolution of sperm conjugation in spiders. *Arthropod Structure and Development* 41: 561–573.
- Lipke, E., M.J. Ramírez, and P. Michalik. 2014. Ultrastructure of spermatozoa of Orsolobidae (Haplogynae, Araneae) with implications on the evolution of sperm transfer forms in Dysderoidea. *Journal of Morphology* 275: 1238–1257.
- Lopez, A., and L. Boissin. 1975. Observation de spermatozoides non enkystés chez une araignée du genre *Phoroncidia* (Araneae, Theridiidae). *Bulletin de la Société Zoologique de France* 100: 583–587.
- Lüpold, S., S. Calhim, S. Immler, and T.R. Birkhead. 2009. Sperm morphology and sperm velocity in passerine birds. *Proceedings of the Royal Society of London B, Biological Sciences* 276: 1175–1181.
- Maddison, W.P., and D.R. Maddison. 2011. Mesquite: a modular system for evolutionary analysis. Version 2.75. Online resource (<http://mesquitemproject.org>).
- Malo, A.F., et al. 2006. Sperm design and sperm function. *Biology Letters* 2: 246–249.
- Marotta, R., M. Ferraguti, C. Erséus, and L.M. Gustavsson. 2008. Combined-data phylogenetics and character evolution of Clitellata (Annelida) using 18s rDNA and morphology. *Zoological Journal of the Linnean Society* 154: 1–26.
- Martin, O.Y., and S.L. Goodacre. 2009. Widespread infections by the bacterial endosymbiont *Cardinium* in Arachnids. *Journal of Arachnology* 37: 106–108.
- Mello-Leitão, C.F. d.e. 1934. Especies brasileiras do genero *Loxosceles* Lowe. *Anais da Academia Brasileira de Ciências* 6: 69–73.
- Metcalfe, J.A., and S.R. Bordenstein. 2012. The complexity of virus systems: the case of endosymbionts. *Current Opinion in Microbiology* 15: 546–552.
- Michalik, P. 2007. Spermatozoa and spermiogenesis of *Liphistius* cf. *phuketensis* (Mesothelae, Araneae, Arachnida) with notes on phylogenetic implications. *Arthropod Structure and Development* 36: 327–335.
- Michalik, P. 2009. The male genital system of spiders (Arachnida, Araneae) with notes on the fine structure of seminal secretions. *Contributions to Natural History* 12: 959–972.
- Michalik, P., and G. Alberti. 2005. On the occurrence of the 9+0 axonemal pattern in the spermatozoa of sheetweb spiders (Linyphiidae, Araneae). *Journal of Arachnology* 33: 569–572.
- Michalik, P., and G. Hormiga. 2010. Ultrastructure of the spermatozoa in the spider genus *Pimoa*: new evidence for the monophyly of Pimoidae plus Linyphiidae (Arachnida: Araneae). *American Museum Novitates* 3682: 1–17.
- Michalik, P., and B.A. Huber. 2006. Spermiogenesis in *Psilochorus simoni* (Berland, 1911) (Pholcidae, Araneae): evidence for considerable within-family variation in sperm structure and development. *Zoology* 109: 14–25.
- Michalik, P., and E. Lipke. 2013. Male reproductive system of spiders. In W. Nentwig (editor), *Spider ecophysiology*, 173–187, Springer: Heidelberg.
- Michalik, P., and M.J. Ramírez. 2014. Evolutionary morphology of the male reproductive system, spermatozoa and seminal fluid of spiders (Araneae, Arachnida)—current knowledge and future directions. *Arthropod Structure and Development* 43: 291–322.
- Michalik, P., and G. Uhl. 2005. The male genital system of the cellar spider *Pholcus phalangioides* (Fuesslin, 1775) (Pholcidae, Araneae): development of spermatozoa and seminal secretion. *Frontiers in Zoology* 2: 12.
- Michalik, P., M.R. Gray, and G. Alberti. 2003. Ultrastructural observations of spermatozoa and spermiogenesis in *Wandella orana* Gray, 1994 (Araneae: Filistatidae) with notes on their phylogenetic implications. *Tissue and Cell* 35: 325–337.
- Michalik, P., J. Haupt, and G. Alberti. 2004a. On the occurrence of coenospermia in mesothelid spiders (Araneae: Heptathelidae). *Arthropod Structure and Development* 33: 173–181.
- Michalik, P., P. Sacher, and G. Alberti. 2006. Ultrastructural observations of spermatozoa of several tetragnathid spiders with phylogenetic implications (Araneae, Tetragnathidae). *Journal of Morphology* 267: 129–151.
- Michalik, P., R. Dallai, F. Giusti, and G. Alberti. 2004b. The ultrastructure of the peculiar synspermia of some Dysderidae (Araneae, Arachnida). *Tissue and Cell* 36: 447–460.
- Michalik, P., B. Knoflach, K. Thaler, and G. Alberti. 2005a. The spermatozoa of the one-palped spider *Tidarren argo* (Araneae, Theridiidae). *Journal of Arachnology* 33: 562–568.
- Michalik, P., A. Aisenberg, R. Postiglioni, and E. Lipke. 2013. Spermatozoa and spermiogenesis of the wolf spider *Schizocosa malitiosa* (Lycosidae, Araneae) and its functional and phylogenetic implications. *Zoomorphology* 132: 11–21.
- Michalik, P., R. Dallai, F. Giusti, D. Mercati, and G. Alberti. 2005b. Spermatozoa and spermiogenesis of *Holocnemus pluchei* (Scopoli, 1763) (Pholcidae, Araneae). *Tissue and Cell* 37: 489–497.

- Morrow, E.H. 2004. How the sperm lost its tail: the evolution of aflagellate sperm. *Biological Reviews* 79: 795–814.
- Nicolet, A.C. 1849. Aracnidos. In C. Gay (editor), *Historia física y política de Chile*. *Zoología* 3: 319–543.
- Nixon, K.C. 2002. WinClada, ver., 1.00.08, Published by the author: Ithaca, NY.
- Ōsaki, H. 1969. Electron microscope study on the spermatozoon of the Liphistiid spider *Hep-tathela kimurai*. *Acta Arachnologica* 22: 1–12.
- Penney, D. 2000. Miocene spiders in Dominican Amber (Oonopidae, Mysmenidae). *Paleontology* 43: 343–357.
- Pitnick, S. 1996. Investment in testis and the cost of making long sperm in *Drosophila*. *American Naturalist* 148: 57–80.
- Pitnick, S., D. Hosken, and T.R. Birkhead. 2009. Sperm morphological diversity. In T.R. Birkhead, D. Hosken, and S. Pitnick (editors), *Sperm biology—an evolutionary perspective*, 69–149, Academic Press: Amsterdam.
- Platnick, N.I., and N. Dupérré. 2009a. The goblin spider genera *Opopaea* and *Epectris* (Araneae, Oonopidae) in the New World. *American Museum Novitates* 3649: 1–43.
- Platnick, N.I., and N. Dupérré. 2009b. The American goblin spiders of the new genus *Escaphiella* (Araneae, Oonopidae). *Bulletin of the American Museum of Natural History* 328: 1–151.
- Platnick, N.I., and N. Dupérré. 2010a. The goblin spider genera *Stenoconops* and *Australoonops* (Araneae, Oonopidae), with notes on related taxa. *Bulletin of the American Museum of Natural History* 340: 1–111.
- Platnick, N.I., and N. Dupérré. 2010b. The Andean goblin spiders of the new genera *Niarchos* and *Scaphios* (Araneae, Oonopidae). *Bulletin of the American Museum of Natural History* 345: 1–120.
- Platnick, N.I., and N. Dupérré. 2011. The Andean goblin spiders of the new genera *Paradysderina* and *Semidysderina* (Araneae, Oonopidae). *Bulletin of the American Museum of Natural History* 364: 1–121.
- Platnick, N.I., J.A. Coddington, R.R. Forster, and C.E. Griswold. 1991. Spinneret morphology and the phylogeny of haplogyne spiders (Araneae, Araneomorphae). *American Museum Novitates* 3016: 1–73.
- Platnick, N.I., N. Dupérré, D. Ubick, and W. Fannes. 2012a. Got males?: the enigmatic goblin spider genus *Triarieris* (Araneae, Oonopidae). *American Museum Novitates* 3756: 1–36.
- Platnick, N.I., et al. 2012b. Tarsal organ morphology and the phylogeny of goblin spiders (Araneae, Oonopidae), with notes on basal genera. *American Museum Novitates* 3736: 1–52.
- Platnick, N.I., L. Berniker, and A.B. Bonaldo. 2013. The South American goblin spiders of the new genera *Pseudodysderina* and *Tinadysderina* (Araneae, Oonopidae). *American Museum Novitates* 3787: 1–43.
- Platnick, N.I., L. Berniker, and C. Viquez. 2014. The goblin spider genus *Costarina* (Araneae, Oonopidae), part 2: the Costa Rican fauna. *American Museum Novitates* 3794: 1–75.
- Ramírez, M.J. 2000. Respiratory system morphology and the phylogeny of haplogyne spiders (Araneae, Araneomorphae). *Journal of Arachnology* 28: 149–157.
- Reynolds, E.S. 1963. The use of lead citrate at high pH as electron-opaque stain in electron microscopy. *Journal of Cell Biology* 17: 208–212.
- Richardson, H.H., L. Jarett, and E.H. Finke. 1960. Embedding in epoxy resins for ultrathin sectioning in electron microscopy. *Stain Technology* 35: 313–323.
- Roewer, C.F. 1942. *Katalog der Araneae von 1758 bis 1940*. Bremen: Natura, 1: 1–1040.
- Saalfeld, S., R. Fetter, A. Cardona, and P. Tomancak. 2012. Elastic volume reconstruction from series of ultra-thin microscopy sections. *Nature Methods* 9: 717–720.
- Saupe, E.E., et al. 2012. New *Orchestina* Simon, 1882 (Araneae: Oonopidae) from Cretaceous ambers of Spain and France: first spiders described using phase-contrast X-ray synchrotron microtomography. *Palaeontology* 55: 127–143.
- Spurr, A.R. 1969. A low-viscosity epoxy resin embedding medium for electron microscopy. *Journal of Ultrastructure Research* 26: 31–43.
- Talarico, G., L.F.G. Hernandez, and P. Michalik. 2008. The male genital system of the New World Ricinulei (Arachnida): ultrastructure of spermatozoa and spermiogenesis with special emphasis on its phylogenetic implications. *Arthropod Structure and Development* 37: 396–409.
- Tripepi, S., and A. Saita. 1985. Ultrastructural analysis of spermiogenesis in *Admetus pomilio* (Arachnida, Amblypygi). *Journal of Morphology* 184: 111–120.
- Uhl, G. 1993. Mating behaviour and female sperm storage in *Pholcus phalangioides* (Fuesslin) (Araneae). *Memoirs of the Queensland Museum* 33: 667–674.
- Uhl, G. 2000. Female genital morphology and sperm priority patterns in spiders (Araneae). In S. Toft, and N. Scharff (editors), *European Arachnology 2000*: 145–156, Aarhus University Press: Aarhus.
- Uhler, P.R. 1896. Summary of the Hemiptera of Japan presented to the United States National Museum by Professor Mitzukuri. *Proceedings*

- of the United States National Museum. Washington 19: 255–297.
- Vanthournout, B., J. Swaegers, and F. Hendrickx. 2011. Spiders do not escape reproductive manipulations by *Wolbachia*. *BMC Evolutionary Biology* 11: 15.
- Vöcking, O., G. Uhl, and P. Michalik. 2013. Sperm dynamics in spiders (Araneae): ultrastructural analysis of the sperm activation process in the garden spider *Argiope bruennichi* (Scopoli, 1772). *PLoS ONE* 8: e72660. [doi: 10.1371/journal.pone.0072660].
- Watanabe, K., F. Yukuhiro, Y. Matsuura, T. Fukatsu, and H. Noda. 2014. Intrasperm vertical symbiont transmission. *Proceedings of the National Academy of Science* 111: 7433–7437.
- Werren, J.H., L. Baldo, and M.E. Clark. 2008. *Wolbachia*: master manipulators of invertebrate biology. *Nature Reviews Microbiology* 6: 741–751.
- White-Cooper, H., and N. Bausek. 2010. Evolution and spermatogenesis. *Philosophical Transactions of the Royal Society of London B, Biological Sciences* 365: 1465–1480.
- Wiehle, H. 1953. Spinnentiere oder Arachnoidea (Aranea) IX: Orthognatha-Cribellatae-Haplogynae-Entelegynae. *Die Tierwelt Deutschlands* 42: 1–150.
- World Spider Catalog. 2015. World spider catalog, version 16. Natural History Museum Bern. Online resource (<http://wsc.nmbe.ch>), accessed January 14, 2015.

## APPENDIX 1: STUDY SPECIES

- Cinetomorpha* sp. (Iguazú): 2 ad ♂ [PM-0069; PM-0073]: Parque Nacional Iguazú (primary forest with Palm Trees), Misiones, ARGENTINA (S 25°41'24.2" W 054°28'48.8", 257 m, 27.02.2012; leg: K. Huckstorf, M. Izquierdo, P. Michalik, G. Rubio, C.S. Wirkner, det: C.J. Grismado).
- Escaphiella ramirezi* Platnick and Dupérré, 2009: 1 ad ♂ [PM-0092]: Parque Nacional Iguazú (Macuco Trail), Misiones, ARGENTINA (S 25°40.712' W 054°26.955', 205 m, 24.02.2012; leg: K. Huckstorf, M. Izquierdo, P. Michalik, G. Rubio, C.S. Wirkner, det: C. Grismado).
- Gamasomorpha* cf. *vianai* Birabén, 1954: 2 ad ♂ [PM-35; PM-49]: Parque Nacional Calilegua (Seccional Aguas Negras), Jujuy, ARGENTINA (S23°45'43.3", W64°51'04.7", 605 m, 6-11.12.2008; leg: M. Burger, P. Carrera, C. Grismado, M. Izquierdo, F. Labarque, C. Mattoni, P. Michalik, A. Ojanguren, G. Rubio, det: C. Grismado).
- Neotrops poguazu* Grismado and Ramírez, 2013: 1 ad ♂ [PM-0074]: Parque Nacional Iguazú (Primary forest with Palm Trees), Misiones, ARGENTINA (S 25°41'24.2" W 054°28'48.8", 257 m, 27.02.2012; leg: K. Huckstorf, M. Izquierdo, P. Michalik, G. Rubio, C.S. Wirkner, det: C. Grismado).
- Neotrops pombero* Grismado and Ramírez, 2013: 3 ad ♂ [PM-0070; PM-0071; PM-0075]: Parque Nacional Iguazú (Primary forest with Palm Trees), Misiones, ARGENTINA (S 25°41'24.2" W 054°28'48.8", 257 m, 27.02.2012; leg: K. Huckstorf, M. Izquierdo, P. Michalik, G. Rubio, C.S. Wirkner, det: C. Grismado). 3 ad ♂ [PM-0080; PM-0095; PM-0096]: Parque Nacional Iguazú (Apepú Field Station), Misiones, ARGENTINA (S 25°33.814' W 054°17.758', 216 m, 29.02.2012; leg: K. Huckstorf, M. Izquierdo, P. Michalik, G. Rubio, C.S. Wirkner, det: C. Grismado).
- Neotrops waorani* Grismado and Ramírez, 2013: 1 ad ♂ [PM-EC-066]: Parque Nacional Yasuni (Botanical trail), Orellana, ECUADOR (S 00°40.428', W 076°23.90', 168 m, 03.12.2009; leg: Niarchos expedition, det: C. Grismado).
- Neoxyphinus termitophilus* (Bristowe, 1938): 2 ad ♂: Parque Nacional Iguazú (Garganta del Diablo), Misiones, ARGENTINA (S25°42'16.7" W54°26'28.2", 250 m, 16-20.05.2005; leg.: M. Ramírez, F. Labarque, P. Michalik). 1 ad ♂: Parque Nacional Iguazú (Sendero Macuco), Misiones, ARGENTINA (S25°40'45" W54°26'57.4" 250 m, 16-20.05. 2005; leg.: M. Ramírez, F. Labarque, P. Michalik). 3 ad ♂ [PM-0076, PM-0090, PM-0091]: Parque Nacional Iguazú (Macuco trail, close to C.I.E.S.), Misiones, ARGENTINA (S 25°40.712' W 054°26.955', 205 m, 24.02.2012; leg: K. Huckstorf, M. Izquierdo, P. Michalik, G. Rubio, C.S. Wirkner, det: C. Grismado). 1 ad ♂ [PM-0093]: Parque Nacional Iguazú (Apepú Field Station), Misiones, ARGENTINA (S 25°33.814' W 054°17.758', 216 m, 29.02.2012; leg: K. Huckstorf, M. Izquierdo, P. Michalik, G. Rubio, C.S. Wirkner, det: C. Grismado).
- Niarchos scutatus* Platnick and Dupérré, 2010: 1 ad ♂ [PM-EC 004]: Yanayacu Biological Station (stream trail), Napo, ECUADOR (S 0°35.955', W 77°53.431', 2130 m, 25. 11.2009; leg: Niarchos expedition, det: C. Grismado).
- Oonops* sp. (Ibiza): 1 ad ♂ [PBI\_OON 51523]: Cala S'Aguila, Ibiza, SPAIN (2010; leg: P. Michalik, det: N. Platnick).
- Opopaea apicalis* Simon, 1893b: 2 ad ♂: Monroe County, Big Pine Key, Long Beach NKD Refuge, Long Beach Drive (Florida) (N 24°38.716' W 81°19.900'; 25.04.2008; leg: P. Sierwald, det: P. Michalik).
- Orchestina* sp. 1 (Chile): 5 ad ♂ [PM-0028; PM-0029; PM-0030; PM-0032; PM-0033]: Monumento Natural Contulmo, Malleco, CHILE (S 38.1314° W 73.18648°, 341 m, 10.02.2012; leg: K. Huckstorf, M. Izquierdo, P. Michalik, M.J. Ramírez, C.S. Wirkner, det: C.J. Grismado). 3 ad ♂ [PM-0039; PM-0040; PM-0041]: Parque Nacional Chiloé (Sendero Tepual, near Cucao), Chiloé, CHILE (S 42.61766° W 74.10120°, 15 m, 15.02.2012; leg: K. Huckstorf, M. Izquierdo, P. Michalik, M.J. Ramírez, C.S. Wirkner, det: C.J. Grismado).

- Orchestina* sp. 2 (Argentina): 1 ad ♂ [MACN-Ar 17718, PBI\_OON 14879 (PM-41)]; Parque Nacional Calilegua (Seccional Aguas Negras), Jujuy, ARGENTINA (S 23°45'43.3", W 64°51'04.7", 605 m, 6-11.12.2008; leg: C. Grismado, M. Izquierdo, F. Labarque, G. Rubio, M. Burger, P. Michalik, P. Carrera, A. Ojanguren, C. Mattoni, det: C.J. Grismado).
- Paradysderina fusciscuta* Platnick and Dupérré, 2011: 1 ad ♂ [PM-EC086 (PBI 43143)]; Otonga forest, Pichincha, ECUADOR (S 00°25.179', W 078°59.824', 1803 m, 07.12.2009; leg: Niarchos expedition, det: C. Grismado).
- Paradysderina yanayacu* Platnick and Dupérré, 2011: 3 ad ♂ [PM-EC001 (PBI 30842); PM-EC024 (PBI 43144); PM-EC044 (PBI 584); PM-EC046 (PBI 46489)]; Yanayacu Biological Station (stream trail), Napo, ECUADOR (S 0.60022°, W 77.89039°W, 2180 m, 25-30.11.2009; leg: Niarchos Expedition, det: C. Grismado).
- Scaphios yanayacu* Platnick and Dupérré, 2010: 3 ad ♂ [PM-EC 005; PM-EC 045; PM-EC 047]; Yanayacu Biological Station (stream trail), Napo, ECUADOR (S 0°35.955', W 77°53.431', 2130 m, 24-25.11.2009; leg: Niarchos expedition, det: C. Grismado).
- Silhouettella loricatea* (Roewer, 1942): 1 ad ♂: Tarragona, SPAIN (23.06.2004; leg/det: M. Burger).
- Stenoconops peckorum* Platnick and Dupérré, 2010: 2 ad ♂ [PBI\_OON 00010483; FMNH-INS 0000 034 721]; Little Torch Key, Torchwood Hammock, Jolly Roger Estate, Florida (Nov. 2007, leg: P. Sierwald, det: N. Platnick).
- Tinadysderina otonga* Platnick, Berniker and Bonaldo, 2013: 2 ad ♂ [PM-EC085 (PBI 43146); PM-EC087 (PBI 43145)]; Otonga forest, Pichincha, ECUADOR (S 00°25.179', W 078°59.824', 1803 m, 07.12.2009; leg: Niarchos expedition det: C. Grismado).

## APPENDIX 2: CHARACTER MATRIX

|  |        |       |       |          |          |       |       |        |      |
|--|--------|-------|-------|----------|----------|-------|-------|--------|------|
| <i>Cinetomorpha</i> sp. (Iguazú)       | 32000  | 00100 | 02000 | 03050    | -5020    | 0?0?1 | 0111? | 00002  | 100? |
| <i>Escaphiella ramirezi</i>            | 32000  | 0000? | 03000 | 03050    | 34000    | 0?011 | 0101? | 01002  | 0011 |
| <i>Giamasomorpha</i> cf. <i>vianai</i> | 32000  | 00000 | 02000 | 03050    | -5020    | 0?0?1 | 0111? | 00002  | 1?0? |
| <i>Neotrops poguazu</i>                | 32000  | 00101 | 12110 | 00020    | [12]0121 | 03001 | 0111? | 00002  | 2?00 |
| <i>Neotrops pombero</i>                | 32000  | 00101 | 12110 | 00020    | [12]0121 | 03001 | 0111? | 10002  | 2200 |
| <i>Neotrops waorani</i>                | 32000  | 00101 | 12110 | 00020    | 20121    | 03001 | 0111? | 00002  | 2?00 |
| <i>Neoxyphinius termitophilus</i>      | 31010  | 00000 | 02000 | 010[36]0 | 02310    | 00?00 | 10111 | ?10022 | 1000 |
| <i>Niarachos scutatus</i>              | 32000  | 0???0 | 0?0?0 | 0?0?0    | ?0000    | 0?0?1 | 0101? | 011-2  | 0?0? |
| <i>Oonops domesticus</i>               | ??000  | 000?0 | 03100 | 01000    | 10200    | 0-001 | 0101? | 11001  | ??00 |
| <i>Oonops</i> sp. (Ibiza)              | 31000  | 00000 | 03000 | 00000    | [12]0200 | 0?001 | 1101? | 011-2  | 0200 |
| <i>Opopaeca apicalis</i>               | 31???? | 0?--- | ----? | ----     | ---3-    | ----  | ----1 | -000?  | ?-0- |
| <i>Orchestina</i> sp. 1 (Chile)        | 32000  | 00000 | 02000 | 02011    | -5000    | 000?1 | 0101? | 20002  | 0001 |
| <i>Orchestina</i> sp. 2 (Argentina)    | 3?0?0? | 00000 | 02?0? | ?201?    | -5000    | 000?1 | 0101? | 20002  | 0001 |
| <i>Paradysderina yanayacu</i>          | 31000  | 00000 | 02000 | 01030    | 02000    | 0?001 | 0111? | 10002  | 1000 |
| <i>Paradysderina fusiscuta</i>         | 31000  | 00000 | 02000 | 01030    | 02000    | 0?001 | 0111? | 10002  | 1000 |
| <i>Scaphiops yanayacu</i>              | 31000  | 0???0 | 0?3?0 | 0?0?0    | ?0000    | 0?011 | 0101? | 011-2  | 0?0? |
| <i>Silhouetella toricatula</i>         | 310?0  | 00000 | 020?0 | 03050    | -5020    | 0?0?1 | 0111? | 00002  | 100? |
| <i>Stenoonops peckorum</i>             | 3?0?0? | 0?000 | 02000 | 03050    | 3400?    | ?0011 | 01?0? | 1?0?2  | 0?0? |
| <i>Timadysderina otonga</i>            | 31000  | 00100 | 12000 | 010[36]0 | 02000    | 0?0?1 | 0111? | 10002  | 000? |